To the Graduate Council:

I am submitting herewith a thesis written by Brian T. Sheldon entitled "An Oxygen Isotope Study of Illitization and Diagenesis in Appalachian Vertic Paleosols." I have examined the final copy of this thesis for form and content and recommend that it be accepted in partial fulfillment of the requirements for the degree of Master of Science, with a major in Geology.

Dr. Claudia I. Mora, Major Professor

We have read this thesis
and recommend its acceptance:

Accepted for the Council:

Associate Vice Chancellor and
Dean of the Graduate School

STATEMENT OF PERMISSION TO USE

In presenting this thesis in partial fulfillment of the requirements for a Master's degree at the University of Tennessee, Knoxville, I agree that the Library shall make it available to borrowers under rules of the Library. Brief quotations from this thesis are allowable without special permission, provided that accurate acknowledgment of the source is made.

Permission for extensive quotation from or reproduction of this thesis may be granted by my major professor, or in her absence, by the Head of Interlibrary Services when, in the opinion of either, the proposed use of the material is for scholarly purposes. Any copying or use of the material in this thesis for financial gain shall not be allowed without my written permission.

Signature 

Date 1-5-95

AN OXYGEN ISOTOPE STUDY OF ILLITIZATION AND DIAGENESIS IN APPALACHIAN VERTIC PALEOSOLS

A Thesis
presented for the
Master of Science
Degree
The University of Tennessee, Knoxville

Brian T. Sheldon
May, 1995

Dedication

For my Father,

HERBERT C. SHELDON JR.

whose extreme interest and enthusiasm in my
personal and professional life have made
his memory a very powerful driving force.

ACKNOWLEDGMENTS

When I first entered the graduate program in geology at the University of Tennessee, I had very little understanding (its called being naive) of active scientific research. Now on the verge of graduating, I walk away with many new friends, a greater appreciation of hard work, and most importantly with a "hands-on" feel of how science progresses. There are many people to be thanked for these accomplishments. First and foremost I would like to thank my advisors Dr. Claudia Mora and Steven Driese for inviting me in on this project and providing the financial support necessary to get the project done. I would like to further thank Claudia for being actively involved in this project, and for teaching me organizational and writing skills that will serve me well, especially in the environment of last minute panic. Field trips with Steve were valuable learning experiences and taught me such basics as the need for sampling bags! I would like to express my appreciation to my third committee member Dr. Otto Kopp, who aside from helping me get my first publication, was an excellent source of information on laboratory techniques. The entire committee was invaluable in making the final draft of this thesis a much better manuscript.

There are several people who contributed directly to this thesis and should be thanked. Dr. Samuel Savin was gracious enough to lend the use of several laboratories (and equipment therein) at Case Western Reserve University. Dr. Savin and Dr. Crawford Elliott, also of Case Western Reserve University, were instrumental in teaching me the finer points of clay sample preparation. I am further indebted to Dr. Elliott for performing the very lengthy and time consuming K/Ar analyses. I am very grateful to the secretaries Cindy Turner, Melody Branch, and Denise Stansberry, who do their job so well that many of the little oddities associated with graduate school often go

unappreciated. Ian Richards not only taught me to sing Neil Young tunes opera style (which sounded really bad), but also was extremely patient in showing me my way around a very unforgiving silicate line. Most importantly, Ian further instilled the idea that the quality of scientific interpretation can only be as good as the quality of data collection. A huge thanks goes to an excellent field geologist, Mike Caudill, who through many discussions and field excursions taught me much about paleosols and depositional environments, as well as a little about life in general. Lastly, Andy Stefaniak is thanked for his contribution of graphical artistry on the paleosol schematic profiles.

To all my friends here at that University of Tennessee....many thanks. For fear of accidentally leaving anybody unlisted, I resolve to saying you know who you are. You have made my experience here at UT a memorable one, and I hope our paths continue to cross. There are a few friends I wish to acknowledge because they have gone through the meat grinder with me. Tony Tingle sparked my interest in the world of bluegrass flatpickin, and I'd like to thank him for getting me interested in something I'll take with me to the grave. Thanks also to Landon Davidson .....for the planes, buses, boats, taxis, and automobiles, and of course for all of our politically correct conversations.

By far and away the greatest amount of my appreciation goes to my Mom, Dad, Brother, and very best friend, computer consultant, and future wife Amy Halleran for giving me a strong foundation on which to live my life and view this world. I could not have accomplished what I have without them.

ABSTRACT:

Paleoclimate interpretations based on paleosol stable isotope proxies require preservation of original pedogenic signatures and thorough understanding of mineral paragenesis (i.e., pedogenic or diagenetic). This study examined the oxygen isotope compositions of clays and pedogenic carbonate in three approximately time-equivalent vertic paleosols to establish the extent to which these minerals approached isotopic equilibrium at pedogenic and burial diagenetic temperatures. The paleosols are preserved in the late Mississippian Mauch Chunk (PA), Hinton (WV), and Pennington (TN) Formations, which were buried to 7-8 km, 3-4 km, and <3 km, respectively, within the Appalachian Basin. Preserved macro- and micromorphological features indicate that these paleosols were composed of $>$ 30 %, chiefly smectitic, clay which experienced repeated cycles of wetting and drying as a result of strongly seasonal precipitation during pedogenesis. Presently, the paleosols are composed predominantly of discrete illite, which is inferred to have been authigenically produced through the smectite-to-illite transition. Size separations were made to isolate the smallest naturally occurring size fraction of clays, as determined by laser particle scattering. This size fraction was then analyzed to evaluate its mineralogy (using X-ray diffraction) and its oxygen isotope composition.

Previous studies have documented the strong control of the smectite-to-illite transition on the isotopic evolution of pore fluids. Therefore, three

possible environments of illite formation in the paleosols, defined by different temperatures and pore fluid oxygen compositions, were considered: 1) illitization occurs in the pedogenic environment and is kinetically driven by repeated cycles of wetting and drying smectitic clays, 2) illitization is thermally driven as result of increased depths of burial, and 3) illitization occurs in response to a pulse of hot, saline, orogenic fluids migrating through the paleosols. Illite-calcite equilibration temperatures, calculated equilibrium pore-fluid compositions estimated from appropriate O-isotope fractionation factors, and radiogenic (K/Ar) age dating were used to evaluate which environment best explains illitization within each paleosol.

Illite and pedogenic calcite in the more-deeply buried Mauch Chunk and Hinton paleosols no longer preserve pedogenic signatures. Instead, calculated equilibration temperatures for the Mauch Chunk (180 °C) and Hinton (110 °C) indicate that these mineral phases most likely acquired their oxygen signatures during burial-driven illitization. Compaction of the paleosols subsequent to clay dewatering may have effectively prevented later orogenic fluids from migrating through them. That vertic paleosols behave as isotopically closed systems is supported by the preservation of isotopic equilibration temperatures that are below, and, in the case of the Mauch Chunk, well below, maximum burial temperatures.

Interpretation of the Pennington data is more difficult. The method of

illite formation must account for three important parameters defined by the data: 1) illitization of the paleosol is extensive despite very shallow depths of burial, 2) calcite retained a pedogenic oxygen isotope signature which indicates it did not undergo isotopic exchange during smectite dewatering and illite formation, and 3) the Pennington "parent" and paleosol materials have identical oxygen isotope compositions and have gone through the same degree of illitization. Individually, none of the defined environments of illite formation can account for all of these parameters. Therefore, the pathway of Pennington illitization is best explained by a combination of different methods of illite formation. In this case, illitization most likely began in the pedogenic environment and continued to be driven during burial diagenesis. Illitization initiated in the pedogenic environment may have allowed coarsening and ordering of illite to proceed at the low temperature and low water/rock conditions necessary for the preservation of pedogenic oxygen isotope compositions in calcite. Extended periods of time in the shallow burial environment would account for extensive illitization and masking of mineralogical and isotopic differences between "parent" and paleosol illites. The results of this study suggest that oxygen isotopes in vertic paleosols are not well suited for paleoclimate interpretations, but are best suited for evaluating the physical and chemical conditions of diagenesis.

LIST OF FIGURES

LIST OF FIGURES (continued) PAGE

LIST OF TABLES

I. INTRODUCTION

The stable carbon isotope compositions of pedogenic carbonates (rhizoconcretions) from vertic paleosols of the Appalachian Basin have been used to estimate carbon dioxide levels (pCO_2) in the middle-to-late Paleozoic atmosphere (Mora and Driese, 1993), using Cerling's (1991) soil carbonate paleobarometer. Comparison of Mora and Driese's (1993) estimates to those predicted by the long-term carbon cycle (Berner, 1991) confirm a mid-to-late Paleozoic decline in atmospheric pCO_2 (Fig. 1). The most important assumption associated with estimates of this type is that the original pedogenic carbon signature has been preserved. The fact that rhizoconcretions from time-equivalent paleosols yield similar estimates of pCO_2 despite forming in different depositional environments and experiencing different burial histories, suggests that pedogenic carbon isotope compositions were preserved through diagenetic recrystallization (Mora et al., 1991; Mora and Driese, 1993).

The oxygen isotope composition of pedogenic calcretes may contain additional paleoclimate information. Oxygen compositions may be used to reconstruct approximate paleotemperatures and meteoric water compositions, if the original pedogenic signatures have not been diagenetically altered (Cerling, 1984, 1991; Salomons and Mook, 1986). However, unlike the carbon isotope ratios of pedogenic calcretes, oxygen

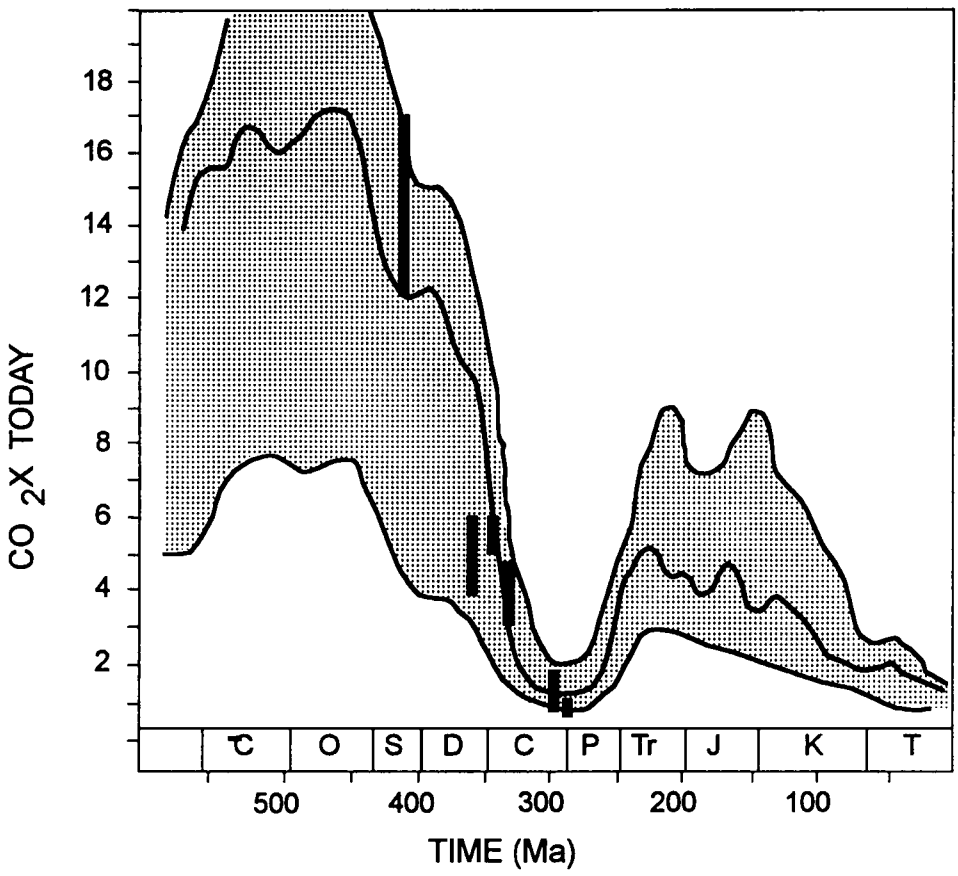

Figure 1. Estimates of Paleozoic atmospheric CO_2 from vertic paleosols using soil carbonate barometer of Cerling (1991) compared to Berner's (1993) carbon cycle model. Vertic paleosols confirm a Mid-to-Late Paleozoic decline in P_{CO2}. The upper and lowermost lines define the error of Berner's model. Data of Mora and Driese (1993) and Mora (1994, pers. comm.)

isotope signatures are not constant for time-equivalent carbonates (Fig. 2). Instead, O-isotope values vary by as much as 15 ‰ and generally become more depleted with increased depth of burial (Mora et al., 1993). This depletion trend suggests that oxygen isotope compositions of pedogenic carbonates may be better suited to evaluate the physicochemical conditions of burial diagenesis rather than the pedogenic environment.

The objective of this study is to characterize the oxygen isotope systematics of vertic paleosols by examining the isotopic evolution of pedogenic carbonate and the clays comprising the matrix of the paleosol. The focus of the study is three approximately time-equivalent, late Mississippian vertic paleosols that experienced different depths of burial within the Appalachian Basin. Each of these paleosols has passed through the smectite-to-illite transition. This mineralogical transformation has been documented to exert strong control on the chemical and oxygen isotope evolution of porewater (Hower et al., 1976; Yeh and Savin, 1977; Suchecki and Land, 1983), and should therefore have affected the pore fluids to which paleosol illites and carbonates were exposed. Establishing whether pedogenic carbonates approach oxygen isotope equilibrium with coexisting illite might provide insight on the relative timing of the acquisition of measured oxygen isotope values in both of these phases. If the carbonates and clays approach oxygen isotope equilibrium, it may indicate the

Figure 2. Mississippian calcrete stable isotope compositions from various types of paleosols. Regardless of different burial depths, carbon isotope compositions are fairly uniform within a given type of paleosol. Carbon compositions are even more uniform within a given type of carbonate morphology (rhizolith or nodule). In contrast, oxygen isotope compositions are more variable (by 15 %) and become isotopically lighter in paleosols (i.e., Mauch Chunk) that have been more deeply buried. References to the numbered fields are: 1,3,6,7,8 Mora and Driese, unpublished data; 2,4 Stefaniak et. al., 1993; 5, Caudill et. al., 1992; 9, Wright and Vanstone, 1991; 10, Goldstein, 1991.

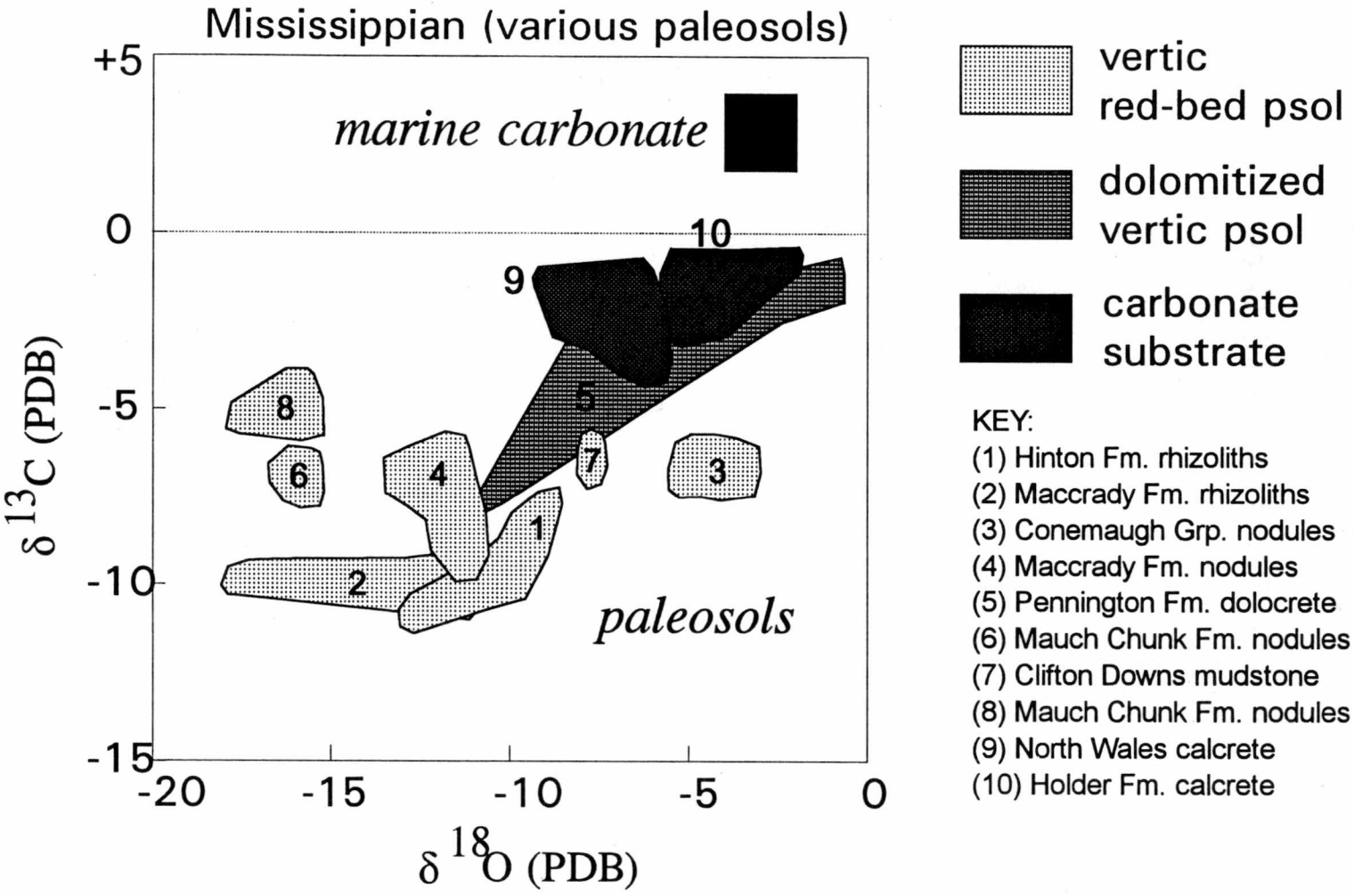
Mississippian (various paleosols)
+5
0
-5
-10
-15
-20
-15
-10
-5
0
δ 13C (PDB)
δ 18O (PDB)
marine carbonate
paleosols
1
2
3
4
5
6
7
8
9
10
vertic red-bed psol
dolomitized vertic psol
carbonate substrate
KEY:
(1) Hinton Fm. rhizoliths
(2) Maccrady Fm. rhizoliths
(3) Conemaugh Grp. nodules
(4) Maccrady Fm. nodules
(5) Pennington Fm. dolocrete
(6) Mauch Chunk Fm. nodules
(7) Clifton Downs mudstone
(8) Mauch Chunk Fm. nodules
(9) North Wales calcrete
(10) Holder Fm. calcrete

Figure. 2

carbonates recrystallized in the presence of diagenetic fluids that were compositionally controlled by the dewatering of smectitic clays. Calculated illite-calcite oxygen isotope equilibration temperatures and estimates of pore fluid oxygen composition based on equilibrium fractionation with both of these mineral phases, could then potentially be used to reconstruct the physicochemical conditions under which the smectite-to-illite transition occurred. If oxygen isotope equilibrium between calcite and illite is not approached it may indicate the pedogenic carbonate was not affected during illitization, or that the carbonate exchanged oxygen with later diagenetic fluids.

Establishing the conditions in which the clays and pedogenic carbonates assumed their measured O-isotope compositions was accomplished by performing a detailed mineralogical and isotopic examination of the clay minerals, and by constraining the temperatures at which the clays and pedogenic carbonate approached O-isotope equilibrium. The results of this study are useful in determining the value of these minerals to studies of paleoclimate or diagenesis.

II. THE SMECTITE-TO-ILLITE TRANSITION

The smectite-to-illite transition is widely recognized as a diagenetic reaction involving the replacement of smectite layers by illite, with increasing depths of burial (Burst,1969; Hower et al., 1976). Although the mechanism of illite formation is still being debated and seems to be variable for different sedimentary basins, it is agreed that this transition is not simply a smectite dewatering event (Hower et al.,1976). Instead, the smectite-to-illite transition predominantly involves the fixation of K^+ and Al^{3+} into, and the displacement of Si^{4+} and Ca^{2+} out of, the structural layers of smectite (Hower et al., 1976). Such reconstructive chemical changes make clay deposits with high concentrations of smectite particularly susceptible to isotope exchange with post-formational fluids (O'Neil and Kharaka, 1976; O'Neil, 1987).

Isotopic studies performed by Yeh and Savin (1977) and Suchecki and Land (1983) have documented oxygen isotope responses to this diagenetic transition in Texas Gulf Coast shales and the Great Valley sequence, respectively. Yeh and Savin (1977) found that significant isotopic exchange between clays, particularly the finest size fraction, and pore fluid occurs with increased depths of burial. As a result of exchange with higher temperature fluids, clay oxygen isotope values became more negative in samples that were more deeply buried. At shallow depths of burial (<3km),

only the finest size fraction (<0.1 μm) of clays show isotopic depletion characteristic of oxygen exchange. Yeh and Savin (1977) concluded that the smallest size fractions were the most likely to achieve oxygen equilibrium with pore fluids. To test for equilibrium, they attempted to confirm measured well temperatures using quartz-illite, quartz-calcite, and calcite-illite oxygen isotope thermometers. The two calcite thermometers produced unrealistic temperature estimates, indicating calcite was not in equilibrium with quartz or illite. They interpreted disequilibrium to be the result of calcite exchanging with pore fluids after the silicates had attained their measured O-isotope values. Isotopic temperatures obtained using the finest quartz and clay size fractions showed good agreement with measured well temperatures above 80 °C. A temperature of 80 °C correlates with burial depths of Gulf Coast shales (3000 m) in which the smectite-to-illite transition has been found to be actively occurring (Hower et al., 1976). Yeh and Savin (1977) concluded that significant isotopic exchange (enough to achieve oxygen isotope equilibrium) occurs between the finest clay fraction and pore fluids, in concert with dehydration and conversion of smectite to illite.

Suchecki and Land (1983) used carbon, hydrogen, and oxygen isotopes of sandstones and mudstones in the Great Valley Sequence of northern California to model thermal and fluid evolution during burial

diagenesis. Using oxygen isotope equilibrium fractionation data, they modelled an illite/smectite ^{18}O depletion (+22 to +16 ‰ SMOW) that resulted from an increasing percentage of illite layers replacing smectite within the illite/smectite complex. The oxygen isotope composition of hypothetical pore fluids in equilibrium with a given illite/smectite was also calculated. The initial temperature, temperature gradient, and relative amounts of illite converted to smectite were considered as well as the open- or closed-system nature of reequilibration for clay minerals and pore fluids. Finally, the oxygen isotope compositions of other mineral phases that may coexist in equilibrium with calculated pore fluids and illite/smectite at any given temperature were estimated. Their results indicate that calculated and measured compositions of authigenic quartz, chlorite, and calcite were in good agreement, suggesting that these phases formed in near isotopic equilibrium with pore fluids that became increasingly enriched in ^{18}O with depth. Sharp increases in D/H ratios of illite/smectite at 3000 m (100 °C) coincided with late stage dehydration and conversion of smectite to illite. Coincident with this mineralogic transformation was a buffering of the oxygen isotope composition of pore fluids from compositions similar to sea water (approximately 0.0 SMOW) to compositions of +8 ‰ SMOW. The study by Suchecki and Land (1983) clearly illustrates the control that the

smectite-to-illite transition can have on the oxygen isotope composition of pore fluids.

III. HYPOTHESIS

Vertic paleosols provide a unique opportunity to use oxygen isotope ratios to evaluate physicochemical conditions of the burial diagenetic environment. Their distinctive physical characteristics such as sepic plasmic microfabrics, large silt-filled cracks, pseudoanticlines, mukkara, pedogenic slickensides, and their angular blocky ped textures are comparable to the physical characteristics of Holocene Vertisols. Vertisols require a >30 % (chiefly smectitic) clay component and form in climates with strongly seasonal precipitation that leads to wet/dry cycling of these clays (Dudal and Eswaran, 1988). Shrinking and swelling of the smectitic clay generates the distinctive physical characteristics by which vertic paleosols and Vertisols are identified. The clay component of the three paleosols studied in this investigation is at present dominantly illitic, suggesting these paleosols have passed through the smectite-to-illite transition. Based on what is known about oxygen isotope responses to this mineralogic transformation, the oxygen isotope signatures of paleosol clays can potentially be used to evaluate physicochemical conditions of the diagenetic environment. It is hypothesized that authigenically produced illite equilibrated with pore fluids strongly influenced by dewatering associated with the smectite-to-illite transition.

Pedogenic carbonates, which potentially preserve paleoclimate

information, may recrystallize and exchange in response to mineralogic transformations occurring in the paleosol matrix. Evaluating the extent to which illite and calcite approach isotopic equilibrium will allow the relative timing of recrystallization/production of these two mineral phases to be established. If isotopic equilibrium was approached, equilibration temperatures and pore fluid oxygen compositions can be estimated. Carbonate and clay oxygen isotope signatures should be consistent with illite formation and carbonate recrystallization in the presence of fluids buffered by smectite dewatering. If oxygen isotope equilibrium is not approached, it suggests that carbonates and clays acquired their isotopic signatures in the presence of different fluids, at different times.

IV. GENERAL STRATIGRAPHY AND PALEOSOL LOCATION

The paleosols studied in this investigation are middle-to-late Chesterian in age and occur in the Mauch Chunk Formation of Pennsylvania, the Hinton Formation of West Virginia, and the Pennington Formation of Tennessee (Fig. 3). Each of these formations are red-bed sequences that were deposited in association with incipient Alleghanian clastic wedges that actively filled the Appalachian Basin from late Mississippian to early Permian time (Meckel, 1970). The Mauch Chunk is part of the Pottsville Clastic wedge and the Pennington is part of the Pennington-Lee clastic wedge (Fig. 4). The Hinton received sediment from both clastic wedge source areas (Fig. 4). In general, the Mauch Chunk, Hinton, and Pennington Formations represent depositional and pedogenic environments of increasing marine influence. Vertical tectonics active during the Mississippian (Donaldson and Shumaker, 1981) resulted in development of varied arrays of depositional environments in the near-shore Hinton and Pennington Formations. Extreme care must therefore be exercised in locating the stratigraphic position of preserved vertic paleosols, and in interpreting the paleoenvironments represented.

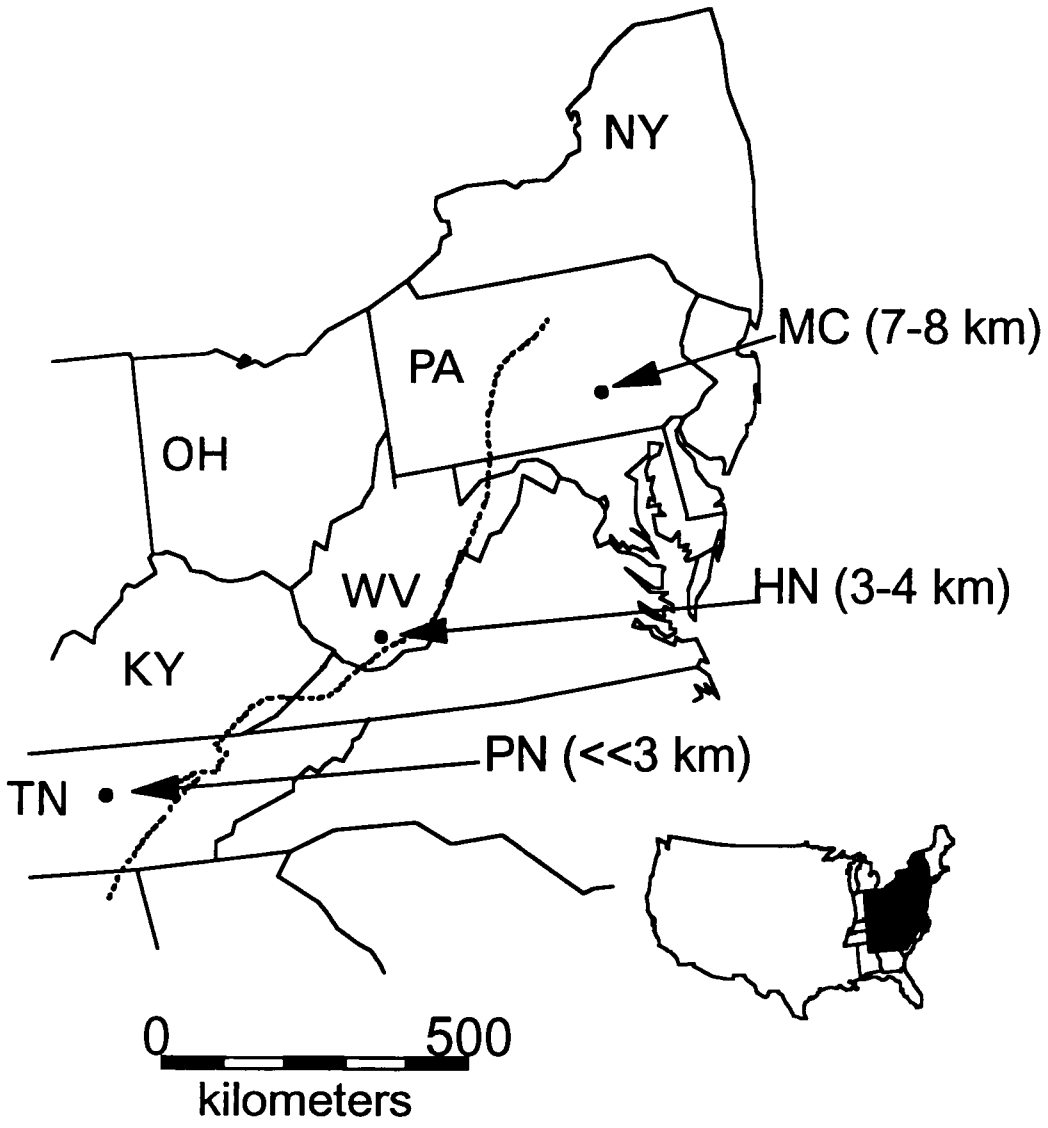

Figure 3. Location of field areas with estimated burial depths for each paleosol in parantheses. PN = Pennington, HN = Hinton, MC = Mauch Chunk. Dotted line approximates the western limit of Alleghanian thrust faults.

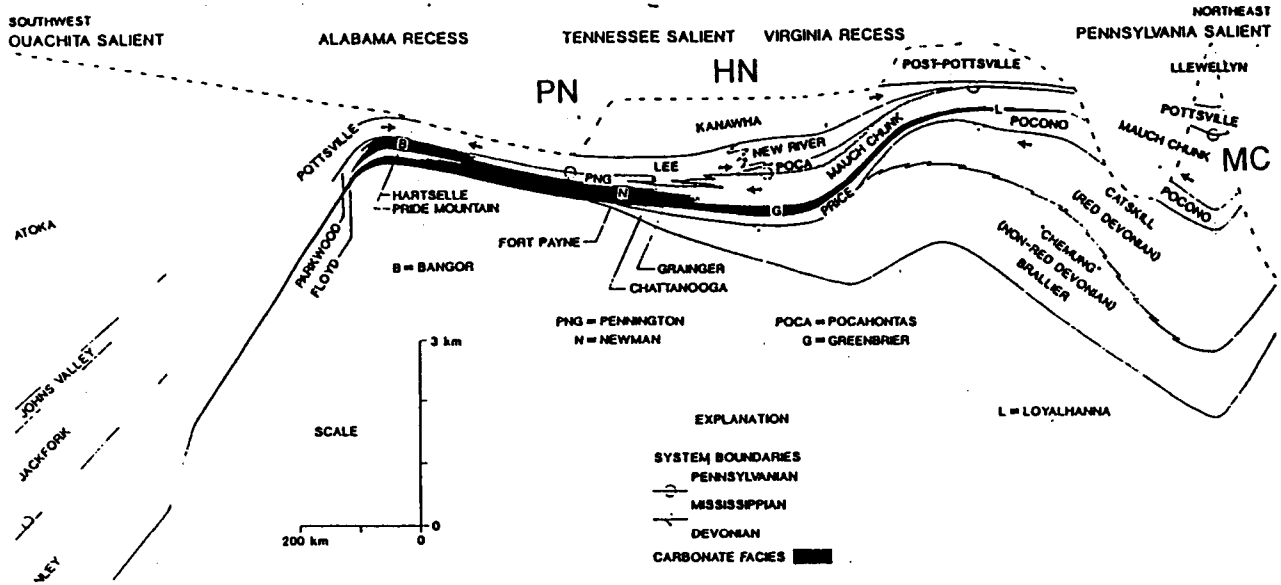

Figure 4. Northeast-southwest cross section of the Appalachian basin showing Alleghanian clastic wedges (from Hatcher, 1989). The location of the paleosols is denoted by PN (Pennington), HN (Hinton), MC (Mauch Chunk). Note the Hinton is located where the northeastward prograding Pennington clastics merge with southwestward prograding Mauch Chunk clastic facies.

V. DEPOSITIONAL ENVIRONMENTS AND BURIAL HISTORIES

MAUCH CHUNK PALEOSOL

The Mauch Chunk Formation in Pennsylvania is a terrestrial sequence primarily composed of alluvial and delta-plain sediments (Edmunds et al., 1979; Englund et al., 1985; Donaldson and Shumaker, 1981). The stratigraphy near the locality of the Mauch Chunk paleosol is characterized by repetitively stacked 2-5 meter thick fining-upward sequences of alternating nonred sandstones and red siltstones and mudstones (Driese et al., 1993). This sequencing was interpreted by Stancel (1980) and Morrow (1984) to be characteristic of a depositional environment associated with a coarse-grained, low sinuosity, meandering stream system. The sandstone intervals are believed to be fluvial in origin, with the silt and mudstones representing floodplain deposits (Stancel, 1980; Morrow 1984). The Mauch Chunk paleosol studied in this project developed in the silt and mudstones of the floodplain deposits (Driese et al., 1993).

The location of the Mauch Chunk paleosol to the East of all Alleghanian thrust faults (Fig. 3) indicates the burial of this paleosol was both depositionally and structurally controlled. Burial was initially caused by deposition as sedimentation associated with the Alleghanian orogeny was initiated prior to the thrusting stages of this mountain-building event (Hatcher et al.,1989). Most of the burial of the Mauch Chunk and anthracite

region was probably the result of stacked thrust sheets (Levine, 1986). Based primarily on coalification patterns (Levine, 1986), Conodont Alteration Indices (Epstein et al., 1977), and estimated isopachs (Beaumont et al., 1988), peak burial conditions of the Mauch Chunk paleosol have been estimated to be 7-8 km and 230-260 °C (Fig. 3).

HINTON PALEOSOL

The Hinton Formation in West Virginia represents a variety of depositional environments, with coastal plain, tidal flat, shallow marine and barrier bar units being represented (Englund et al., 1985). The Hinton paleosol is found in a stratigraphic sequence dominated by grayish-red shale and siltstone that Englund et al. (1985) believe represent a transition from marine to more terrestrial conditions. At the Hinton outcrop, vertic paleosols have developed in silt and mudstones that are associated with channel sandstones. This relationship is similar to the Mauch Chunk, and indicates the Hinton paleosol developed in fluvial overbank deposits. The Hinton paleosol, however, developed in a coastal plain (as opposed to upper alluvial plain) setting.

The Hinton field area is located to the west of Alleghanian thrusting (Fig. 3), which indicates the burial of this paleosol was strictly the result of depositional overburden. Conodont Alteration Indices (Epstein et al., 1977)

and isopachs generated by Beaumont et al. (1988) suggest that this paleosol had a maximum burial depth of approximately 4 km, with peak temperatures of 140 °C.

PENNINGTON PALEOSOL

The Pennington Formation consists of a mixed siliciclastic-carbonate sequence composed of dolomite, limestone, fine-grained sandstone, conglomeratic sandstone, and red, green, and gray shale (Milici, 1974; Milici et al., 1979). In Tennessee, the Pennington Formation comprises nondeltaic littoral deposits underlain by offshore carbonates and overlain by coal-bearing deltaic deposits (Milici, 1974). The Pennington paleosol studied in this investigation is bounded by marine deposits, indicating a coastal marine setting. More specifically, Caudill et al. (1992, and submitted) suggest that this paleosol developed on a flat, low-lying coastal plain situated adjacent to a clastic lagoon. The lagoon was separated from an area of offshore carbonate production by a barrier or tidal bar complex (Caudill et al., submitted). The Pennington paleosol developed in marginal marine clays (Caudill et al., 1992).

The location of the Pennington paleosol to the West of all Alleghanian thrust sheets (Fig. 3) indicates that the burial of this paleosol was strictly a function of depositional overburden. Conodont Alteration Indices and

isopach data suggest maximum burial conditions of this paleosol was < 3km and 70-100 °C.

VI. PALEOSOL LOCATION, DESCRIPTION, AND SAMPLING

The Mauch Chunk paleosol is located in east-central Pennsylvania (Dauphin County) along I-80 near the summit of Nescopeck Mountain. Descriptions of this paleosol are taken from Driese et al. (1993). The legend of symbols used in the schematic section of this and all three paleosols is shown in Figure 5. The "Nescopeck" paleosol is 2.25 meters thick and can be divided into three different horizons (Fig. 6). The top 80 cm is composed of a stage III calcrete (Machette, 1985) that consists of vertically stacked micrite nodules (pedogenic) embedded in grayish red, silty clay matrix. Clasts of this calcrete can be found in the overlying non-red sandstone that erosively cuts the paleosol. Beneath the calcic horizon is a 60-80 cm thick grayish red, silty claystone with well-developed blocky ped structures. Pedogenic slickensides of modest scale are present in this second horizon. The lowermost horizon is a clayey siltstone that is dominated by large, non-calcified root traces and extensive color mottling. The paleosol grades downward into a ripple- laminated siltstone that shows little evidence of pedogenic modification.

Four Mauch Chunk clay samples were chosen based on association with pedogenic carbonate and availability from an existing suite of samples (Fig. 6). This suite represented a vertical section through the paleosol with samples taken every 10 cm. Pedogenic carbonates used in paleoatmospheric pCO_2 estimates by Mora et al. (1991; 1993) are from the

Legend

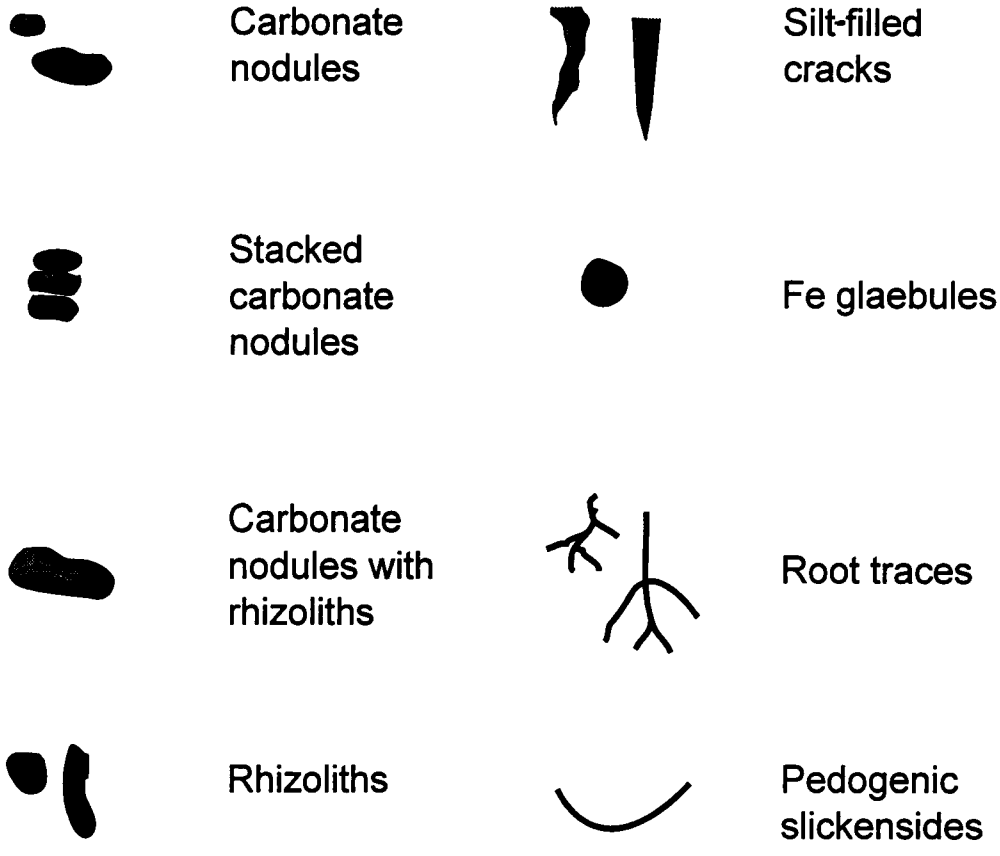

Fiugre 5. Legend for symbols used in paleosol schematic sections (figures 6,7, and 8).

Mauch Chunk Paleosol

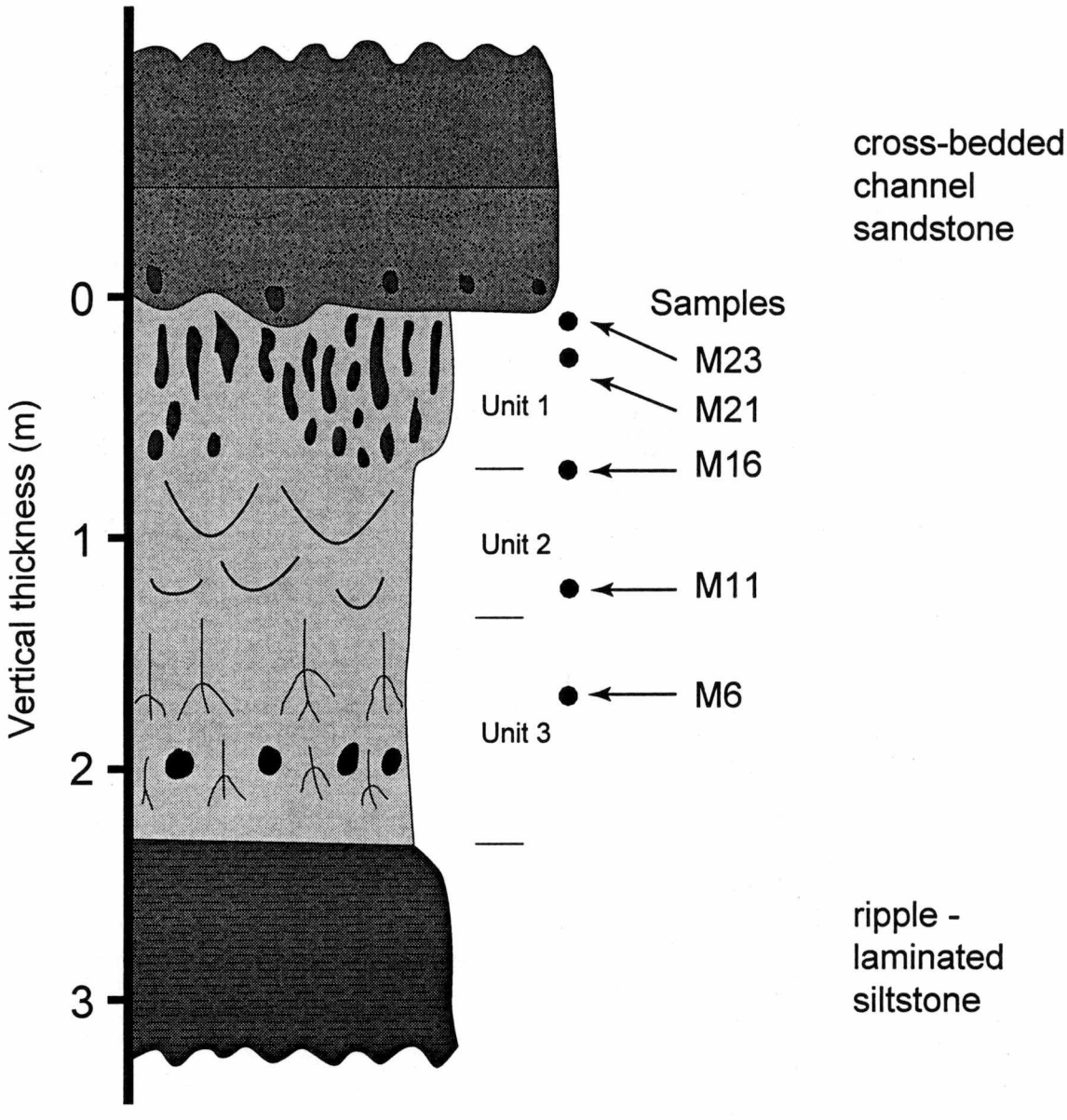

Figure 6. Schematic Profile of the Mauch Chunk Paleosol including sample locations (adopted from Driese, 1993).

stage III calcrete at the top of the paleosol.

The Hinton paleosol is located on Green Lawn Road in Elton, West Virginia in northern Sommers County. The paleosol is a 2.0 meter thick composite paleosol that has been erosively truncated by a cross-bedded channel sandstone (Fig. 7). Four distinguishable horizons make up the paleosol. The top horizon is a silty red/brown mudstone that has a moderate platy structure and sparse small pedogenic slickensides scattered throughout. The maximum thickness of this top horizon is 10 cm, but its overall thickness is variable dependent on the amount of channel scouring above. Beneath the top horizon is an 85 cm thick, dark red/brown mudstone that has a very well developed, medium, blocky structure and has small (2-3 cm) disorthic carbonate nodules distributed throughout. Diagnostic of horizon 2 are two size generations of vertical/sub-vertical cracks. Large cracks, some 5 cm in apparent width and extending 150 cm into the paleosol, are filled with fine-grained sandstone and have gleyed margins in the lower, more narrow portion of the crack. Smaller cracks with gleyed margins reach 20-30 cm in length. Also characteristic of this second horizon are abundant large, curved slickensides that converge to form pseudo-anticlines and intersect to form parallelipipeds. The contact between unit two and unit three is very gradual, with unit three (30 cm thick) being marked by a less well developed structure and fewer slickensides and

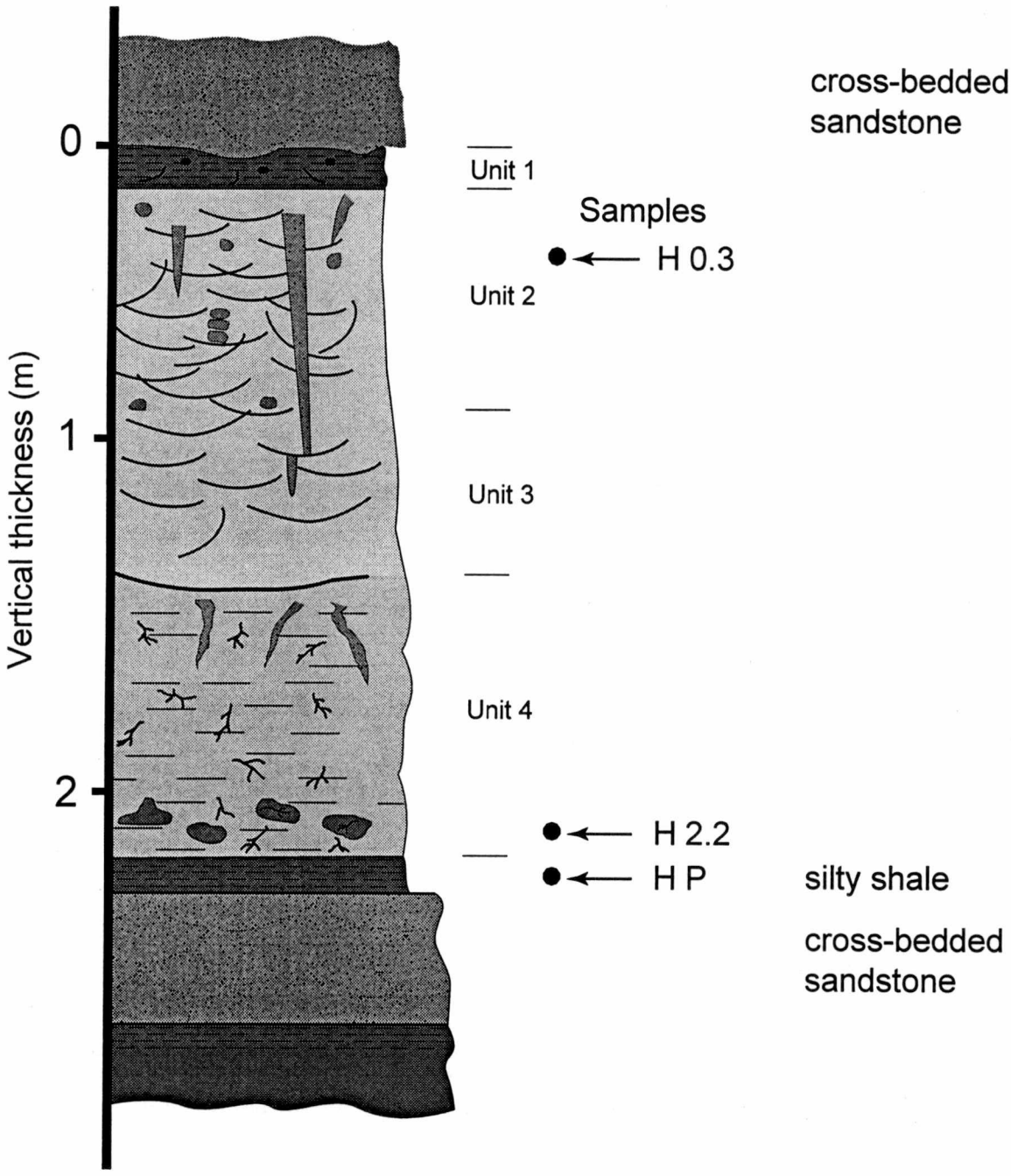

Figure 7. Schematic profile of the Hinton Paleosol including sample locations. The pedogenically unaltered silty shale at the base of the paleosol was sampled (HP) and is considered to be the "parent" material for soil development.

cracks. Unit four is 75 cm thick and is a coarse, platy- structured, brown/red mudstone. Vertical to sub-vertical cracks 20-60 cm in length are common to this fourth horizon. Also very abundant in unit four are small (2-5 cm), downward branching, gleyed root traces. A zone, 5-20 cm thick, composed of large 3-6 cm disorthic carbonate nodules is found 20 cm above a clear contact with an underlying laminated shale. The shale unit is 10 cm thick and shows no signs of pedogenic alteration. This shale is assumed to be the "parent" material of the Hinton paleosol.

Several carbonate nodules and three clay samples were taken from the Hinton paleosol (Fig. 7). Small disorthic carbonate nodules were taken from unit 2, but carbonate sampling concentrated on the large, disorthic nodules of unit 4. Clays associated with the carbonates of units 2 and 4 were taken, as well as a sample from the pedogenically unaltered "parent" material.

The Pennington paleosol is exposed in roadcut along Interstate 40, just west of Monterey, Tennessee. The paleosol is approximately 1.5 m thick and comprises four morphological units that show marked lateral variations in thickness. The schematic profile shown in Figure 8 is through the flank of a pseudo-anticline where sampling was performed. Descriptions of this paleosol are taken from Caudill et al. (1992) and Caudill et al., (submitted).

Pennington Paleosol

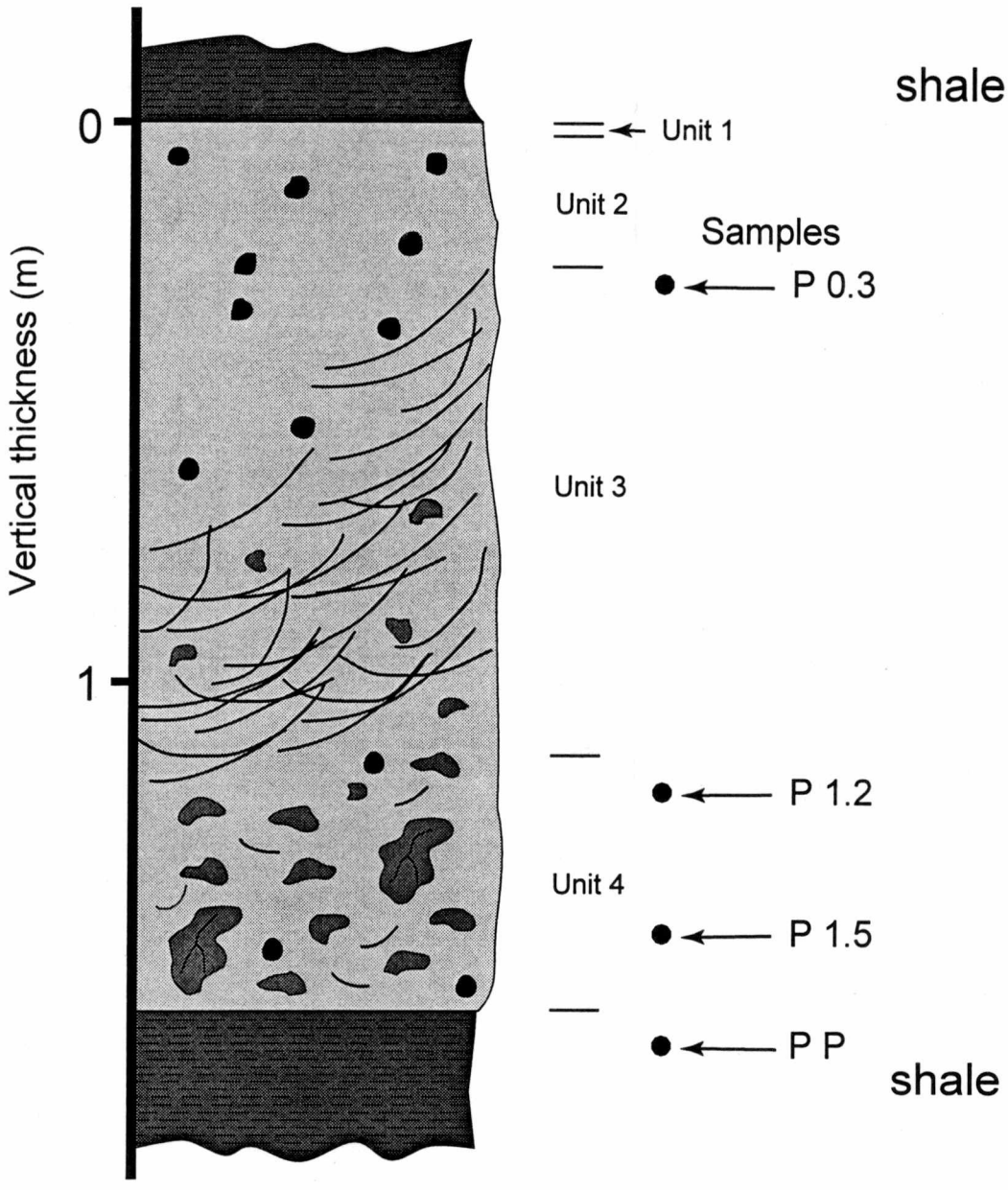

Figure 8. Schematic profile of the Pennington Paleosol including sample locations. The pedogenically unaltered shale at the base of the paleosol was sampled (PP). This is considered to be the "parent" material for soil development.

Unit 1 is a hard, massive, dolomicritic crust that is 0-15 cm thick. The basal contact of unit 1 is clear and wavy. Unit 2 (0-80 cm thick) is a dark olive gray, noncalcareous silty claystone. Common to this second unit are small pedogenic slickensides as well as small (0.1 - 1 cm), disseminated sesquioxide concretions. Unit 2 has a distinctive moderate granular structure with a wavy and gradual basal contact. Unit 3 (0-85 cm thick) is a dark reddish brown, weakly calcareous silty claystone. Common to this third unit are many small slickensides as well as large, arcuate slickensides that converge to form pseudo-anticlines. Medium, sub-angular blocky aggregates result from intersecting slickensides. Disorthic, tuberous dolomicrite nodules are fairly common in unit 3. Unit 4 (20-70 cm thick) is also a dark reddish brown, silty claystone, but has a moderate, coarse angular blocky structure with few wedge-shaped structural aggregates. Many large slickensides in the top 10 cm are subhorizontal. Tuberous, disorthic dolomicrite nodules (1-10 cm in diameter), some of which are vertically stacked and considered to be rhizoconcretions, are common in this fourth horizon. A few non-dolomitized carbonate nodules were found at the very bottom of this unit. Fine (<0.5 cm) sesquioxide nodules are scattered throughout unit 4, which has a gradual contact with a semi-fissile to fissile, dark greenish gray clay shale below. This 10-100 cm thick shale has

preserved sedimentary layering and is assumed to be the "parent" material for the Pennington paleosol.

VII. ANALYTICAL METHODS AND INSTRUMENTATION

CLAY SAMPLE PREPARATION

Mauch Chunk and Hinton clay samples were crushed using a mortar and pestle into 1-2 mm pieces and then wet sieved to remove any clay size particles artificially generated by crushing. The sieved material was then ultrasonically disaggregated to obtain the clay size fraction. Pennington samples were dissaggregated by placing them in water overnight. All disaggregated material was chemically treated following the method of Jackson (1975) to remove iron oxides, organic, and carbonate material. These phases would contaminate oxygen isotope analyses and also act as cements that prevent clean size separations. A detailed outline of Jackson's (1975) methods are given in Appendix A.

Determining whether or not these chemical treatments affected the O-isotope compositions of the clays is very important. Yeh (1974) and Eslinger (1971) treated identical sets of clay samples with chemicals that had different oxygen isotope signatures. They found that the oxygen isotope composition of the clays were identical between sets, and concluded that the chemical treatments did not affect clay oxygen values. Savin and his students have performed this experiment on numerous clay samples and have had similar results (Savin, pers. comm.). Therefore, it is assumed that

chemical treatments used in this project did not affect the measured oxygen isotope composition of the clays.

Following chemical treatments, all samples were dialysized in distilled, deionized water to remove residual chemicals, particularly those that acted as flocculants. Clay-size separates were then obtained using centrifugation. The smallest clay-size fractions required a flocculant (usually 1 ml/L nitric acid or 5 ml/L 1.0 M sodium acetate-acetic acid buffer) so that the amount of sample suspension could be reduced for storage. All size fractions were stored in a methanol/water (4 drops/ 100 ml) suspension to prevent bacterial growth. Nitric acid, sodium acetate-acetic acid buffer, and methanol were removed by dialysis for 3-4 days, just prior to isotope and XRD analyses.

PARTICLE SIZE SEPARATION

Size separations were achieved using centrifugation to isolate naturally existing clay size populations. Natural size populations were determined at Case Western Reserve University using a Spectrex Particle Size Analyzer (1.0 μm -100 μm) and a NICOMP 370 submicron particle size analyzer. Both the Spectrex and the NICOMP make use of laser scattering techniques. Because smaller size fractions are more likely to be authigenic, the most crucial size separation was the one chosen to isolate the smallest size fraction. Size separations proceeded from largest to smallest to make

the cleanest split possible for the smallest size fraction.

MINERALOGICAL IDENTIFICATION

Mineralogical identifications were made using X-ray diffraction (XRD) techniques. All XRD analyses were performed on a Siemans D500 powder diffractometer using Cu Kα radiation (λ = 1.542 Å). Oriented samples were prepared by settling sample suspension on to a glass slide and then drying the suspension in a 40 °C atmosphere. Glycolation was achieved using a glycol atmosphere at 60 °C for 20 hrs. Heat treatments were performed at 550 °C for one hour. Samples were step scanned from 4 - 40° 2θ using a .02° θ step. A minimum of two elutriated slides were prepared for each sample analyzed. X-ray diffraction plots for every sample are shown in Appendix B.

A first order approximation of the percentage of illite and chlorite in the smallest size fraction was obtained by comparing the areas of the illite and chlorite 003 peaks (Moore and Reynolds, 1989). Areas were determined by multiplying peak height by peak width at half peak height (Fig. 9; Appendix B). Deconvolution programs were not employed and best estimates of baselines were drawn using "artistic license". It was assumed that chlorite and illite had the same relative intensity ratios so that peak areas could be correlated to relative percentages of these two minerals in

Figure 9. X-ray diffraction plot showing method used to obtain first order approximations of the percentages of illite and chlorite in the finest size fraction. The plot shows estimates where the peak area of both the chlorite 003 and 004 peaks are compared to the illite 003 peak. Inferred background for the chlorite 003 peak was done using "artistic license". Estimated percentages were given a 15 % margin of error.

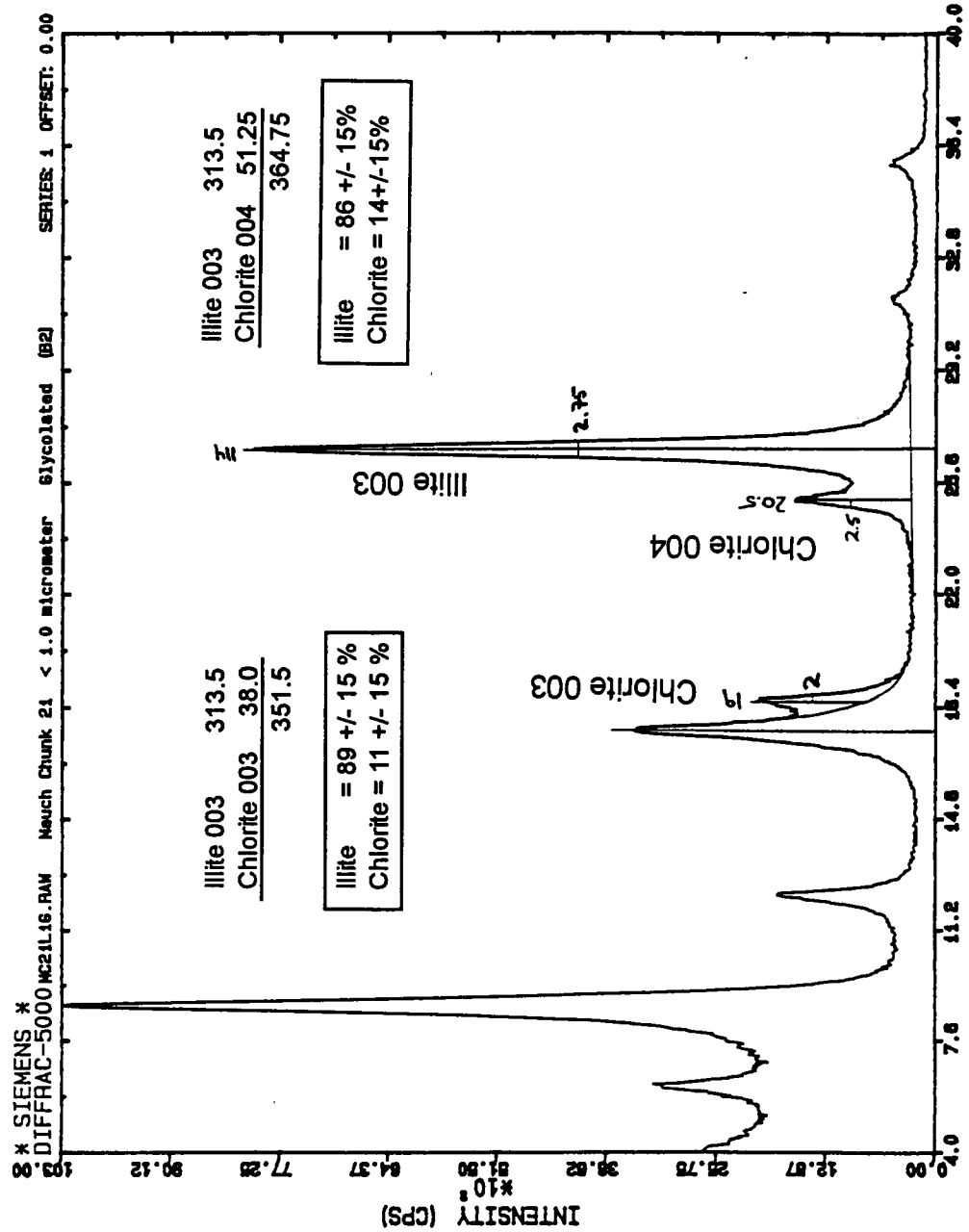
* SIEMENS *
DIFFRAC-5000 MC21L16.RAW Mauch Chunk 21 < 1.0 micrometer Glycolated (B2) SERIES: 1 OFFSET: 0.00
INTENSITY (CPS)
*10³
TWO - THETA (DEGREES)
Illite 003
Chlorite 004
Chlorite 003
2.75
20.5
2.5
19
2
Illite 003 313.5
Chlorite 003 38.0
351.5
Illite = 89 +/- 15 %
Chlorite = 11 +/- 15 %
Illite 003 313.5
Chlorite 004 51.25
364.75
Illite = 86 +/- 15%
Chlorite = 14+/-15%

Figure 9

the sample. Error associated with this technique was assumed to be +/- 15%. Isotopic interpretations took into account the possibility of a 30% error. In some cases the area of the chlorite 003 could not be determined, and the 004 peak was used instead (Fig. 10). With the exception of the Pennington and Hinton "parent" material samples, estimates of %chlorite based on 004 peaks were the same as estimates obtained using the 003 peak, within the 15 % margin of error. Illite and chlorite percentages reported are averages from two or more XRD analyses.

The type of illite/smectite (I/S) ordering and the percentage of illite layers in the I/S were determined using the methods of both Srodon (1984) and Moore and Reynolds (1989). Peak positions of the illite 002 and illite 003 were plotted on Srodon's (1984) figure 2 to evaluate if the illite present was discrete illite or ordered illite/smectite. The difference in $°2\theta$ ($\Delta 2\theta$) between the I/S 001/002 peak and the I/S 002/003 peak was measured and then compared to Moore and Reynolds (1989) table 7.3 to get the %illite layers and the accompanying Reichweite ordering.

CLAY ISOTOPE ANALYSIS

Prior to weighing clay samples for oxygen isotope extraction, adsorbed and interlayer water was reduced by outgassing at 175 °C without vacuum for 8-12 hrs. Remaining water, and water adsorbed during sample

Figure 10. Example of estimating illite and chlorite percentages when the chlorite 003 peak could not be used.

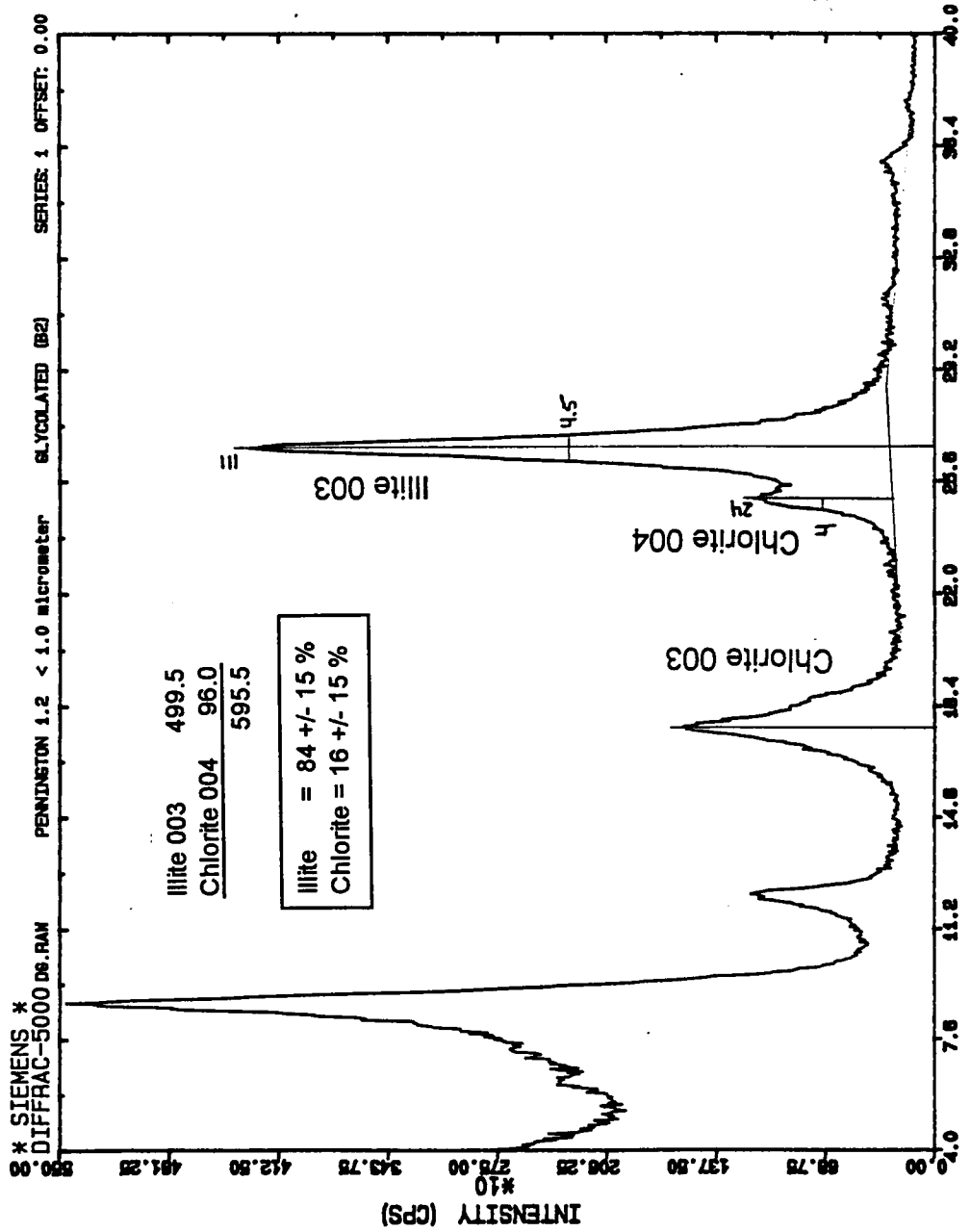
* SIEMENS *
DIFFRAC-5000 DG.RAW
PENNINGTON 1.2 < 1.0 micrometer GLYCOLATED (B2)
SERIES: 1 OFFSET: 0.00
INTENSITY (CPS)
*10
TWO - THETA (DEGREES)
Illite 003
Chlorite 004
Chlorite 003
Illite 003 499.5
Chlorite 004 96.0
595.5
Illite = 84 +/- 15 %
Chlorite = 16 +/- 15 %

Figure 10

loading, was removed by outgassing under vacuum at 175 °C for 7-9 hrs. Oxygen was obtained from clay samples by reaction with BrF_5 (Clayton an Mayeda, 1963) at 550 °C for 16 hrs, and then converted to carbon dioxide gas for oxygen isotope ratio analysis. Isotope ratios were measured on a fully automated, triple collector, VG903 mass spectrometer, and are reported in standard δ notation as per mil (‰) deviations from Standard Mean Ocean Water (SMOW) (Craig, 1961a). Reference gas was CO_2 liberated from Chihuahuan calcite. In this study, the NBS-28 quartz standard ($\delta^{18}O$ = 9.64 ‰) yielded $\delta^{18}O$ = 9.56 ‰. Precision (standard deviation from the mean of replicate extractions) throughout the experiment was 0.25 ‰ and 0.30 ‰ for NBS-28 and a laboratory feldspar standard, respectively. In all cases, the clay oxygen value reported is the mean of two or more oxygen extractions that had similar oxygen yields. Precision was <.40 ‰ for 100% of the samples and <0.30 ‰ for 80 % of the samples. Results of all isotopic analyses, including those for standards, are given in Appendix C.

CARBONATE ISOTOPE ANALYSIS

Carbonates were only sampled from the Hinton paleosol; the Mauch Chunk and Pennington carbonates were previously analyzed and are reported elsewhere (Mora et al., 1991; Caudill et al., 1992; Driese et al., 1993; and

unpublished data). Large disorthic carbonate nodules taken from unit 4 in the Hinton were thin sectioned and petrographically analyzed to establish that these nodules are pedogenic in origin (see criteria, TABLE 6, Mora et al., 1993). Cathodoluminescence microscopy was used to help determine if any diagenetic recrystallization had occurred. Several rhizoliths (all micritic sheaths) within four different carbonate nodules were identified in thin section and micro-sampled using a dental drill. Powdered samples were heated at 375 °C for 1hr to remove organics, reacted for 12hrs with 100 % H_3PO_4 at 25 °C (McCrea, 1950), and then analyzed on the VG903 mass spectrometer. All samples analyzed are reported in standard δ notation relative to PDB and SMOW. Precision for all samples, including the Chihuahuan calcite standard was +/- 0.2 ‰. All isotopic values are given in Appendix D.

K/Ar AGE DATING

Potassium/Argon age dating was performed to determine the timing of illite formation. Four samples of the smallest size fraction and one sample of the largest size fraction were analyzed to establish diagenetic and detrital ages, respectively. K/Ar analyses were performed by Dr. W. Crawford Elliott at Case Western Reserve University. Methods used are outlined in Elliott and Aronson (1987).

VIII. RESULTS

CLAY SIZE POPULATIONS

Each of the paleosols studied has unique particle size distributions. Based on the results of the particle size analyses, three particle-size ranges were isolated from the Mauch Chunk and Hinton paleosols, and two were chosen for the Pennington. All Mauch Chunk samples were separated into > 3.0 μm, 1-3 μm, and < 1.0 μm. Limited sample supply of Mauch Chunk samples made size separations designed to obtain the finest size population (0.2 μm) in the Mauch Chunk samples unreasonable. There was not sufficient quantities of this size fraction for XRD and oxygen isotope analyses. The finest split in the Mauch Chunk was therefore < 1.0 μm to isolate a clay population roughly 0.5 μm in size. Hinton sample H.3 was separated into > 2.0 μm, 0.5-2.0 μm, and < 0.5 μm. H2.2 was separated into >2.0 μm, 0.8-2.0 μm, and < 0.8 μm. Hinton "parent" material (HP) was separated into 1.0-5.0 μm and < 1.0 μm. Volumetrically, the Pennington samples were the finest grained with a bulk of the clays being < 1.0 μm in size. All Pennington samples were separated into 1.0-5.0 μm and < 1.0 μm fractions.

MINERALOGY

The mineralogy of the three paleosols was very consistent. Illite, chlorite, and quartz make up the largest size fraction, whereas the smallest

size fraction is composed only of illite and chlorite. Very minor amounts of quartz contamination do exist in samples PP, HP (Appendix B). The decrease in intensity of the quartz peaks below XRD detection limits with decreasing size fraction is illustrated in Figure 11.

Estimates of the percent of illite in the smallest size fraction was >75% in all three paleosols (TABLE 1). Estimated illite percentages were consistently greater in the Pennington clays. Plotting of the < 1.0 μm illite 002 and 003 peaks on Srodon's (1984) diagram indicates that illite in each paleosol is discrete illite/smectite (Fig.12), although small percentages (<5%) of smecitite layers may be in some of these samples. The higher sensitivity parameters used by Srodon to identify these smectitic components could not be used in this study, primarily because of different sample mounting procedures. The °$\Delta 2\theta$ parameter used by Moore and Reynolds (1989) showed good agreement with the Srodon plot. The °$\Delta 2\theta$ was >8.38 for every sample, which actually falls off of Moore and Reynold's (1989) table 7.3 towards a >90 % illitic illite/smectite (closer to discrete illite/smectite).The Reichweite ordering for all of these samples is R3.

Comparison of the illite 001 peak width at half peak height, supports the relative depths of burial estimated for each paleosol (Fig. 13). The

Figure 11. Typical size fraction comparison showing the decrease in intensity of quartz peaks below detection limits in the smallest size fraction. The decrease in quartz peak intensity is best illustrated by the 20.9 20 peak (labelled Q).

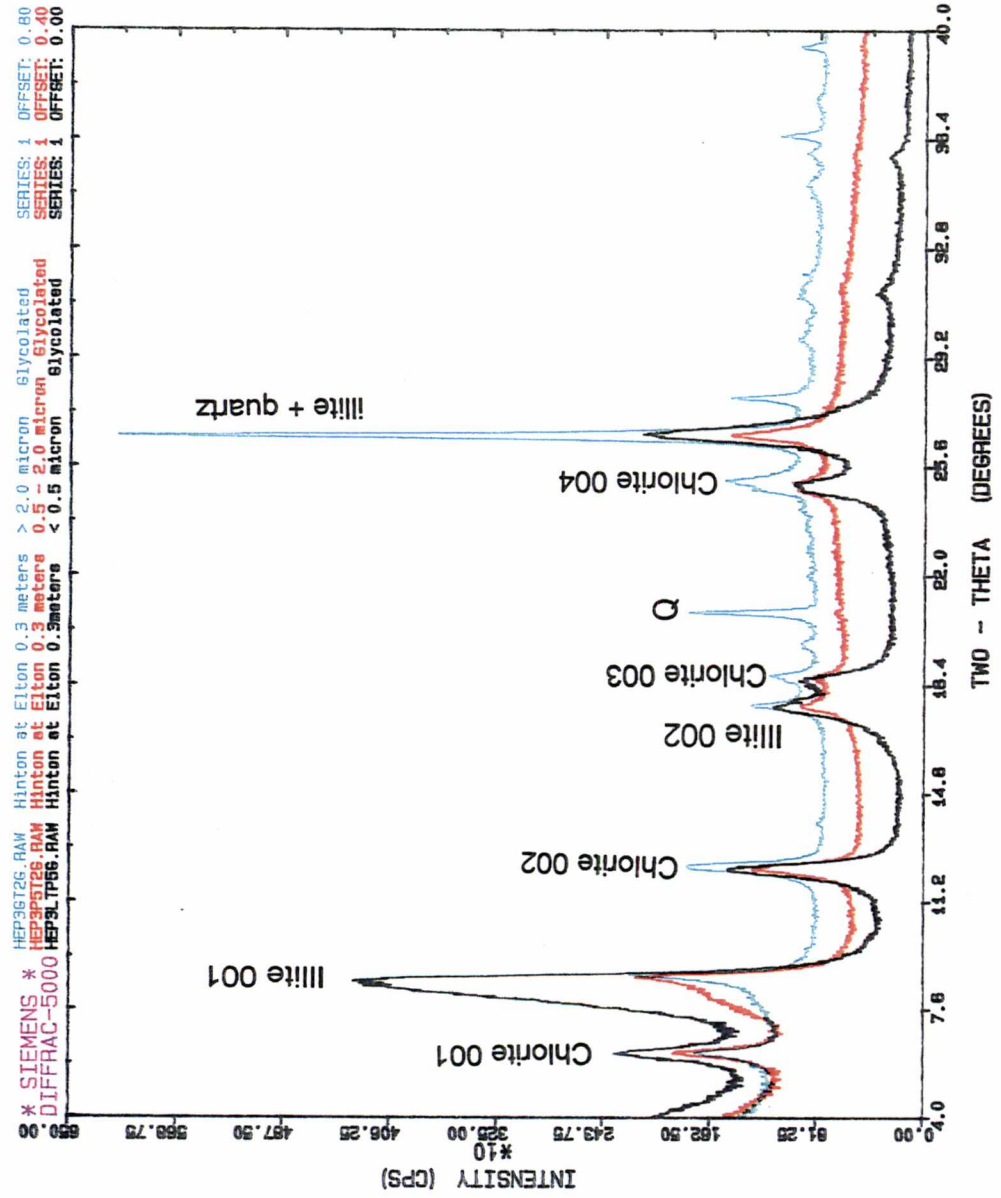
* SIEMENS *
DIFFRAC-5000
HEP3GT26.RAW Hinton at Elton 0.3 meters > 2.0 micron Glycolated
HEP3P5T26.RAW Hinton at Elton 0.3 meters 0.5 - 2.0 micron Glycolated
HEP3LTP56.RAW Hinton at Elton 0.3meters < 0.5 micron Glycolated
SERIES: 1 OFFSET: 0.80
SERIES: 1 OFFSET: 0.40
SERIES: 1 OFFSET: 0.00
Illite + quartz
Chlorite 004
Q
Chlorite 003
Illite 002
Chlorite 002
Illite 001
Chlorite 001
INTENSITY (CPS)
*10
TWO - THETA (DEGREES)

Figure 11

Table 1: Summary of mineralogical data.

Sample	Size fraction	Mineralogy	%Illite* 003/003	%Illite** 003/004
M23	< 1.0 μm	Chlorite, Illite	80 +/- 15%	79 +/- 15%
M21	< 1.0 μm	Chlorite, Illite	88 +/- 15%	85 +/- 15%
M16	< 1.0 μm	Chlorite, Illite	81 +/- 15%	81 +/- 15%
M11	< 1.0 μm	Chlorite, Illite	90 +/- 15%	85 +/- 15%
H.3	< 0.5 μm	Chlorite, Illite	87 +/- 15%	74 +/- 15%
H2.2	< 0.8 μm	Chlorite, Illite	89 +/- 15%	74 +/- 15%
HP	< 1.0 μm	Chlorite, Illite	85 +/- 15%	67 +/- 15%
P.3	< 1.0 μm	Chlorite, Illite	98 +/- 15%	86 +/- 15%
P1.2	< 1.0 μm	Chlorite, Illite	NA***	80 +/- 15%
P1.5	< 1.0 μm	Chlorite, Illite	NA***	79 +/- 15%
PP	< 1.0 μm	Chlorite, Illite	94 +/- 15%	57 +/- 15%

* illite percentages estimated using the peak areas of the illite 003 and the chlorite 003 peaks.

** illite percentages estimated using the peak areas of the illite 003 and the chlorite 004 peaks.

*** Chlorite 003 peaks could not be used for measurements.

Figure 12. Plot of the average illite 002 and 003 peak positions on Srodon's (1984) diagram. All samples, with the exception of one Hinton samples, plotted in the discrete illite field. Possible sources of error for the Hinton samples are sample mounting problems or slight quartz contamination.

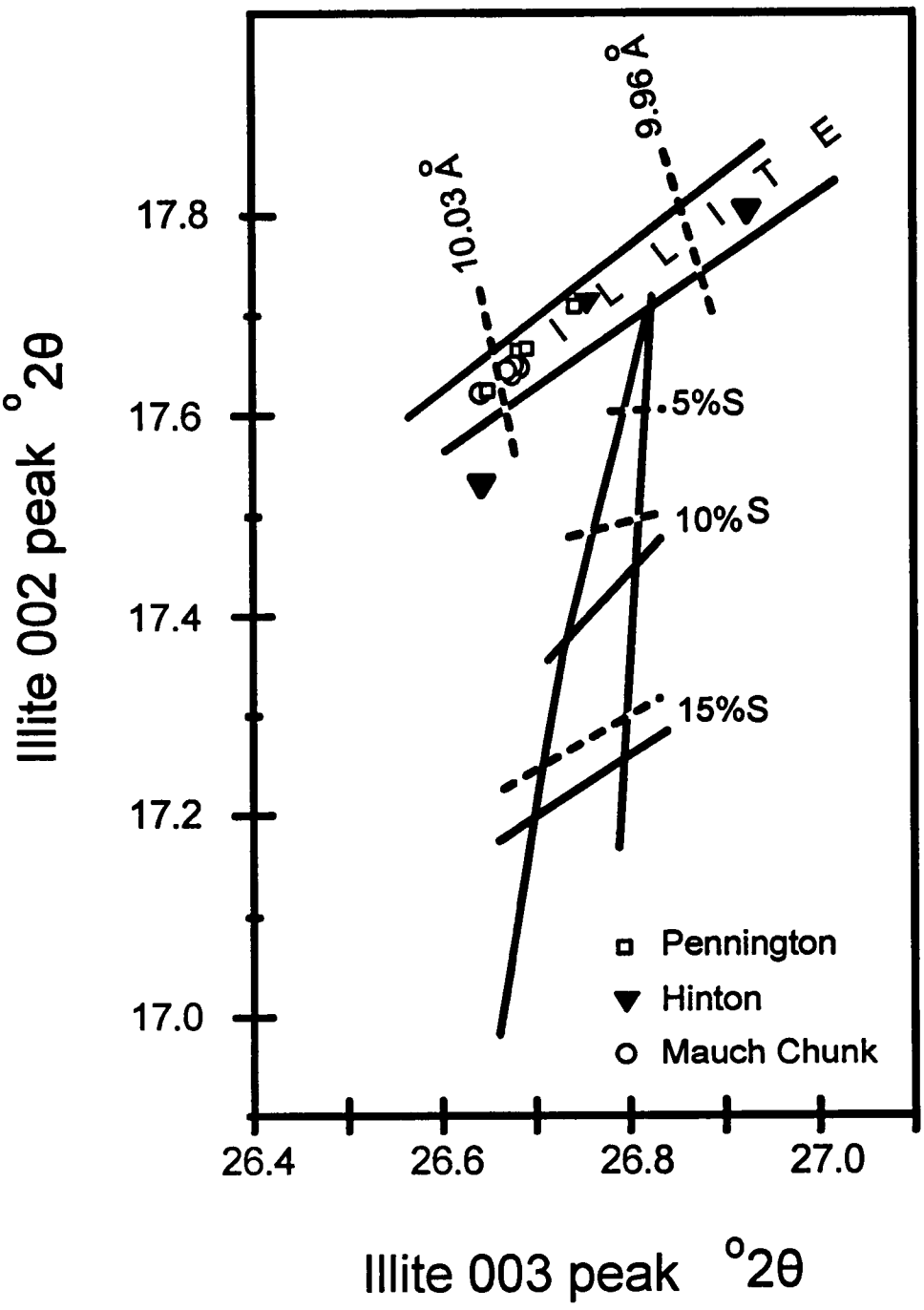
17.8
17.6
17.4
17.2
17.0
26.4
26.6
26.8
27.0
Illite 002 peak °2θ
Illite 003 peak °2θ
10.03 Å
9.96 Å
5%S
10%S
15%S
Pennington
Hinton
Mauch Chunk

Figure 12

Figure 13. X-ray diffraction plot illustrating the differences in the illite 001 peak width at half peak height. The relative depths of burial for each paleosol is supported by the increase in sharpness of the illite 001 peak from the Pennington to the Mauch Chunk.

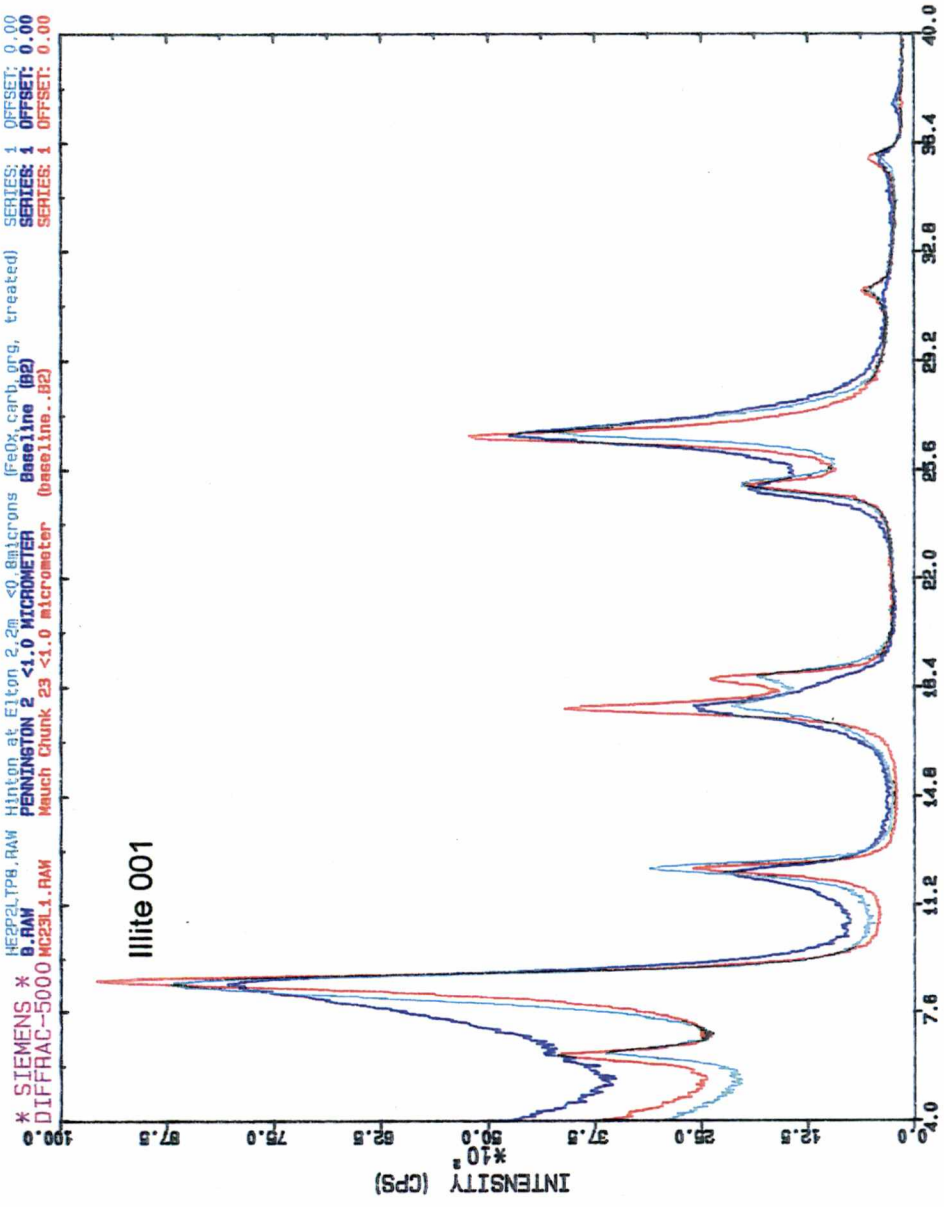
* SIEMENS *
DIFFRAC-5000
HE2P2LTP8.RAW
8.RAW
MC23L1.RAW
Hinton at Elton 2.2m <0.8microns (FeOx,carb,org, treated)
PENNINGTON 2 <1.0 MICROMETER
Mauch Chunk 23 <1.0 micrometer
Baseline (B2)
(baseline..B2)
SERIES: 1 OFFSET: 0.00
SERIES: 1 OFFSET: 0.00
SERIES: 1 OFFSET: 0.00
Illite 001
INTENSITY (CPS)
*10³
100.0
87.5
75.0
62.5
50.0
37.5
25.0
12.5
0.0
4.0
7.6
11.2
14.8
18.4
22.0
25.6
29.2
32.8
36.4
40.0
TWO - THETA (DEGREES)

Figure 13

Mauch Chunk illite has the sharpest 001 peak; the Pennington illite has the widest 001 peak.

CLAY OXYGEN ISOTOPES

Clay oxygen values show a trend of being more negative in more deeply buried paleosols (Fig. 14). Mean values recorded for the Pennington, Hinton, and Mauch Chunk are +17.2 ‰, +15 ‰, and +12.2 ‰ (SMOW), respectively. The $\delta^{18}O$ value for illite from paleosol "parent" material in the Pennington and Hinton Formation paleosols did not differ from the $\delta^{18}O$ of clay samples taken from the paleosols. A limited supply of sample material precluded the separation of chlorite from illite by magnetic separation. Attempts to remove chlorite by chemical treatments were unsuccessful. These experiments are described in Appendix E. Therefore, the isotopic compositions reported here for "illite" include a mixture of illite and chlorite. The possible effects of chlorite are further examined in the discussion below.

CARBONATE OXYGEN ISOTOPES

Petrographic analysis of Hinton carbonates indicated that these nodules were pedogenic in nature. All nodules are composed primarily of rhizoliths in the form of concentric micritic sheaths. In several instances, organic material was preserved in the core of these concentric rings.

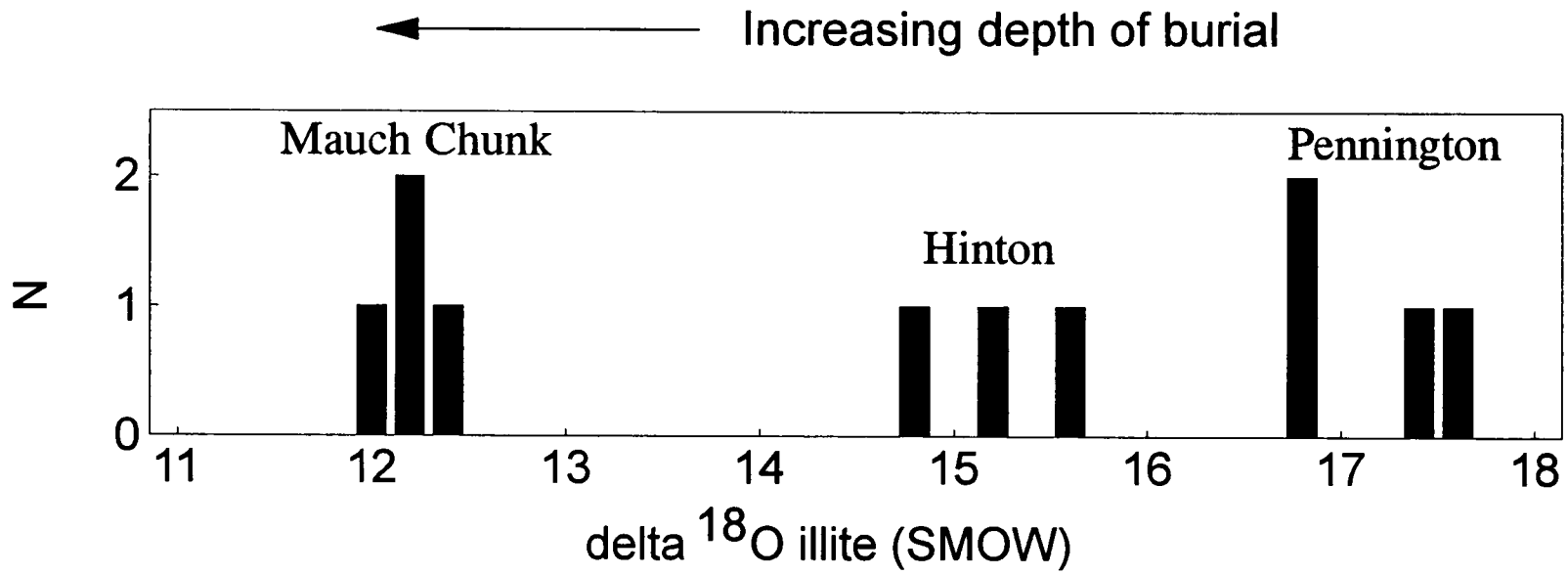

Figure 14. Clay oxygen compositions illustrating ^{18}O depletion with increased depth of burial. Note that "parent" material in both the Pennington and Hinton paleosols have similar oxygen compositions to actual paleosol samples.

The average O-isotope composition of Hinton pedogenic calcite was +18.6 ‰ (SMOW). When this value is compared to the previously measured Pennington and Mauch Chunk carbonates, they exhibit the same trend found in the paleosol clays: depletion in ^{18}O with increased depths of burial (Fig. 15).

K/Ar AGE DATING

The results of the K/Ar analysis are summarized in Table 2. The large size fraction (sample P1.2 > 2 μm) yielded an age of 382 +/- 6 Ma (Fig.16). This age is older than late Chesterian time and indicates the illite in the coarse size fraction is detrital, formed prior to the time of deposition. Because active pedogenesis was coeval with the time of deposition, a "pedogenic" age is bracketed as being late Chesterian time (Fig. 16). All samples composed of the < 1.0 μm size fraction had ages younger than late Chesterian time, which indicates that illite < 1.0 μm in size was produced in the diagenetic environment after active pedogenesis (deposition). Diagenetic ages for the < 1.0 μm size fraction supports the hypothesis that this size fraction was authigenically produced. The possibility of some detrital contamination occurring in the < 1.0 μm size fraction is addressed in the discussion.

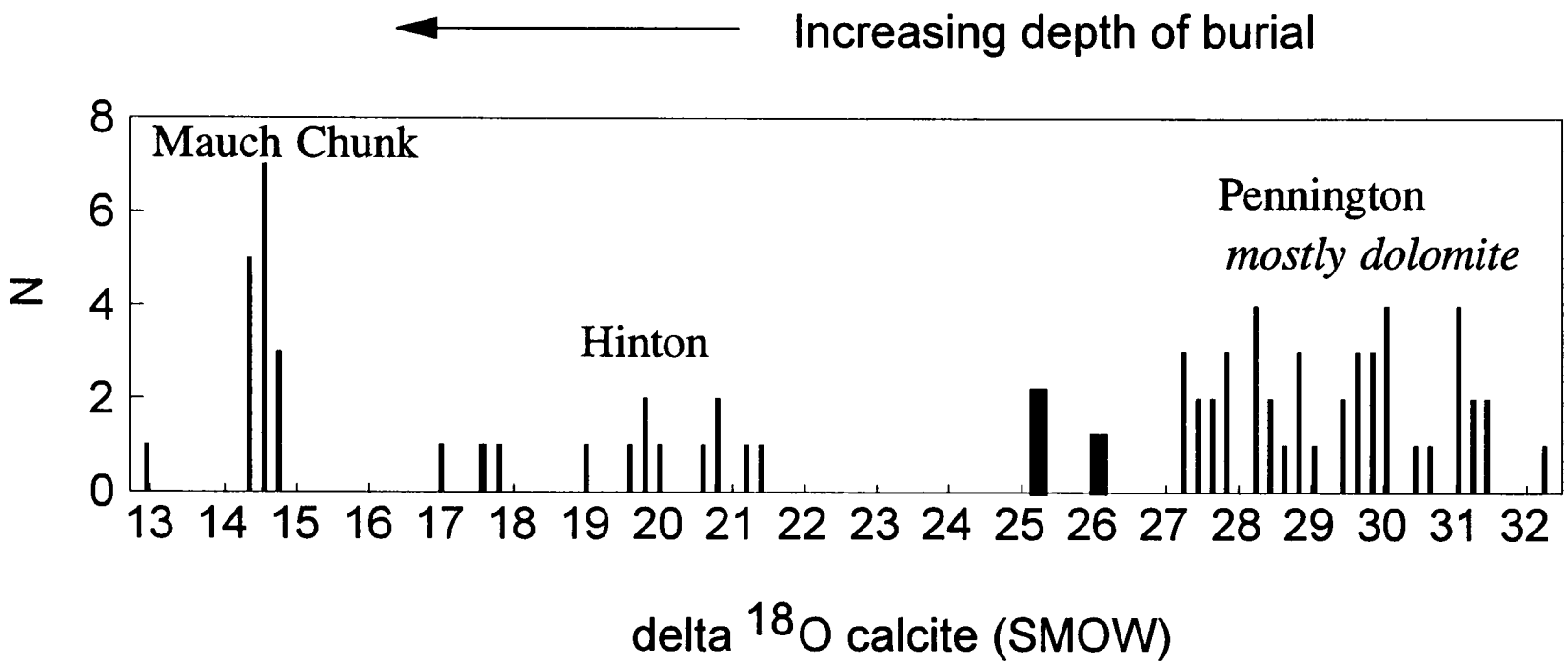

Figure 15. Carbonate oxygen compositions illustrating the same ^{18}O depletion trend as clay oxygen values with increasing depth of burial. Pennington carbonate oxygen compositions used in this study are indicated by the bolded bars (25 and 26 SMOW), which were for calcite found near the bottom of the paleosol. Data for the Mauch Chunk and Pennington are from Mora et. al., (1993).

TABLE 2: Summary of K/Ar Analysis

SAMPLE	K_2O (%)	^{*40} Ar rad (%)	^{*40} Ar mole/gm ($x10^{-9}$)	K-Ar age (Ma)
H.3 (<0.5μm)	5.558	94.04	2.770	317 +/- 7
M11 (<1.0μm)	7.209	96.79	3.301	293 +/- 7
P.3 (<1.0μm)	5.905	92.04	2.615	282 +/- 7
P1.5 (<1.0μm)	5.412	91.10	2.312	275 +/- 7
P1.2 (>2.0μm)	3.360	91.45	2.508	382 +/- 7
LP6 biotite *	12.40	91.13	1.901	122 +/- 3

* LP6 biotite is a interlaboratory standard at Case Western Reserve University. LP6 biotite has an accepted value of 19.30×10^{-10} mol ^{*40}Ar/g (Odin, 1982).

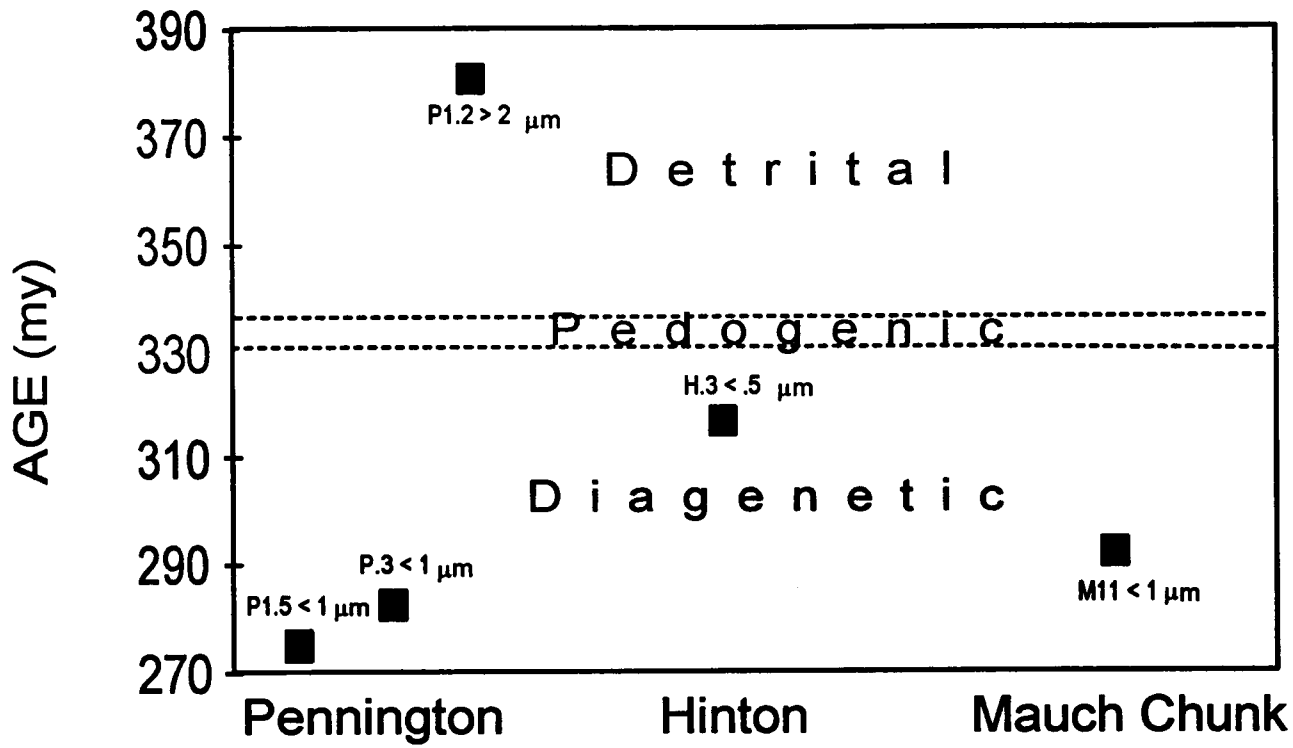

Figure 16. Plot of illite K/Ar age dates which show the smallest size fraction yield diagenetic ages. Diagenetic ages support the hypothesis that illite in the smallest size fraction was authigenically produced during the smectite-to-illite transition.

IX. DISCUSSION

The presence of predominantly discrete illite in the < 1.0 μm size fraction indicates that extensive illitization has occurred in each of the paleosols studied. Because vertic features, characteristic of the macromorphology of these paleosols, require a large, chiefly smectitic, clay component for their formation, it is assumed that the < 1.0 μm illites in these paleosols were primarily produced authigenically during the smectite-to-illite transition. The physicochemical conditions of the environment(s) which best explain the measured oxygen isotopic compositions of calcite and illite were determined using K/Ar age dating (Fig 16), calculated calcite-illite O-isotope equilibration temperatures (Fig. 17), and calculated fluid evolution curves, which show the oxygen isotope evolution of pore fluids in equilibrium with average measured illite and calcite $\delta^{18}O$ values (Figs. 18 - 23). K/Ar age dating potentially records the time of illite formation as potassium (usually from detrital K-feldspar and micas) is incorporated into illite and ^{40}Ar is lost (Faure, 1986). Isotopic equilibration temperatures (Fig. 17) were calculated using measured $\delta^{18}O$ values and the fractionation factors of Savin and Lee (1988; illite-H_2O) and Friedman and O'Neil (1977; calcite-H_2O). Oxygen isotope fluid evolution curves were created for the range of temperatures that each paleosol may have experienced. Fluid evolution curves were calculated using the average measured oxygen value

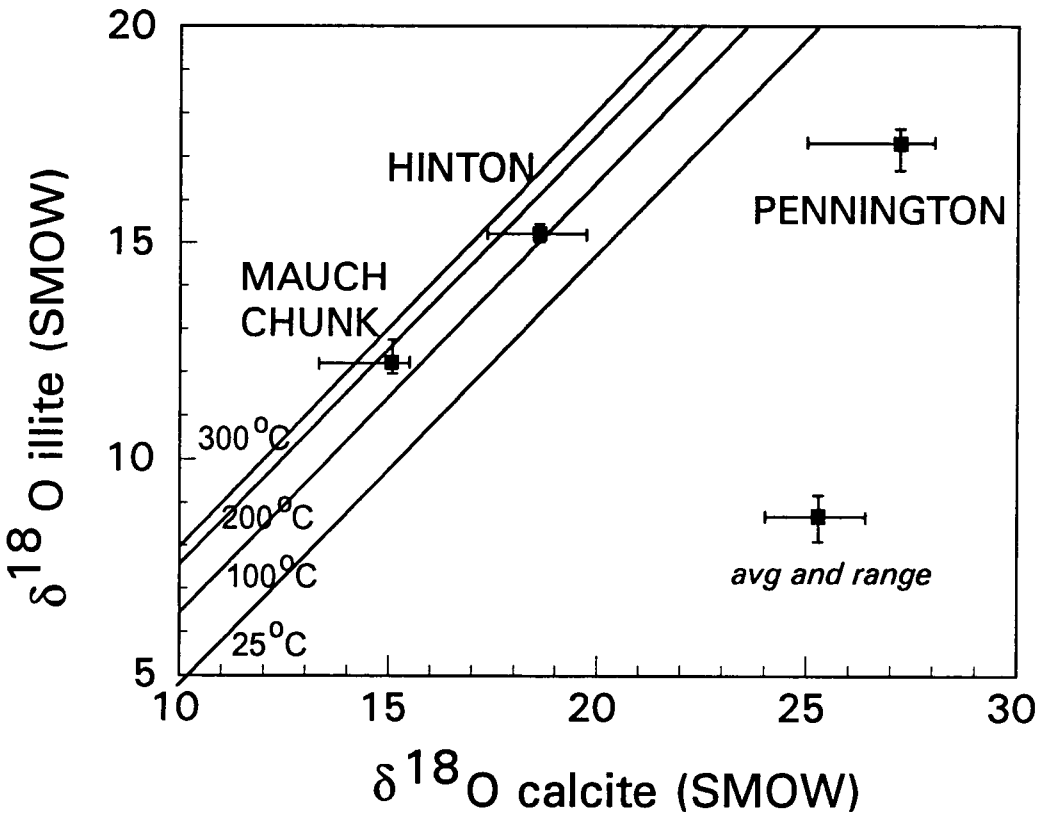

Figure 17. delta-delta plot showing calculated illite-carbonate equilibration temperatures. Isopleths were generated using the illite-water fractionation factor of Savin and Lee (1988) and the calcite-water fractionation factor of Friedman and O'Neil (1977). Note that Pennington clays and carbonates do not approach O-isotope equilibrium at any reasonable geologic temperature.

Figure 18. Mauch Chunk calcite-based oxygen isotope fluid evolution curve. The fluid evolution curve (the line) represents the oxygen isotope composition of a fluid that would have been in isotopic equilibrium with the measured calcite value. If the fluid evolution curve passes through a given environment (boxes), it indicates that calcite is consistent with having obtained its measured oxygen value in that environment (under the conditions defined by that environment).

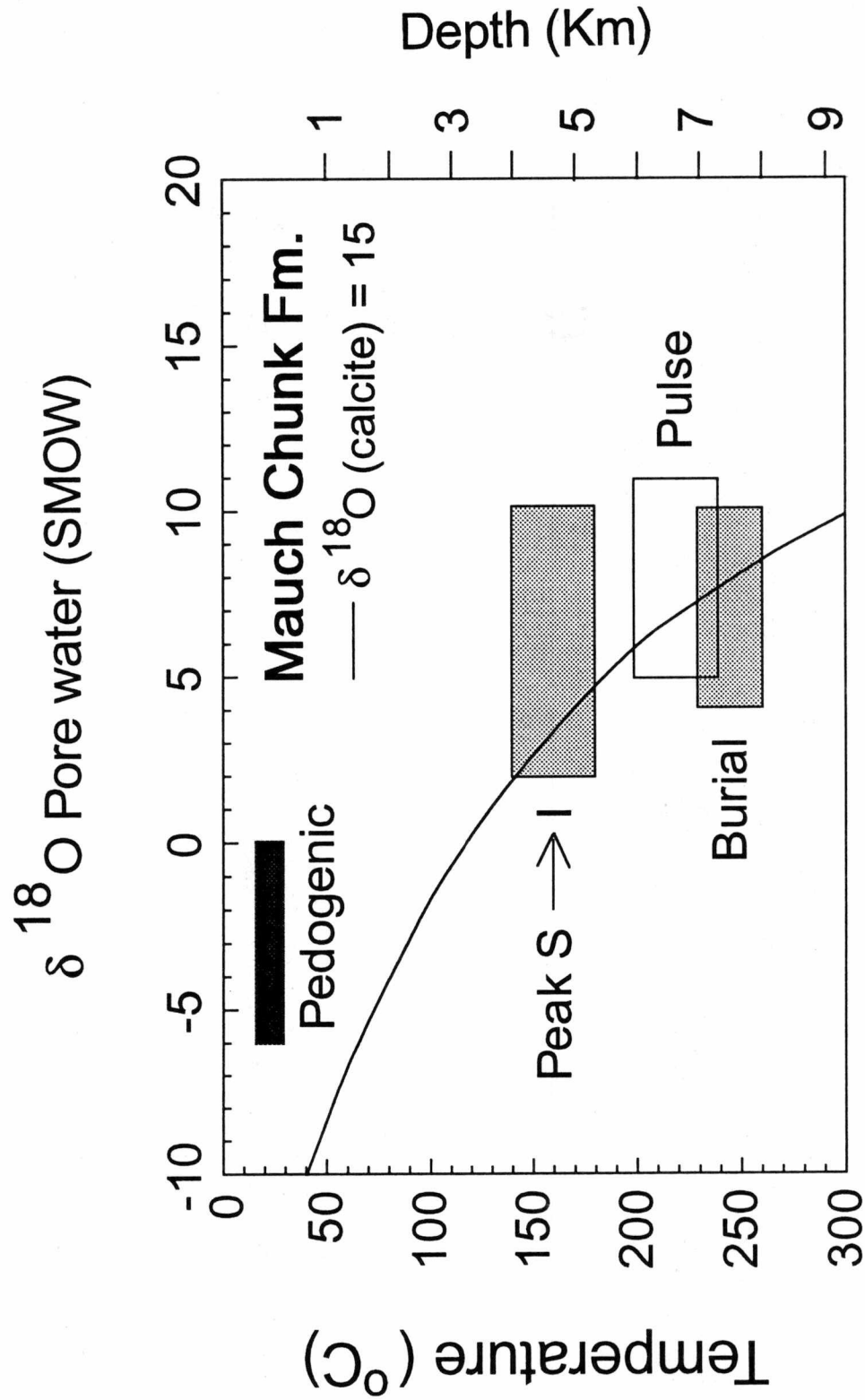
Depth (Km)
1
3
5
7
9
δ 18O Pore water (SMOW)
-10
-5
0
5
10
15
20
Temperature (°C)
0
50
100
150
200
250
300
Mauch Chunk Fm.
— δ 18O (calcite) = 15
Pedogenic
Peak S → I
Pulse
Burial

Figure 18

Figure 19. Mauch Chunk illite-based oxygen isotope fluid evolution curve. The fluid evolution curve (solid line) represents the oxygen isotope composition of a fluid that would have been in isotopic equilibrium with the measured illite value. The dashed and dotted lines are fluid evolution curves corrected for estimated chlorite contamination (average of 15 % chlorite for the Mauch Chunk). The different corrections are explained in the text. Not shown is a chlorite corrected curve where chlorite contamination was estimated to be as great as 50 %. The 50 % chlorite corrected curve fell just to the right of the detrital corrected (dotted) curve and did not change the interpretation of the isotopic data. If a fluid evolution curve passes through a given environment (boxes), it indicates that illite is consistent with having obtained its measured oxygen value in that environment (under the conditions defined by that environment).

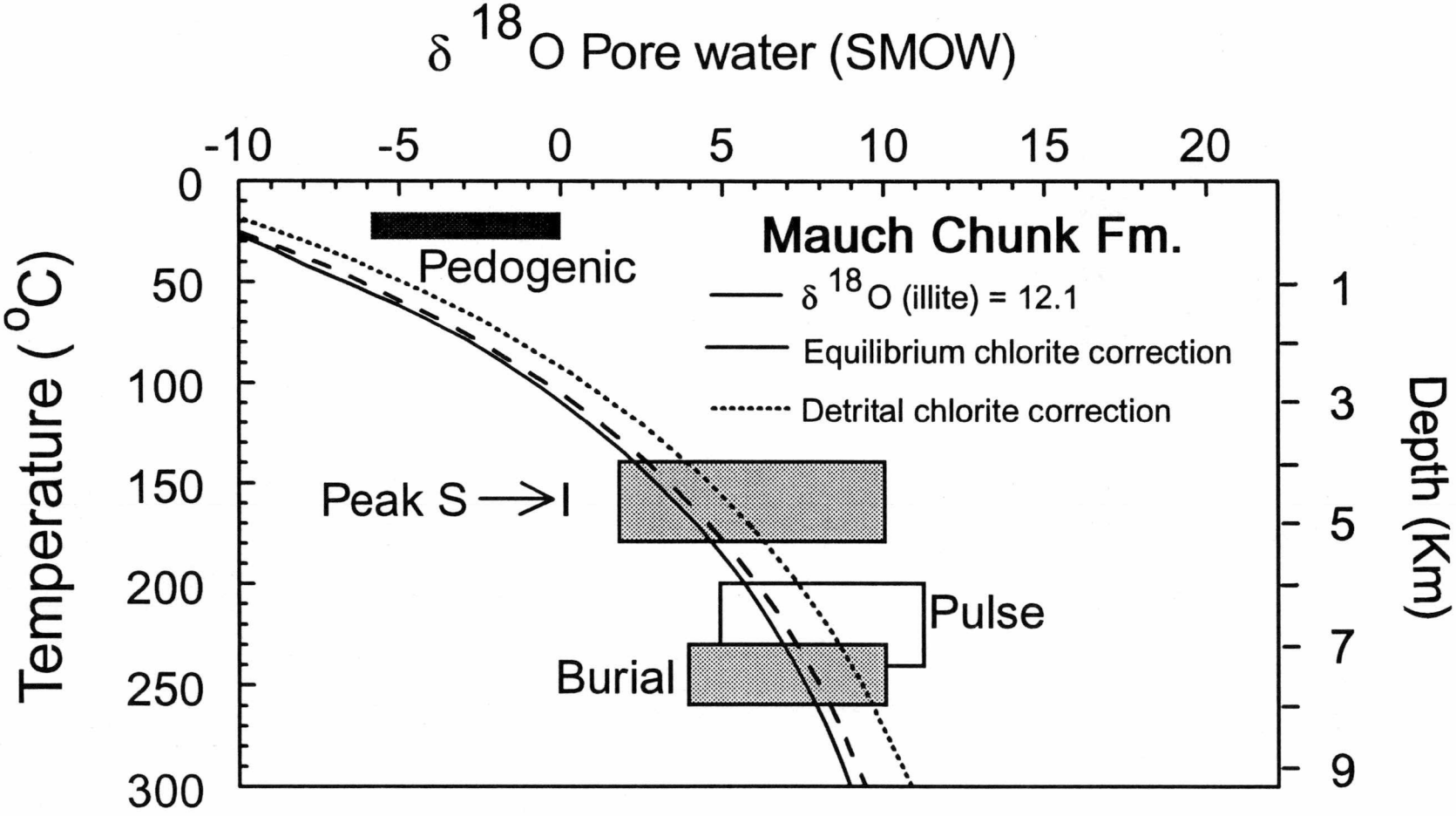
δ 18O Pore water (SMOW)
-10
-5
0
5
10
15
20
0
50
100
150
200
250
300
Temperature (°C)
Pedogenic
Mauch Chunk Fm.
δ 18O (illite) = 12.1
Equilibrium chlorite correction
Detrital chlorite correction
Peak S → I
Pulse
Burial
1
3
5
7
9
Depth (Km)

Figure 19

Figure 20. Hinton calcite-based oxygen isotope fluid evolution curve. The fluid evolution curve (the line) represents the oxygen isotope composition of a fluid that would have been in isotopic equilibrium with the measured calcite value. If the fluid evolution curve passes through a given environment (boxes), it indicates that calcite is consistent with having obtained its measured oxygen value in that environment (under the conditions defined by that environment).

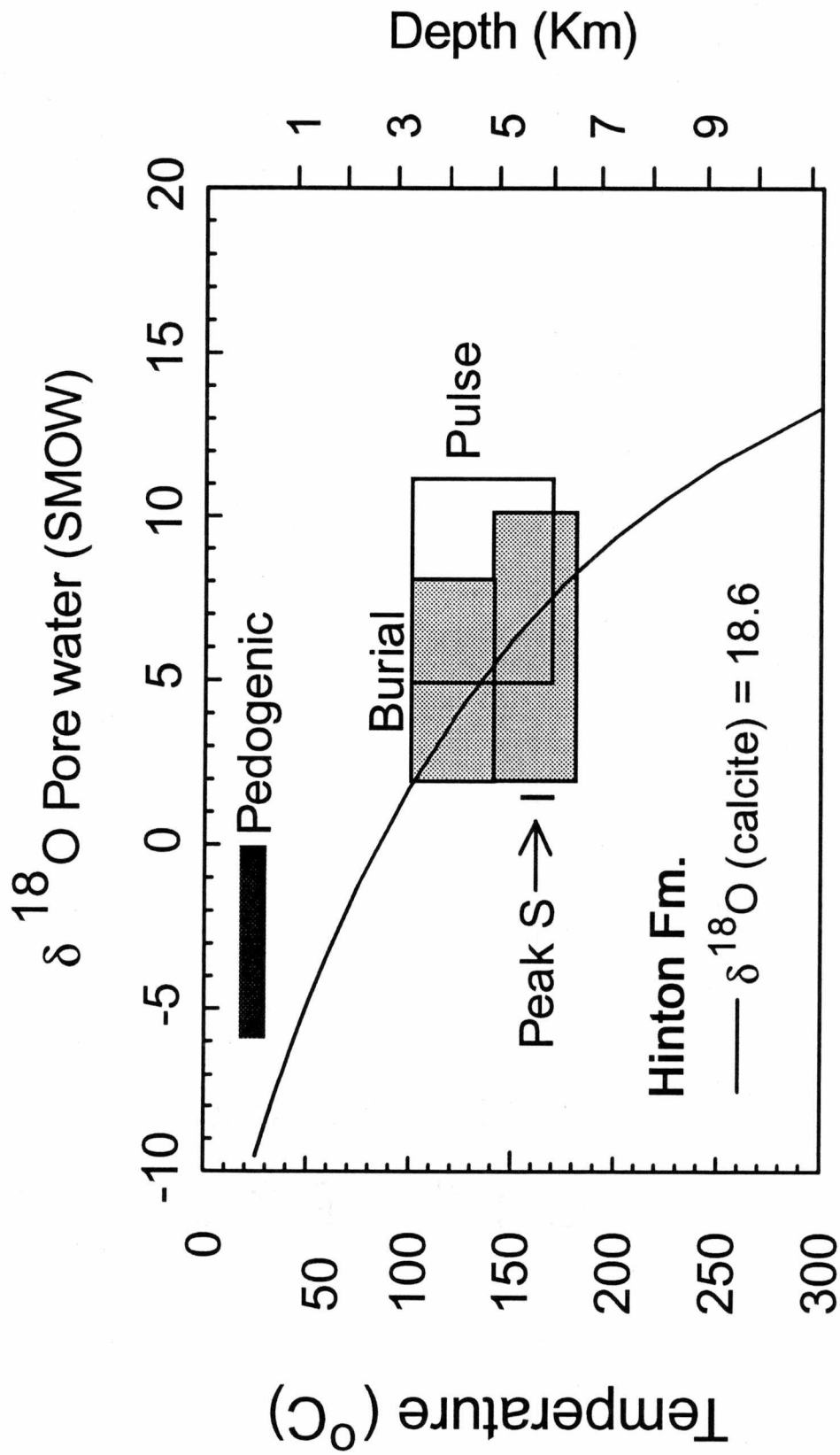
Depth (Km)
1
3
5
7
9
δ 18O Pore water (SMOW)
-10
-5
0
5
10
15
20
Temperature (°C)
0
50
100
150
200
250
300
Pedogenic
Burial
Pulse
Peak S → I
Hinton Fm.
δ 18O (calcite) = 18.6

Figure 20

Figure 21. Hinton illite-based oxygen isotope fluid evolution curve. The fluid evolution curve (solid line) represents the oxygen isotope composition of a fluid that would have been in isotopic equilibrium with the measured illite value. The dashed and dotted lines are fluid evolution curves corrected for estimated chlorite contamination (average of 13 % chlorite for the Hinton). The different corrections are explained in the text. Not shown is a chlorite corrected curve where chlorite contamination was estimated to be as great as 50 %. The 50 % chlorite corrected curve fell just to the right of the detrital corrected (dotted) curve and did not change the interpretation of the isotopic data. If a fluid evolution curve passes through a given environment (boxes), it indicates that illite is consistent with having obtained its measured oxygen value in that environment (under the conditions defined by that environment).

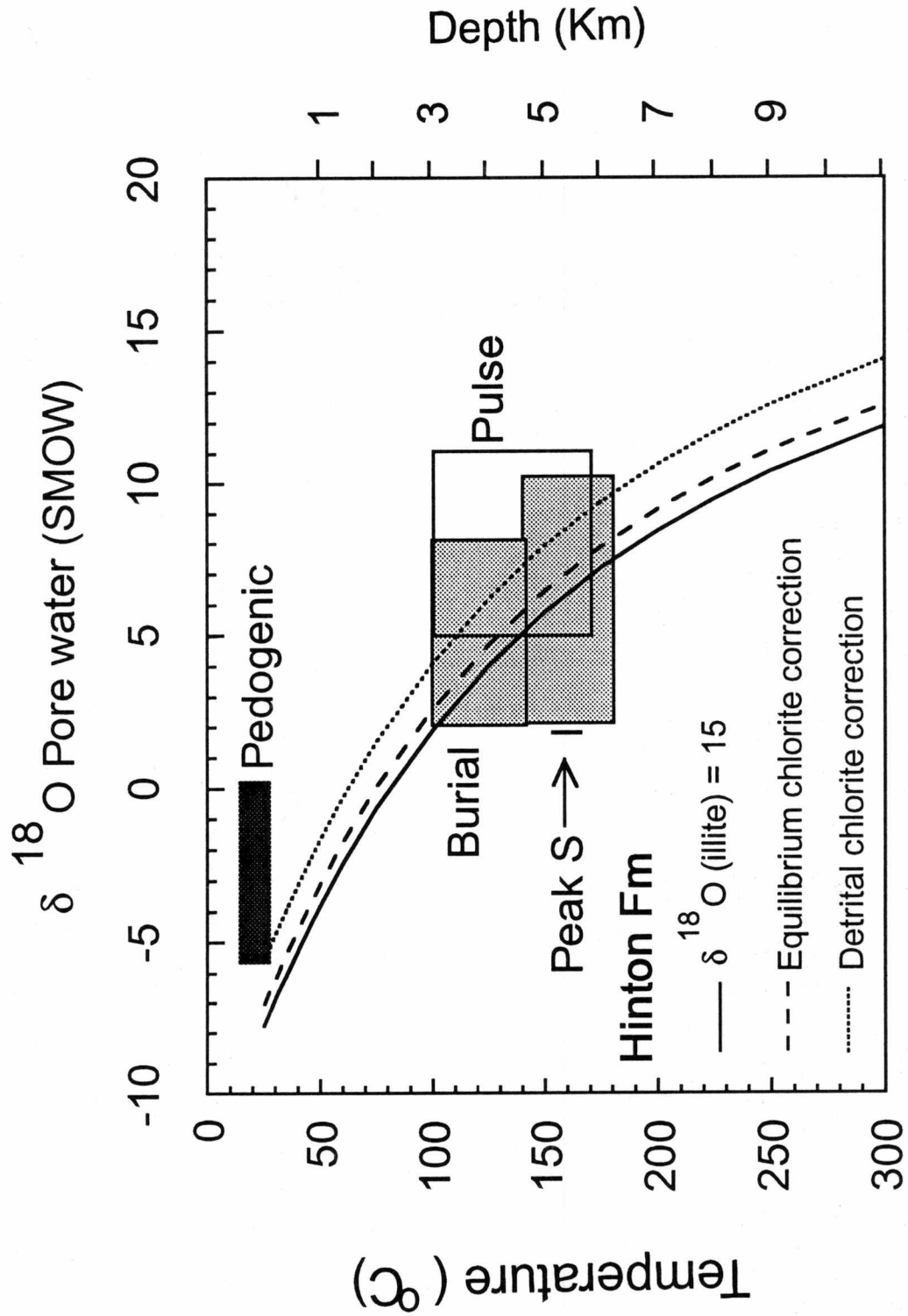
Depth (Km)
1
3
5
7
9
δ 18O Pore water (SMOW)
-10
-5
0
5
10
15
20
Temperature (°C)
0
50
100
150
200
250
300
Pedogenic
Burial
Pulse
Peak S⟶ I
Hinton Fm
δ 18O (illite) = 15
Equilibrium chlorite correction
Detrital chlorite correction

Figure 21

Figure 22. Pennington calcite-based oxygen isotope fluid evolution curve. The fluid evolution curve (the line) represents the oxygen isotope composition of a fluid that would have been in isotopic equilibrium with the measured calcite value. If the fluid evolution curve passes through a given environment (boxes), it indicates that calcite is consistent with having obtained its measured oxygen value in that environment (under the conditions defined by that environment).

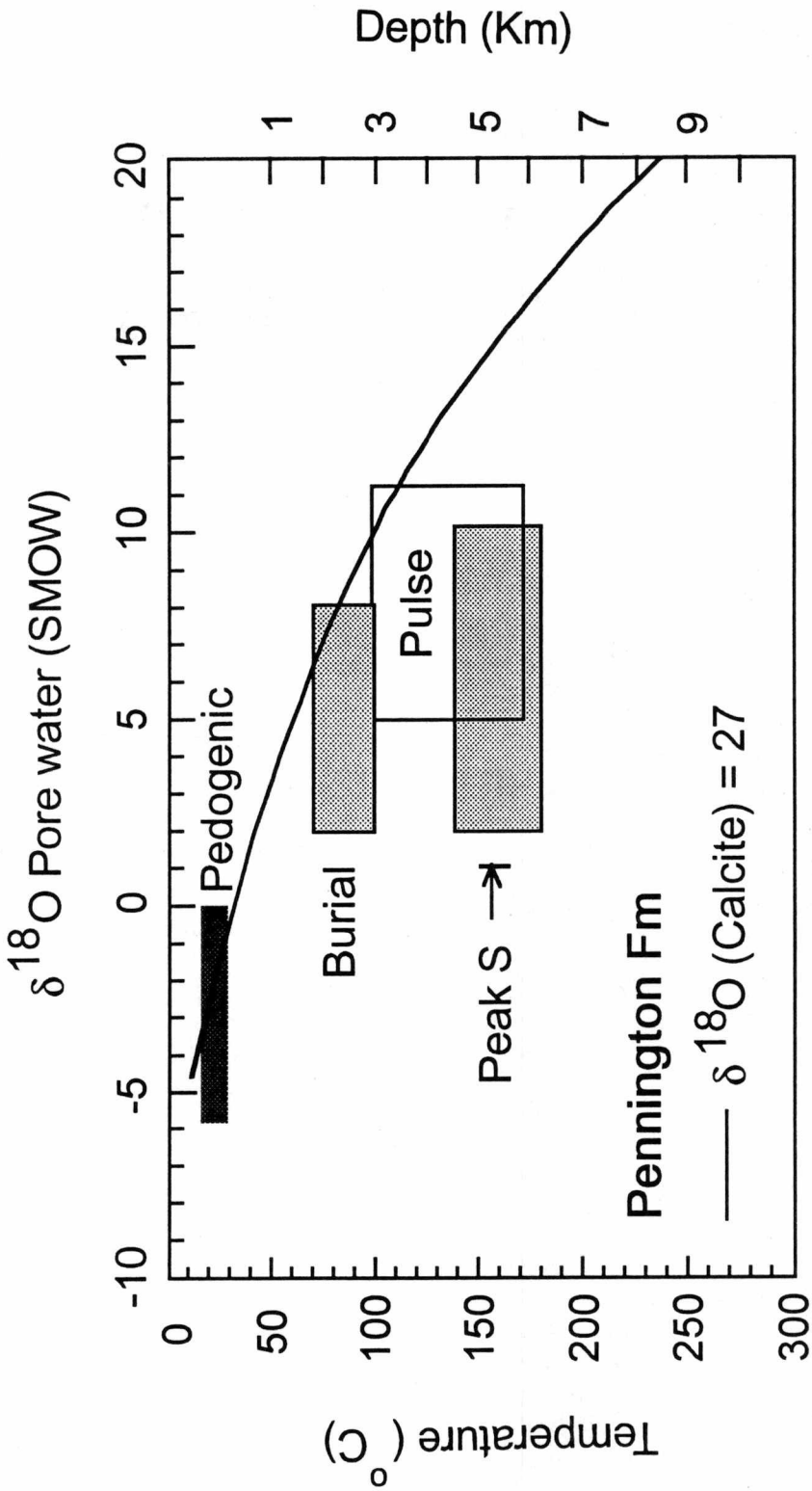
Depth (Km)
1
3
5
7
9
δ18O Pore water (SMOW)
20
15
10
5
0
-5
-10
Pedogenic
Burial
Pulse
Peak S
Pennington Fm
δ18O (Calcite) = 27
Temperature (°C)
0
50
100
150
200
250
300

Figure 22

Figure 23. Pennington illite-based oxygen isotope fluid evolution curve. The fluid evolution curve (solid line) represents the oxygen isotope composition of a fluid that would have been in isotopic equilibrium with the measured illite value. The dashed and dotted lines are fluid evolution curves corrected for estimated chlorite contamination (average of 12 % chlorite for the Pennington). The different corrections are explained in the text. Not shown is a chlorite corrected curve where chlorite contamination was estimated to be as great as 50 %. The 50 % chlorite corrected curve fell just to the right of the detrital corrected (dotted) curve and did not change the interpretation of the isotopic data. If a fluid evolution curve passes through a given environment (boxes), it indicates that illite is consistent with having obtained its measured oxygen value in that environment (under the conditions defined by that environment).

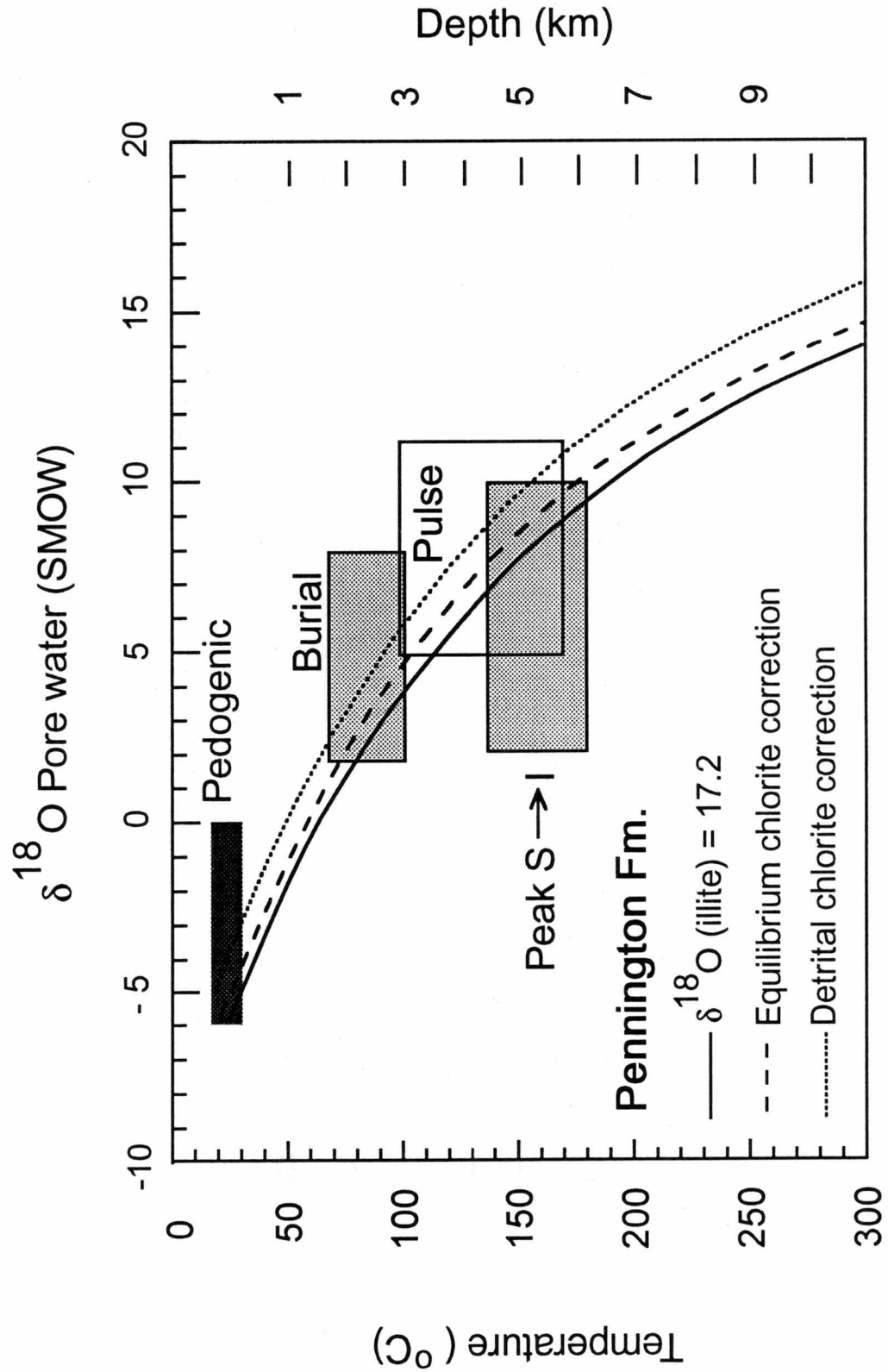
Depth (km)
1
3
5
7
9
δ^{18}O Pore water (SMOW)
-10
-5
0
5
10
15
20
Temperature (°C)
0
50
100
150
200
250
300
Pedogenic
Burial
Pulse
Peak S→I
Pennington Fm.
δ^{18}O (illite) = 17.2
Equilibrium chlorite correction
Detrital chlorite correction

Figure 23

of calcite and "illite" (illite without chlorite contamination removed). Two additional fluid evolution curves were calculated to correct the measured $\delta^{18}O$ for the contribution of oxygen from chlorite. One correction assumes that chlorite was authigenically produced by the smectite-to-illite transition and is therefore in isotopic equilibrium with illite. The other correction assumes all chlorite was detrital and has a $\delta^{18}O$ of +7‰ SMOW, a typical value for chlorite in a regionally metamorphosed rock. Both corrections are based on: 1) average estimated chlorite percentages for each paleosol; 2) the measured $\delta^{18}O$ clay value; and 3) the chlorite-water fractionation factor of Wenner and Taylor (1971). These two approaches reasonably bracket the $\delta^{18}O$ of pure illite in these samples and indicate that the interpretation of these data is insensitive to the chlorite contamination. For example, the interpretations were unaffected assuming as much as 50 % chlorite contamination and an equilibrium chlorite-illite correction, as described above.

Three possible methods of illitization are considered for each of the paleosols examined. Each method corresponds to a different environment in which calcite and illite may have acquired their measured oxygen values. The environments are defined by reasonable temperature and $\delta^{18}O$ pore fluid estimates for individual paleosols. A summary of the temperature and $\delta^{18}O$ compositions of these environments in each of the paleosols is given in

Table 3; references used to constrain temperature and fluid compositions are given in Table 4 . Explanations of each of the environments are as follow:

PEDOGENIC ENVIRONMENT: Laboratory experiments done by Mamy and Gaultier (1975) and more recently by Eberl et al. (1986) have shown that, in the presence of a potassium source, wetting and drying cycles can cause illitization of smectite at near-surface conditions. The study done by Eberl et al. (1986) found that at 30 °C smectites subjected to as many as 100 wet/dry cycles produced randomly interstratified illite/smectite, and occasionally partial R1 ordering. More importantly, they also found that the percentage of illite layers produced was proportional to both the original layer charge of the smectite and to the number of wetting and drying cycles. Wet/dry cycling of smectitic clays is a physical process that is a fundamental characteristic of vertic soils, thus vertic paleosols are likely candidates for the natural production of illite by wetting and drying. The pedogenic environment is defined by illite forming at surface soil temperatures of 15-30°C in the presence of meteoric water having a $\delta^{18}O$ value in the broad range 0.0 to -6.0 ‰ SMOW.

BURIAL ENVIRONMENT: The burial environment includes all temperature and fluid oxygen compositions experienced after the paleosols were covered. However, for the purposes of this study, the burial

TABLE 3: Summary of temperature and $\delta^{18}O$ ranges for the three possible environments of illitization.

ENVIRONMENT	TEMPERATURE RANGE	$\delta^{18}O$ RANGE (SMOW)
Pedogenic	15 - 30 °C	-6.0 to 0.0 ‰
Peak Smectite/Illite	140 - 180 °C	+2.0 to +10 ‰
Pennington Burial	70 - 100 °C	+2.0 to + 8.0 ‰
Pennington Pulse	100 - 170 °C	+5.0 to +11.0 ‰
Hinton Burial	100 - 140 °C	+2.0 to +8.0 ‰
Hinton Pulse	100 - 170 °C	+5.0 to +11.0 ‰
Mauch Chunk Burial	230 -260 °C	+4.0 to +10.0 ‰
Mauch Chunk Pulse	200 - 240 °C	+5.0 to +11.0 ‰

TABLE 4: Summary of references used to define the three environments of illitization. S → I = Smectite-to-illite, PN = Pennington, HN = Hinton, MC = Mauch Chunk

ENVIRONMENT	PARAMETER	REFERENCE	DATA TYPE
Pedogenic	$\delta^{18}O$ & T(°C)	Inferred from modern conditions	
Peak S → I	$\delta^{18}O$ & T(°C)	Eslinger and Savin, 1973b	O-isotope
		Yeh and Savin, 1977	O-isotope
		Yeh, 1980	O-isotope
		Suchecki and Land, 1983	O-isotope
		Eslinger and Yeh, 1986	O-isotope
PN,HN,MC Burial	$\delta^{18}O$	Yeh and Savin, 1977	O-isotope
		Yeh, 1980	O-isotope
		Suchecki and Land, 1983	O-isotope
		Eslinger and Yeh, 1986	O-isotope
PN, HN Burial	T(°C)	Epstein et al., 1977	CAI
		Beaumont et al., 1988	Isopachs
MC Burial	T(°C)	Epstein et al., 1977	CAI
		Bajak, 1981	Fluid inclusion
		Levine, 1986	Coalification
		Beaumont et al., 1988	Isopachs
		Roden and Miller, 1989	Apatite fission
PN,HN,MC Pulse	$\delta^{18}O$	Dorobek, 1989	O-isotope
		Battles, 1993	O-isotope
		Montanez and Read, 1992	O-isotope
PN,HN Pulse	T(°C)	Roedder, 1979	Fluid inclusion
		Hearn et al., 1987	Fluid inclusion
		Battles, 1993	Fluid inclusion
MC Pulse	T(°C)	Orkan and Voight, 1985	Fluid inclusion
		Orkan, 1986	Fluid inclusion
		Hearn et al., 1987	Fluid inclusion
		Dorobek, 1989	Fluid inclusion

environment is divided into two fields, defining peak smectite-to-illite and peak burial conditions. These two fields bracket the physicochemical conditions under which calcite and illite were most likely to have acquired their final oxygen isotope compositions. Temperatures and fluid compositions defining the peak smectite-to-illite field are those that have been commonly observed in several other studies (Tables 3,4). Reasonable maximum burial temperatures were estimated by compiling Conodont Alteration Indices (CAI), vitrinite reflectance, apatite fission track, and fluid inclusion data (Tables 3,4). These peak temperature estimates were typically made by extrapolation through geographic and stratigraphic differences between the location of the paleosols and the location of the field areas in the referenced studies. Isopach data modelled by Beaumont et al. (1987), coupled with appropriate geothermal gradients, were also used to estimate maximum burial temperatures. A surface temperature of 20 °C and a documented geothermal gradient of approximately 30 °C/km for eastern Pennsylvania (Lacazette, 1991; Zhang and Davis, 1993) were used for the Mauch Chunk paleosol. A geothermal gradient of 25 °C/km and surface temperature of 25 °C as suggested by Beaumont et al. (1988) was used for the Hinton and Pennington paleosols. The lower surface temperature for the Mauch Chunk is a function of altitude associated with the Mauch Chunk paleosol's position high on the alluvial plain. The $\delta^{18}O$ value of burial fluids

were estimated for peak thermal conditions based on typical $\delta^{18}O$ enrichment of pore fluids associated with clay dewatering in other shale-rich sequences (Tables 3,4).

FLUID PULSE ENVIRONMENT: The fluid pulse environment accounts for a widespread, well-documented, high-temperature fluid pulse that migrated through much of the Appalachian Basin in response to the Alleghanian orogeny (Table 4). The timing of fluid migration has been constrained to 270-300 Ma by K/Ar age dating of illite in Ordovician K-bentonites (Elliott and Aronson,1987), and $^{40}Ar/^{39}Ar$ age dating of fluid inclusions in authigenic K-feldspars (Hearn et al., 1987). The temperature of these fluids is documented predominantly by fluid inclusion studies (Tables 3,4), which suggest that the fluids were hotter in areas of the basin where burial depths were greatest during the Alleghanian orogeny. A $\delta^{18}O$ range of +5 to +11 SMOW for these fluids was compiled from Dorobek, (1989); Montanez and Read, (1992); and Battles, (1993) (Table 3).

The three environments of illitization are overlaid on the fluid evolution curves in Figures 18-23. If a fluid evolution curve passes through a given environment it indicates that the measured oxygen isotopic composition of illite and/or calcite is consistent with their formation or recrystallization in that environment.

THE MAUCH CHUNK PALEOSOL

Mauch Chunk fluid evolution curves indicate that the $\delta^{18}O$ values of calcite and illite are consistent with their formation or recrystallization in the burial (both peak smectite-to-illite, and peak burial conditions) and/or the fluid pulse environment (Figs. 18,19). Attempts at resolving which of these environments is/are responsible for illitization must consider the timing of orogenic fluid migration in relation to the burial history of this region. Paleomagnetic ages (Van der Voo, 1979; Kent, 1979; Scotese et al. 1982) and vitrinite reflectance data (Levine, 1986) bracket maximum overburden emplacement and anthracite formation to 285-270 Ma. Comparison of this age range to the 270-300 Ma timing of Alleghanian orogenic fluid migration indicates that the fluid pulse was prior to, and/or coeval with maximum burial. This is consistent with Hearn et al's. (1987) findings that authigenic K-feldspars were generated by orogenic fluids both prior to and during the thrusting and folding stages of the Alleghanian orogeny.

The usefulness of K/Ar age dating to resolve the environment of illitzation in the Mauch Chunk is unfortunately lost as a result of burial depths having approached 7-8 km. K/Ar has a blocking temperature of approximately 150 °C in illite/smectites (Crawford Elliott, pers. comm.); which indicates Mauch Chunk illites are only capable of dating the uplift of

this paleosol through the 150 °C isotherm. Apatite fission track data for middle Devonian sediments in the region indicate unroofing began approximately 250 Ma (Roden and Miller, 1989). Mauch Chunk illites should therefore yield ages much younger the measured 290 Ma. The best explanation for this discrepancy overestimate of unroofing is that the Mauch Chunk sample is a mixture of both detrital and authigenic illite. Preliminary XRD analysis of random powder mounts suggest the $< 1.0\ \mu m$ illite size fraction has a detrital (2M) component, but no quantitative measurements have been done.

Hatcher et al. (1989) noted that Alleghanian thrust faults have displaced the youngest preserved rocks in the Alleghanian synorogenic clastic wedges. This temporal relationship indicates that clastic wedge development preceded Alleghanian thrust loading. Therefore, the Mauch Chunk paleosol may have experienced burial sufficient to drive the smectite-to-illite reaction prior to initiation of Alleghanian thrust faulting and orogenic fluid migration. It is widely believed, however, that maximum burial occurred during the interval 285-270 Ma as a result of thrust loading (Levine,1986). Thrust faulting of the Mauch Chunk Formation may have created new pathways for orogenic fluid migration; Oliver (1986) and Battles (1993) demonstrated that orogenic fluids associated with the

Alleghanian orogeny migrated preferentially through thrust planes and more permeable stratigraphic units.

The calculated illite-calcite equilibration temperature of 180 °C (Fig. 17) suggests that Mauch Chunk pedogenic calcite recrystallized and isotopically equilibrated with authigenic illite during clay dewatering and progressive illitization of the surrounding clay matrix in the paleosol. This temperature is most consistent with the peak smectite-to-illite field (Figs. 18,19), which suggests that illite was formed during this transition in the burial environment. If illitization is burial driven, then retention of the 180 °C isotopic equilibration temperature through maximum burial conditions of 230-260 °C suggests that there was little recrystallization/exchange subsequent to clay dewatering. It is not unreasonable for the Mauch Chunk paleosol to have behaved as a closed system following smectite dewatering and compaction. Freeze and Cherry (1979) noted that clays, particularly after burial, are essentially impermeable to fluid flow. Furthermore, Suchecki and Land (1983), in their study of the Great Valley Sequence, found that calcites in mudstones had equilibrated in a nearly closed system with fluids isotopically buffered by the conversion of smectite-to-illite. They also found that calcites in sandstones from similar stratigraphic intervals were depleted in oxygen by later hydrothermal fluids that preferentially moved through the more porous sandstone medium.

Thus, it seems reasonable that burial compaction associated with smectite dewatering may have progressed enough to prevent orogenic fluids from migrating through the Mauch Chunk paleosol.

Oxygen isotope compositions suggest that Mauch Chunk pedogenic calcite recrystallized and equilibrated with authigenic illite during illitization. The initiation of the smectite-to-illite reaction most likely started in the burial environment and was completed in either the fluid pulse and/or burial regimes. Calculated isotopic equilibration temperatures lower than both peak burial and orogenic fluid pulse temperatures, cannot preclude the possibility of illitization having occurred at these higher temperatures. Calculated illite-calcite isotopic equilibration temperatures are very sensitive to slight errors in the $\delta^{18}O$ of either phase. It is also possible that low equilibration temperatures are the result of retrograde recrystallization of calcite, however, no noticeable retrograde recrystallization fabrics are seen in Mauch Chunk carbonates.

THE HINTON PALEOSOL

Calcite and illite in the Hinton paleosol potentially acquired their oxygen isotope composition in the burial and/or fluid pulse environments (Figs. 20,21). Maximum burial temperatures below the illite/smectite K/Ar blocking temperature of 150 °C indicate that K/Ar ages should date the

timing of illite formation. The age determined for the Hinton sample, 322 +/- 7 Ma, is older than expected when compared to the smallest size fractions dated for the Pennington and Mauch Chunk. However, 322 +/- 7 Ma is consistent with both the pulse (Hearn et al., 1987) and burial environments. One possible explanation of the older age for the Hinton sample is detrital contamination, but that seems unlikely because the Hinton sample was composed of the smallest size fraction dated (< 0.5 μm). The older age for the Hinton is probably closer to a "true" age, and suggests that illitization was completed early in the burial history of this paleosol.

A calculated calcite-illite equilibration temperature of 110 °C (Fig. 17) is equally consistent with either of these environments, however, both the illite and calcite fluid evolution curves pass through this temperature within the burial field only (Figs. 20,21). Establishing if illitization was most likely to have occurred in the fluid pulse or burial environment requires some degree of resolution in the timing of fluid pulse relative to burial depths achieved prior to or during the Alleghanian orogeny. The Hinton paleosol is located in an area unaffected by Alleghanian thrust faulting (Fig. 3), indicating that burial of this paleosol was the result of sedimentation only. Peak burial conditions (approximately 4 km, 130 °C) could have reasonably been achieved prior to 300 Ma assuming an average sedimentation rate of .13 mm/yr. Thrust faults to the east of the Hinton paleosol cut across the

youngest preserved sediments of the Pennington-Lee clastic wedge (Hatcher et al., 1989), indicating that peak burial of the paleosol occurred just prior to or during the thrust emplacement stage of the Alleghanian orogeny. Thus, burial-driven illitization of the Hinton paleosol may have progressed far enough to become fairly impermeable to any orogenic fluid pulse; however, as in the case of the Mauch Chunk paleosol, eliminating the possibility of illitization driven by a fluid pulse would require a more precise knowledge of burial depths during the orogenic fluid migration.

THE PENNINGTON PALEOSOL

The isotopic and mineralogic data for the Pennington paleosol are difficult to interpret. Extensive illitization of the Pennington clays to discrete illite is inconsistent with maximum burial depths of < 3 km and temperatures most likely below 80 °C. Furthermore, calcite in the Pennington paleosol appears to retain its original pedogenic oxygen signature (Fig. 22) and does not approach oxygen equilibrium with surrounding illite at any reasonable geologic temperature (Fig. 17). Each of the three possible environments of illitization will be discussed to see which one might best accounts for extensive illitization, without concurrent alteration of $\delta^{18}O$ of pedogenic calcite.

The illite-based oxygen isotope fluid evolution curves indicate that

Pennington illite was potentially formed by repeated cycles of wetting and drying in the pedogenic environment (Fig. 23). Macromorphological features supporting such cycles include preservation of a well-developed basal slickenside, manganese oxide coatings on large arcuate slickensides, redistribution of carbonate nodules to pseudo-anticlines, and the inferred presence of gilgai. The stage II pedogenic carbonate morphology in the Pennington paleosol probably took 8,000 to 15,000 years to develop (Gile et al., 1966; Machette, 1985), suggesting that the Pennington may have experienced thousands and possibly tens of thousands of wetting and drying cycles. Despite the potential for extensive illitization by wetting and drying in the Pennington paleosol, the production of discrete illite/smectite is questionable. Pedogenic illite production accounts for the preservation of pedogenic oxygen isotope values in coexisting calcites, but begs the question as to why the pedogenically produced illite does not approach O-isotope equilibrium with pedogenic calcite. Furthermore, if this kinetic pathway of illitization is solely responsible for the paleosol illites, then the pedogenically unaltered "parent" material for this paleosol should have greater quantities of smectite present. Instead, the paleosol "parent" material is not only extensively illitized (Fig. 12), but also has the identical oxygen isotope signature as illite in the paleosol (Fig. 14). Thus, although pedogenic illite formation accounts for retention of pedogenic calcite oxygen

signatures, the mineralogic and isotopic similarities between "parent" and paleosol are better explained by some other, diagenetic, origin for illite.

Illite formation in the Pennington is also consistent with the fluid pulse environment (Fig. 23). The K/Ar age dates for the $<1.0\ \mu m$ size fraction of Pennington illite (275, 282 Ma; Table 2) should date the timing of illite formation and are coincident with the timing of fluid migration. Elliott and Aronson (1987) found that shallowly buried Ordovician and Devonian K-bentonites in the southern Appalachian basin were highly illitic (up to 90 % illite) and yielded ages of 270 to 300 Ma. They called upon Alleghanian orogenic fluid flow to explain the high degree of illitization in shallowly buried K-bentonites. Clearly, such fluids had the potential to cause extensive illitization of the Pennington paleosol. If, however, Alleghanian fluids had migrated through the Pennington, some degree of calcite recrystallization would be expected. The high temperature of the fluids (100 °C or more, as suggested by Roedder, 1979) coupled with relatively high water/rock ratios would most likely have caused some degree of calcite recrystallization. We note no petrographic (transmitted light or cathodluminscence) evidence for recrystallization of Pennington calcites, indicating that the paleosol was most likely unaffected by migrating orogenic fluids, or that such fluid flow was very minor. Also, preliminary analysis of XRD patterns of random powder mounts indicate there is a detrital (2M)

component in these samples. Depending on how much of this detrital component is present, the age of the authigenic component would most likely be younger than the timing of fluid migration.

Evidence for and against the formation of Pennington illite in the burial environment is similar to that of the fluid pulse environment. The illite-based fluid evolution curve indicates that illite could have formed in the burial environment, although the peak burial conditions of the Pennington ($<$3km, $<$100 °C) seem at odds with the extensive crystallization of discrete illite. Perry and Hower (1972) and Hower and Aronson (1973) have suggested that long time intervals at slightly elevated temperatures can cause the smectite-to-illite reaction to occur. Thus, illitization in the burial environment may have been aided by the long period of time available for illite formation. Burial of the Pennington paleosol was strictly the result of sediment deposition, with maximum burial conditions occurring just prior to, or coeval with Alleghanian thrusting (Hatcher et al., 1989). Stearns and Reesman (1986) suggested that 1,480 m of uplift occurred at the crest of the Nashville Dome (approximately 100 km to the east of the Pennington paleosol) from Permian(?) to Cretaceous time. Assuming that the flanks of the dome did not undergo as much uplift as the crest, the Pennington paleosol could have potentially been buried for 100-150 Ma. Measured K/Ar dates are older and tighter (Table 2) than might be expected if Pennington

illitization is the product of shallow burial for extended periods of time; however, the presence of a small detrital component in the illite samples dated may result in overestimation of the K/Ar age. Burial-driven illitization would account for the mineralogical and isotopic similarities between Pennington "parent" and paleosol material, but, like the fluid-pulse environment, it fails to explain the lack of calcite recrystallization. Considering the slightly elevated burial temperatures and the amount of time necessary to generate discrete illite in the burial environment, some degree of calcite recrystallization is expected.

Extensive illitization of the Pennington paleosol to discrete illite remains an enigma at this time. None of the three environments of illitization accounts individually for both the lack of calcite recrystallization and the similarities between parent and paleosol material. Therefore, the actual pathway of illitization was most likely some combination of two or all three of these environments. Mature vertic features found in the Pennington paleosol suggest that Pennington illites are likely candidates for the natural production of illite by repeated cycles of wetting and drying. It seems reasonable, therefore, that illitization was initiated in the pedogenic environment. Illitization would have continued in the shallow burial environment, with continued coarsening and isotopic reequilibration of the illite under relatively low water/rock conditions. Low temperatures and low

water/rock conditions would allow for preservation of pedogenic oxygen signatures in the coexisting calcite. Furthermore, completion of illitization in the burial environment would account for the mineralogical and isotopic similarities between "parent" and paleosol material. Although the existing data do not definitively rule out illitization by an orogenic fluid pulse, this mechanism is not required to explain any mineralogic or isotopic observations. Extensive illitization in the Pennington paleosol is most likely the result of both pedogenic and burial-driven illite formation.

X. CONCLUSIONS

The results of this study indicate that the oxygen isotope composition of deeply buried vertic paleosol clays and pedogenic calcites are best suited to evaluate the physicochemical conditions of diagenesis, rather than pedogenesis. Illite and calcite in the Mauch Chunk and Hinton vertic paleosols acquired their final O-isotope compositions in the post-pedogenic environment. The initiation of Alleghanian clastic-wedge development (burial) preceded Alleghanian fluid migration, suggesting that illitization, at one point in time, was burial driven. A later fluid pulse could have potentially migrated through these paleosols if burial compaction had not progressed sufficiently to make the paleosols impermeable to fluid flow. More detailed resolution in the timing of fluid migration relative to active burial is required to evaluate this relationship.

At this time the existing data base does not rule out illitization by orogenic fluids, but this mechanism of illite formation probably did not occur in the paleosols studied. Evidence for Alleghanian fluid migration has predominantly been documented in Cambrian and Ordovician carbonates, and along fault planes in the Valley and Ridge (Elliott and Aronson, (1987); Hearn et al., (1987); Schedl et al., (1992); Montanez and Read (1992), and Battles (1993). In most cases, these brines are interpreted to have been derived from, and migrated through, early Paleozoic sediments. Mississippi

Valley Type deposits believed to be generated by Alleghanian orogenic brines are found almost exclusively in Cambrian and Ordovician carbonates (Hearn et al., 1987). Taking this into account, it seems unlikely that Alleghanian fluids would have affected the Hinton and Pennington paleosols, which were located to the west of Alleghanian thrust faulting. Fluids would have had to have migrated through thick packages of Devonian shales and Mississippian carbonate sequences which were not tectonically fractured. Fluid migration through the Mauch Chunk paleosol, which is located in the Valley and Ridge, can not be similarly discounted. The lack of calcite recrystallization and the high degree of illitization in the shallowly buried Pennington offers the intriguing possibility that illite formation was initiated by multiple cycles of wetting and drying. The similarity in the mineralogical and isotopic composition between "parent" and paleosol material in all of the paleosols studied does not preclude the occurrence of pedogenic illitization. Continued illitization subsequent to pedogenesis (i.e., burial or fluid pulse) may mask isotopic and mineralogical differences between the "parent" and paleosol material.

The recognition of pedogenically altered mudstones in the rock record is increasing. Studies of burial diagenesis based on the illite crystallinity indices must consider the possibility that illitization might have been initiated in the pedogenic environment, as a result of repeated cycles of shrinking and swelling.

XI. FUTURE WORK

Unfortunately, the effects of detrital contamination on $\delta^{18}O$ (illite) is impossible to quantify because pure source material cannot be collected and measured for its $\delta^{18}O$ signature. Future work should therefore concentrate on obtaining a smaller size fraction so as to minimize detrital (2M) illite contamination. Scanning and transmission electron microscopy should be utilized to help confirm the authigenic nature of illite. If all of the detrital illite cannot be removed, an estimate of the percentage of M illites in the fine size fraction can be made using the software program WILDFIRE (Reynolds, 1994).

Additional efforts to remove chlorite from the fine size fraction should be made. Large amounts of the < 0.5 μm or smaller size fraction should be obtained to allow for the possible magnetic separation of chlorite from illite. If magnetic separation of chlorites is not possible, chlorite removal by HCl should be tried again. A lower concentration of HCl, coupled with more washes, lower temperatures (80 °C), and shorter time periods (20 minutes), may not produce the negative results explained in Appendix E. Destruction of chlorite and subsequent O-isotope analysis of pure illite would best determine the $\delta^{18}O$ value of illite. The $\delta^{18}O$ value of illite may also be calculated from estimates of %illite and isotopic analysis of chlorite separates. The latter approach has the advantage of further constraining the

origin of chlorite, possibly leading to a better understanding of mineral reactions occurring in the burial environment.

To further evaluate the possibility of pedogenic illitization, studies of mature, vertic paleosols should concentrate on locating as many subtle differences as possible between "parent" and paleosol material. For example, close examination of XRD plots for both the Hinton and Pennington paleosols show a systematic difference in the chlorite found in "parent" and paleosol material (Figs. 24,25). Increased intensities of even-ordered chlorite peaks relative to odd-ordered peaks in "parent" material chlorite suggests "Parent" chlorite is enriched in iron (Moore and Reynolds, 1989). Assuming that the chlorite in the finest size fraction analyzed was authigenically produced during illitization, the lower iron content of chlorite in the paleosol might be remnant evidence of pedogenic illitization. Detailed chemical work would have to be performed to evaluate this possibility. Additional studies should concentrate on much younger vertic paleosols and modern Vertisols, where the depth of burial can be more accurately constrained and the young age precludes extensive illitization in the burial environment. Two possible study areas are Pliocene Vertisols along the Rio Grande Rift that were studied by Coustausen (1991), and active Vertisols found in southern Texas.

Figure 24. X-ray diffraction plot comparing Pennington "parent" and paleosol chlorite. Note the increased intensity in the even ordered peaks within the "parent" material. If the chlorite was produced during the smectite-to-illite transition, the differences between the "parent" and paleosol material may be the result of pedogenic illitization having affected the paleosol material only. The exact same trend is found between the Hinton "parent" and paleosol material (see Fig. 25).

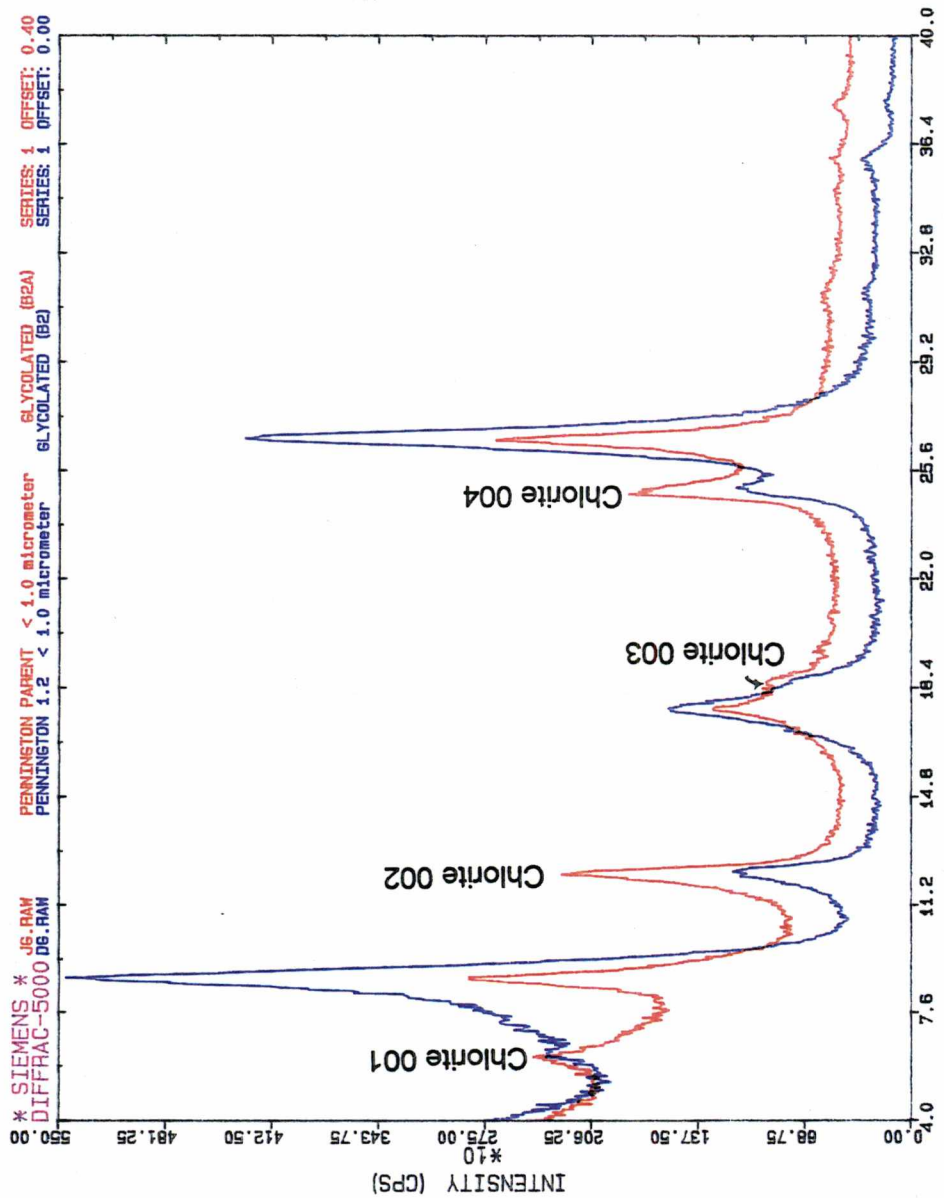
* SIEMENS *
DIFFRAC-5000
JG.RAM
D8.RAM
PENNINGTON PARENT < 1.0 micrometer
PENNINGTON 1.2 < 1.0 micrometer
GLYCOLATED (B2A)
GLYCOLATED (B2)
SERIES: 1 OFFSET: 0.40
SERIES: 1 OFFSET: 0.00
Chlorite 001
Chlorite 002
Chlorite 003
Chlorite 004
INTENSITY (CPS)
*10
550.00
481.25
412.50
343.75
275.00
206.25
137.50
68.75
0.00
4.0
7.6
11.2
14.8
18.4
22.0
25.6
29.2
32.8
36.4
40.0
TWO - THETA (DEGREES)

Figure 24

Figure 25. X-ray diffraction plot comparing Hinton "parent " and paleosol chlorite. Similar to the Pennington paleosol, even ordered chlorite peaks are intensified in the "parent" material.

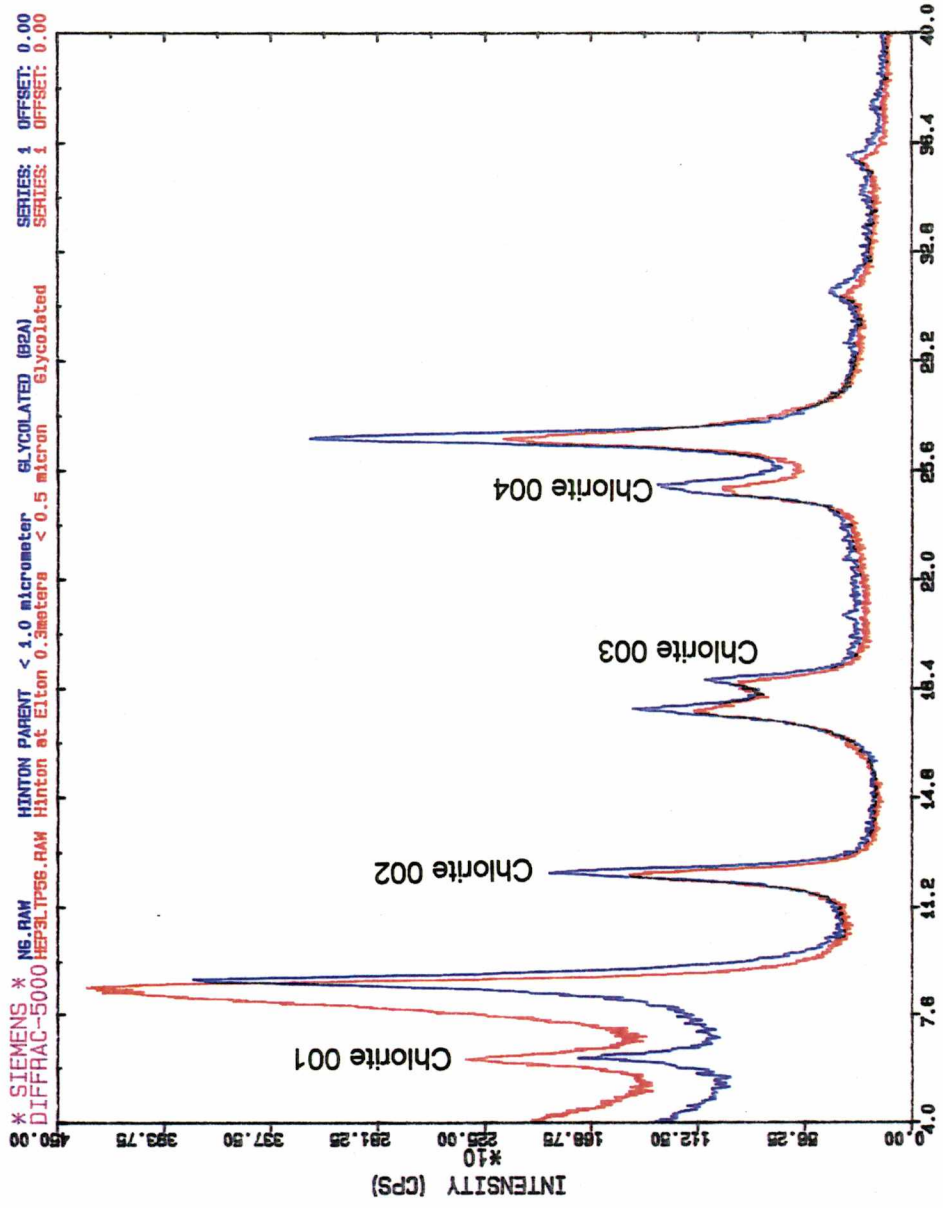
* SIEMENS *
DIFFRAC-5000
NG.RAW
HEP3LTP56.RAW
HINTON PARENT < 1.0 micrometer GLYCOLATED (002)
Hinton at Elton 0.3meters < 0.5 micron Glycolated
SERIES: 1 OFFSET: 0.00
SERIES: 1 OFFSET: 0.00
Chlorite 001
Chlorite 002
Chlorite 003
Chlorite 004
INTENSITY (CPS)
*10
450.00
393.75
337.50
281.25
225.00
168.75
112.50
56.25
0.00
4.0
7.8
11.2
14.8
18.4
22.0
25.6
29.2
32.8
36.4
40.0
TWO - THETA (DEGREES)

Figure 25

LITERATURE CITED

LITERATURE CITED

Battles, D. A., 1993, Fluid geochemistry and fluid migration pathways during the Alleghanian orogeny, central Appalachians: Geological Society of America, Abstracts with programs, v.25, p. 69.

Beaumont, C., Quinlan, G., and Hamilton, J., 1988, Orogeny and stratigraphy: numerical models of the Paleozoic in the eastern interior of North America: Tectonics, v. 7, p. 389-416.

Burst, J.F., 1969, Diagenesis of Gulf Coast clayey sediments and its possible relation to petroleum migration: American Association of Petroleum Geologist Bulletin, v. 53, p. 73-93.

Berner, R.A., 1991, A model for atmospheric CO2 over Phanerozoic time: American Journal of Science, v. 291, p. 339-376.

Caudill, M. R., Mora, C.I., Tobin, K.J., and Driese, S.G., 1992, Preliminary interpretations of paleosols associated with late Mississippian marginal marine deposits, Pennington Formation, Monterey, TN, *in* Driese, S. G., Mora, C.I., and Walker, K.R. (eds.), Paleosols, Paleoweathering Surfaces and Sequence Boundaries: Knoxville, University of Tennessee, Studies in Geology No. 21, p. 57-77.

Cerling, T.E., 1984, The stable isotope composition of modern soil carbonate and its relationship to climate: Earth and Planetary Science Letters, v. 71, p. 229-240.

Cerling, T.E., 1991, Carbon dioxide in the atmosphere: evidence from Cenozoic and Mesozoic paleosols: American Journal of Science, v. 291, p. 377-400.

Clayton, R. N., and Mayeda, T. K., 1963, The use of bromine pentafluoride in the extraction of oxygen from oxides and silicates for isotopic analysis, Geochimica et Cosmochimica Acta, v. 27, p. 43-52.

Craig, H., 1961a, Standard for reporting concentrations of deuterium and oxygen 18 in natural water: Science, v. 133, p. 1833.

Donaldson, A., C., and Shumaker, R. C., 1981, late Paleozoic molasse of Central Appalachians, in Miall, A.D. (ed.), Sedimentology and tectonics in alluvial basins: Geological Association of Canada, Special Paper 23, p. 99-124.

Dorobek, S. L., 1989, Migration of orogenic fluids through the Siluro-Devonian Helderberg Group during late Paleozoic deformation: constraints on fluid sources and implications for thermal histories of sedimentary basins: Tectonophysics, v. 150, p. 25-445.

Driese, S.G., Mora, C.I., and Cotter, E., 1993, Nescopeck creek paleosol, Mauch Chunk Formation near Nescopeck Creek, PA, *in* Driese, S.G. (ed.), Paleosols, Paleoclimate, and Paleoatmospheric CO_2 ; Paleozoic Paleosols of Central Pennsylvania: Knoxville, University of Tennessee, Studies in Geology No. 22, p.91-102.

Dudal, R., and Eswaran, H., 1988, Distribution, properties and classification of Vertisols, *in* Wilding, L.P., and Puentes, R. (eds), Vertisols: Their Distribution, Porperties,Classification, and Management: College Station, TX, Texas A&M University Printing Center, p. 1-22.

Eberl, D. D., Srodon, J., and Northrup, H.R., 1986, Potassium fixation in smectites by wetting and drying: *in* Geochemical Processes at Mineral Surfaces, Davis, J. A., and Hayes, K. F. (eds.), American Chemical Society Symposium Ser., v. 323, p. 296-326.

Edmunds, W.E., Berg, T.M., Sevon, W.D., Piotrowski, R.C., Heyman, L., and Rickard, L.V., 1979, The Mississippian and Pennsylvanian (Carboniferous) systems in the United States-Pennsylvania and New York: U. S. Geological Survey Professional Paper 1110-B, 33p.

Elliott, W. C., and Aronson, J. L., 1987, Alleghanian episode of K-bentonites illitization in the southern Appalachian basin: Geology, v. 15, p. 735-739.

Englund, K.J., Gillespie, W.H., Cecil, C.B., and Windolph, J.F., Jr., 1985, Characteristics of the Mississippian - Pennsylvanian boundary and associated coal-bearing rocks in the southern Appalachians: USGS Open File Report 85-577, 84p.

Epstein, A. G.; Epstein, J. B., and Harris, L. D., 1977, Conodont alteration color- an index to organic metamorphism: United States Geological Survey Professional Paper 995, 27p.

Eslinger, E. V., 1971, Mineralogy and oxygen isotope ratios of hydrothermal and low-grade metamorphic argillaceous rocks [Ph.D. dissertation]: Cleveland, Ohio, Case Western Reserve University.

Eslinger, E.V., and Savin, S.M., 1973b, Oxygen isotope geothermometry of the burial metamorphic rocks of the Precambrian belt supergroup, Glacier National Park, Montana: Geological Society of America Bulletin, v. 84, p. 2549-2560.

Eslinger, E.V., and Yeh, H.W., 1986, Oxygen and hydrogen isotope geochemistry of Cretaceous bentonites and shales from the Disturbed Belt, Montana: Geochimica et Cosmochimica Acta, v. 50, p. 59-68.

Faure, G., 1986, Principles of Isotope Geology, 2nd edition, J. Wiley and Sons, New York, 589p.

Freeze, R.A., and Cherry, J.A., 1979, Groundwater, Prentice Hall, New Jersey 604p.

Friedman, I., and O'Neil, J.R., M., 1977, Compilation of stable isotope fractionation factors of geochemical interest: *in* Data of geochemistry, 6 ed., Fleischer, M., ed., U.S. Geological Survey Professional Paper 440-KK, 12 p..

Gile, L.H., Peterson, F.F., and Grossman, R.B., 1966, Morphological and genetic sequences of carbonate accumulation in desert soils: Soil Science, v. 101, p. 347-360.

Goldstein, R.H., 1991, Stable isotope signatures associated with paleosols, Pennsylvanian Holder Formation, New Mexico: Sedimentology, v. 38, p. 67-77.

Hatcher, R. D., Jr., and others, 1989, Alleghanian orogen, *in* Hatcher, R. D., Jr., Thomas, W.A., and Viele, G.W. (eds.), The Appalachian- Ouachita orogen in the United States: Geological Society of America, The Geology of North America Project, v. F-2, p. 233-318.

Hearn, P. P., Sutter, J. F., and Belkin, H. E., 1987, Evidence for late-Paleozoic brine migration in Cambrian carbonate rocks of the central and southern Appalachians: implications for Mississippi Valley-type sulfide mineralization: Geochimica et Cosmochimica Acta, v. 51, p. 1323-1334.

Hower, J., and Aronson, J.L., 1973, Kinetic aspects of the burial diagenesis of shales [abs]: Clay Mineral Society, 10th Annual Meeting, Banff, p. 35.

Hower, J., Eslinger, E.V., Hower, M.E., and Perry, E.A., 1976, Mechanism of burial metamorphism of agillaceous sediment 1. Mineralogical and chemical evidence: Geological Society of America Bulletin, v. 87, p. 725-737.

Jackson, M. L., 1975, *Soil chemical analysis-Advanced course*, 2nd edition, 10th printing: Madison, Wisconsin, M. L. Jackson, 895p.

Srodon, J., 1984, X-ray powder diffraction identification of illitic materials, Clays and Clay Minerals, v. 32, No. 5, p. 337-349.

Kent, D. V., 1979, Paleomagnetism of the Devonian Onodaga Limestone revisited: Journal of Geophysics Res., v. 84, p. 3576-3588.

Lacazette, A. J., 1991, Natural hydraulic fracturing in the Bald Eagle sandstone in central Pennsylvania and the Ithaca siltstone at Watkins Glen, New York [Ph.D. thesis]: University Park Pennsylvania, Pennsylvania State University, 225 p.

Levine, J. R., 1986, Deep burial of coal bearing strata, Anthracite region, Pennsylvania - sedimentation or tectonics?: Geology, v.14, 577-580.

Machette, M.N., 1985, Calcic soils of the southwestern United States, *in* Weide, D.L. (ed.), Soils and Quaternary Geology of the Southwestern United States: Geological Society of America Special Paper 203, p. 1-21.

Mamy, J., and Gaultier, J.P., 1975, Etude par diffraction Xde la desorption de l'eau fixee dans les espaces interfeuillets des phlogopites alterers [X-ray diffraction study of the dehydration of the interlayer fixed water of altered phlogopite]: Groupe Fr. Argiles Bulletin, v, 26, No. 2, p. 165-171.

McCrea, J. M., 1950, The isotopic chemistry of carbonates and a paleotemperature scale: Journal of Chemical Physics, v. 18, p.849-857.

Meckel, L. D., 1970, Paleozoic alluvial deposition in the central Appalachians, *in* Fisher, G. W., and others (eds), Studies of Appalachian Geology: central and southern New York, Interscience Publishers, p. 49-67.

Milici, R.C., 1974, Stratigraphy and depositional environments of Upper Mississippian and Lower Pennsylvanian rocks in the southern Cumberland Plateau of Tennesee: Geological Society of America Special Paper 148, p. 115-133.

Milici, R.C., Briggs, G., Knox, L.M., Sitterly, P.D., and Statler, A.T., 1979, The Mississippian and Pennsylvanian (Carboniferous) Systems in the United States-Tennessee: U.S. Geological Survey Professional Paper 1110-G, 38p.

Montanez, I.P., and Read, J.F., 1992, Eustatic control on early dolomitization of cyclic peritidal carbonates; evidence from the early Ordovician upper Knox Group, Appalachians: Geological Society of America Bulletin, v. 104(7), p. 872-886.

Moore, D.M., and Reynolds, R.C., 1989, X-ray Diffraction and the Analysis of Clay Minerals: New York, Oxford University Press, 332 p.

Mora, C.I., Driese, S.G., and Seager, P.G., 1991, Carbon dioxide in the Paleozoic atmosphere: evidence from the C-isotopic compositions of pedogenic carbonate: Geology, v. 9, p. 1017-1020.

Mora, C.I., Fastovsky, D.E., and Driese, S.G., 1993, Geochemistry and Stable Isotopes of Paleosols: Knoxville, University of Tennessee, Studies in Geology No.23, 66p.

Mora, C.I., and Driese, S.G., 1993, A steep, mid-to-late Paleozoic decline in atmospheric CO_2 : evidence from soil carbonate CO_2 paleobarometer: Chemical Geology, v. 107, p.217-219.

Morrow, 1984, Senior honors thesis at Bucknell University.

Odin, G. S., 1982, Numerical dating in stratigraphy: New York, John Wiley and Sons, 1040p.

Oliver, J., 1986,Fluids expelled tectonically from orogenic belts: Their role in hydrocarbon migration and other geologic phenomena: Geology, v. 14, p. 99-102.

O'Neil J. R., 1987, Preservation of H, C, and O-isotopic ratios in the low temperature environment, *in* Mineralogical Association of Canada Short Course in Stable Isotope Geochemistry of Low Temperature Fluids, Volume 1: Saskatoon, Saskatchewan.

O'Neil, J.R., and Kharaka, Y.K., 1976, Hydrogen and oxygen isotope exchange between clay minerals and water: Geochemica et Cosmochemica Acta, v. 40, p. 241-246.

Orkan, N. I., and Voight, B., 1983, Fracture geometry and vein mineral paleothermometry-barometry from fluid inclusions, Valley and Ridge Province, Pennsylvania: Geological Society of America, Abstracts with program., v. 15, p. 656.

Orkan, N. I., 1986, Regional joint evolution and paleothermometry-barometry from fluid inclusions in the Valley and Ridge Province of Pennsylvania in relation to the Alleghany orogeny: M.S. paper, Pennsylvania State University, University Park, 194p.

Perry, E.A., and Hower, J., 1972, Late-stage dehydration in deeply buried pelitic sediments: The American Association of Petroleum Geologist Bulletin, v. 56, no. 10, p. 2013-2021.

Reynolds, R.C., 1994, WILDFIRE program available from R.C. Reynolds, Dartmouth College, New Hampshire.

Roedder, E., 1979, Fluid inclusion evidence on the environments of sedimentary diagenesis, a review, *in* Scholle, P. A., and Schluger, P. R. (eds.), Aspects of diagenesis: Society of Economic Paleontologists and Mineralogists Special Publication 26, p. 89-108.

Roden, M. K., and Miller, D. S., 1989, Apatite fission-track thermochronology ot the Pennsylvania Appalachian Basin, *in* Gardner, T. W., and Sevon, W. D. (eds.), Appalchian Geomorphology, v. 2, p. 39-51.

Salomons, W., and Mook, W.G., 1986, Isotope geochemistry of carbonates in the weathering zone, *in* Fritz, P., and Fontes, J. Ch. (eds.), Handbook of Environmental Chemistry, Volume 2, The Terrestrial Environment: Amsterdam, Elsevier Pub. CO., p. 239-270.

Savin, S. M., and Lee, M., 1988, Isotopic studies of phyllosilicates, *in* Hydrous Phyllosilicates (exclusive of micas), Bailey, S. W (ed.), Reviews in Mineralogy, v.19, 189-223.

Schedl, A., McCabe, C., Montanez, I.P., Fullagar, P.D., and Valley, J.W., 1992, Alleghanian Regional Diagenesis, a response to the migration of modified metamorphic fluids derived from beneath the Blue Ridge-Piedmont thrust sheet: Journal of Geology, v. 100 (3), p. 339-352.

Scotese, C. R., Van der Voo, R., and McCabe, C., 1982, Paleomagnetism of the Upper Silurian and Lower Devonian carbonates of New York State: Evidence for secondary magnetizations residing in magnetite: Physics of the Earth and the Planetary Interiors, v. 30, p.385-395.

Srodon, J., 1984, X-ray powder diffraction identification of illitic materials: Clays and Clay Minerals, v. 32, No. 5, p. 337-339.

Stancel, S. G., 1980, Alluvial deposition in the Mauch Chunk - Pottsville transition zone (Upper Mississippian - Lower Pennsyvanian) in east central Pennsylvania: unpublished Master's Thesis, Suny Binghamton, 98 p.

Stearns, R.G., and Reesman, A.L., 1986, Cambrian to Holocene structural and burial history of Nashville Dome: American Association of Petroleum Geologist Bulletin, v. 70, p. 143-154.

Stefaniak, A., Mora, C.I., and Driese, S.G., 1993, Pedogenic and groundwater carbonates in vertic paleosols in the Mississippian Maccrady Formation, southeast West Virginia [abstract]: Geological Society of America, Abstracts with Programs, v. 25, p. A-399.

Sucheki, R. K., and Land, L. S., 1983, Isotopic geochemistry of burial metamorphosed volcanogenic sediments, Great Valley Sequence, northern California: Geochimica et Cosmochimica Acta, v. 47, p. 1487-1499.

Van der Voo, R., 1979, Age of Alleghanian folding in the central Appalachians: Geology, v. 7, p. 297-298.

Wenner, D.B., and Taylor, H.B., Jr., 1971, Temperatures of serpentization of ultramafic rocks based on ^{18}O / ^{16}O fractionation between coexisting serpentine and magnetite: Contributions to Mineralogy and Petrology, v.32, p. 165-185.

Wright, V.P., and Vanstone, S.D., 1991, Assessing the carbon dioxide content of ancient atmospheres using paleo-calcretes. t, p.es: theoretical and empirical constraints: Journal of the Geological Society of London, v. 148, p. 945-947.

Yeh, H.W., 1974, Oxygen isotope studies of ocean sediments during sedimentation and burial diagenesis, Ph.D. Dissertation. Case Western Reserve University.

Yeh, H.W., and Savin, S.M., 1977, The mechanism of burial metamorphism of argillaceous sediments: 3. Oxygen isotope evidence: Geological Society of America Bulletin, v. 88, p. 1321-1330.

Yeh, H.W., 1980, D/H ratios and late-stage dehydration of shales during burial: Geochimica et Cosmochimica Acta, v. 44, p. 341-352.

Zhang, E., and Davis, A., 1993, Coalification patterns of the Pennsylvanian coal measures in the Appalachian foreland basin, western and south-central Pennsylvania: Geological Society of America Bulletin, v. 105, p. 162-174.

APPENDICES

APPENDIX A:

CHEMICAL TREATMENTS OF CLAYS

GENERAL NOTE ON CLAY SAMPLE PREPARATION:

The best rule of thumb to follow in clay sample preparation is to do the least amount of work possible to get the desired results. Each added step potentially changes the clay chemically and/or physically so that results of the study may be skewed or incorrect. Chemical treatments should proceed from treatments designed to remove those phases that make up the greatest percentage of contaminant to those designed to remove the lowest percentage contaminant. Quantitative analysis does not have to be done to determine which contaminant makes up the greatest percentage. Rough estimates can be made just by observation of the sample. For example, if the sample is really red there is probably a fairly decent percentage of iron oxide material. If the sample reacts strongly to HCl there is probably a good amount of carbonate that needs to be removed. For the purposes of this study chemical treatments proceeded from iron oxide, carbonate, to organic material removal.

PREPARING SAMPLE FOR CHEMICAL TREATMENTS

Prior to chemical treatments, samples must be disaggregated so that they are in suspension. Pennington (PN) samples disaggregated simply by placing them in water overnight, but time constraints required that Mauch Chunk (MC) and Hinton (HN) samples be ultrasonically disaggregated. Note, it would have been preferable to allow large amounts of MC and HN samples to disaggregate by letting them sit in distilled deionized water for a couple of months. Steps 1- 8 are for ultrasonic disaggregation and were carried out on MC and HN samples only. Pennington sample was disaggregated until eight 240 ml centrifuge bottles could be filled to 9 cm above the bottom with sample suspension. Steps 9-26 were done for all three paleosols.

1- Crush approximately 400 grams of MC and HN samples into 1-2mm size fraction using mortar and pestle.
2- Wet seive samples through 1000 mesh to remove any artificial clay size fraction created by crushing.
3- To facilitate ultrasonic disaggregation, all crushed and seived material was soaked in distilled deionized water overnight.
4- Add crushed and seived sample (approximately ~1 cm in height) to the bottom of a 200 ml glass beaker. Fill the beaker half full with distilled deionizd water.
5- Place beaker in a 60Hz resonance ultrasonic disaggregater (UD) for 20 to 30 min (do NOT let ultrasonic dissaggregation continue for longer than this ....the sample water gets hot. If the sample water does get hot, the clays may have been damaged. Discard the sample water and the 1-2vmm sample and start over with step four.
6- Decant the now muddy water into a 240 ml centrifuge bottle.

7- Add new distilled deionized water to the same sample in the beaker and repeat steps 4 and 5.
8- Discard sample in the bottom of UD beaker, and repeat steps 4-8 until eight 240 ml centrifuge bottles are filled to 9cm above the bottom with sample suspension.
9- Centrifuge bottles (4 at a time) at 3800 rpm for 30 min. After centrifugation pour a little bit of the supernatant into a glass beaker and make sure that it is clear by comparing it to water . If it is clear, carefully decant and discard all of the supernatant. Go immediately to step 10 (do not let the sample dry...see Sheldon and Kopp, (1994)). If the supernatant is not clear spin the sample again at the same settings. If the sample is still not clear, add ~5 ml of 1 Normal sodium acetate-acetic acid buffer (1N NaAc-HAc). Stir the supernatant gently (do not stir up the clay on the bottom) and then spin again at 3800 rpm for 30 min. 1N NaAc-HAc should cause flocculation and the supernatant should be clear. Decant and discard supernatant. Go immediately to step 10.

REMOVAL OF IRON OXIDES:

Chemical treatments to remove iron oxides should be done in sets of four centrifuge bottles.

10- Add 40 ml of 0.3 Molar sodium citrate ($Na_3C_6H_5O_7$ $2H_2O$) to each centrifuge bottle with sample in it.
11- Add 5 ml of 0.5 Molar sodium bicarbonate ($NaHCO_3$)
12- Stir the solution well until all clay is suspended. There shouldn't be any stuck to the bottom.
13- Warm the four sample solutions in a 70 ^{o}C water bath for 15 min
14- With the sample solutions still in the bath, add 1 g of sodium dithionite ($Na_2S_2O_4$) to one centrifuge bottle. Stir constantly for 1 min. Repeat this step for the last three centrifuge bottles. Stir all four sample solutions occasionally for 20 min while they are still in the bath.
15- Centrifuge all four bottles at 2000 rpm for 20 min. The supernatant should be clear. If it is not centrifuge again at the same settings. Carefully decant and discard clear supernatant. The sample should look less red.
16- Repeat steps 10-15 atleast three more times. These steps should be repeated until all the red is out. Go immediately to step 17, or make sure the sample does not dry out.

REMOVAL OF CARBONATES:

17- Fill each centrifuge bottle to half full with 1N sodium acetate-acetic acid buffer. Stir the solution well.
18- Place the centrifuge tubes in a 50°C water bath and let stand for 4 hrs. IF the water bath can be left on overnight, this reaction can be left alone for 12 hrs.
19- Centrifuge at 3000 rpm for 30 min. Supernatant might be a little yellowish but should be clear (no sample in suspension). Carefully decant and discard supernatant. Go immediately to step 20.

REMOVAL OF ORGANICS:

Organics are removed with 30 % hydrogen peroxide (H_2O_2). The reaction can be very violent so H_2O_2 is added incrementally in small volumes.
20- Add 5 ml of 30% H_2O_2. Stir the sample into solution. Heat in 50°C water bath for 10 min. Repeat this step a total of six times (30 ml of H_2O_2).
21- Once 30 ml of H_2O_2 is added, react the sample solution for 4 hrs at 50°C.
22- Add 5 ml of 1N NaAc-HAc buffer. Centrifuge at 3800 rpm for 60 min. Decant supernatant immediately after centrifugation. You may lose a little bit of sample.

WASHING THE SAMPLE:

Following chemical treatments, excess chemicals must be removed from the clays. This is done with distilled water washes and dialysis.

23- Fill the centrifuge bottles half full with distilled deionized water. Stir the clays into suspension. Centrifuge the bottles at whatever speed and time necessary to get the clays well plastered to the bottom of the bottles. Decant the clear supernatant.
24- Repeat step 23 as many times as possible. You should find that centrifuge speeds and time need to increase to get the clays well plastered on the bottom. This is an indication that the chemicals (flocculants) are being removed. A little less water should be added each time until the last distilled wash is done with maybe a quarter of the bottle full.
25- Dialysize the samples for 3-4 days using Spectra Por1 membrane tubing and clips. Effective dialysis is done with distilled deoinized water moving around the sample dialysis tubes. I used 1L beakers with stir bars. Dialysis tubes were suspended from a ruler that went across the top of the beakers. NOTE: THE DIALYSIS WATER SHOULD BE CHANGED EVERY 2-3hrs THE FIRST DAY. IT SHOULD BE CHANGED 3-4 TIMES EACH OF THE LAST 2-3 DAYS.

26- dry all samples in the oven at 40°C. Samples are now ready for oxygen isotope analysis procedures.

APPENDIX B:

X-RAY DIFFRACTION PLOTS

ARRANGEMENT OF PLOTS FOR EACH SAMPLE:

- 2 plots of the smallest size fraction illustrating the measurements made to estimate illite and chlorite percentages.

- 1 plot comparing baseline to glycolated samples.

- 1 plot comparing baseline to heated samples.

-1 plot showing size fraction comparisons

LEGEND OF PEAK LABELS USED ON ALL XRD PLOTS:

C1 = chlorite 001 peak
C2 = chlorite 002 peak
C3 = chlorite 003 peak
C4 = chlorite 004 peak
C5 = chlorite 005 peak

I1 = illite 001 peak
I2 = illite 002 peak
I3 = illite 003 peak
I4 = illite 004 peak
I5 = illite 005 peak

Q = quartz

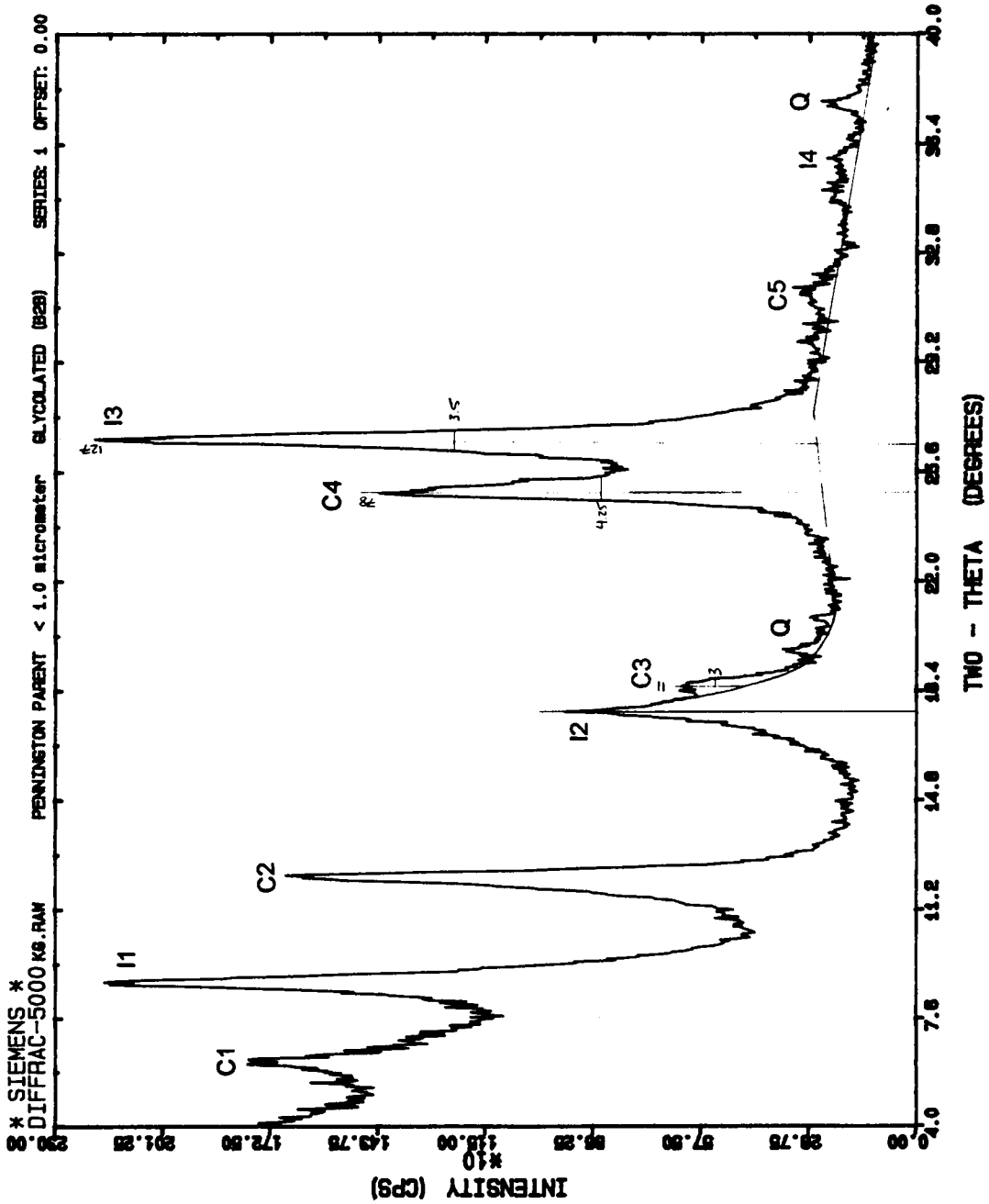
* SIEMENS *
DIFFRAC-5000 KB.RAM
PENNINGTON PARENT < 1.0 micrometer GLYCOLATED (B2B)
SERIES: 1 OFFSET: 0.00
I1
C1
C2
I2
C3
I3
C4
C5
I4
Q
INTENSITY (CPS)
*10
TWO - THETA (DEGREES)

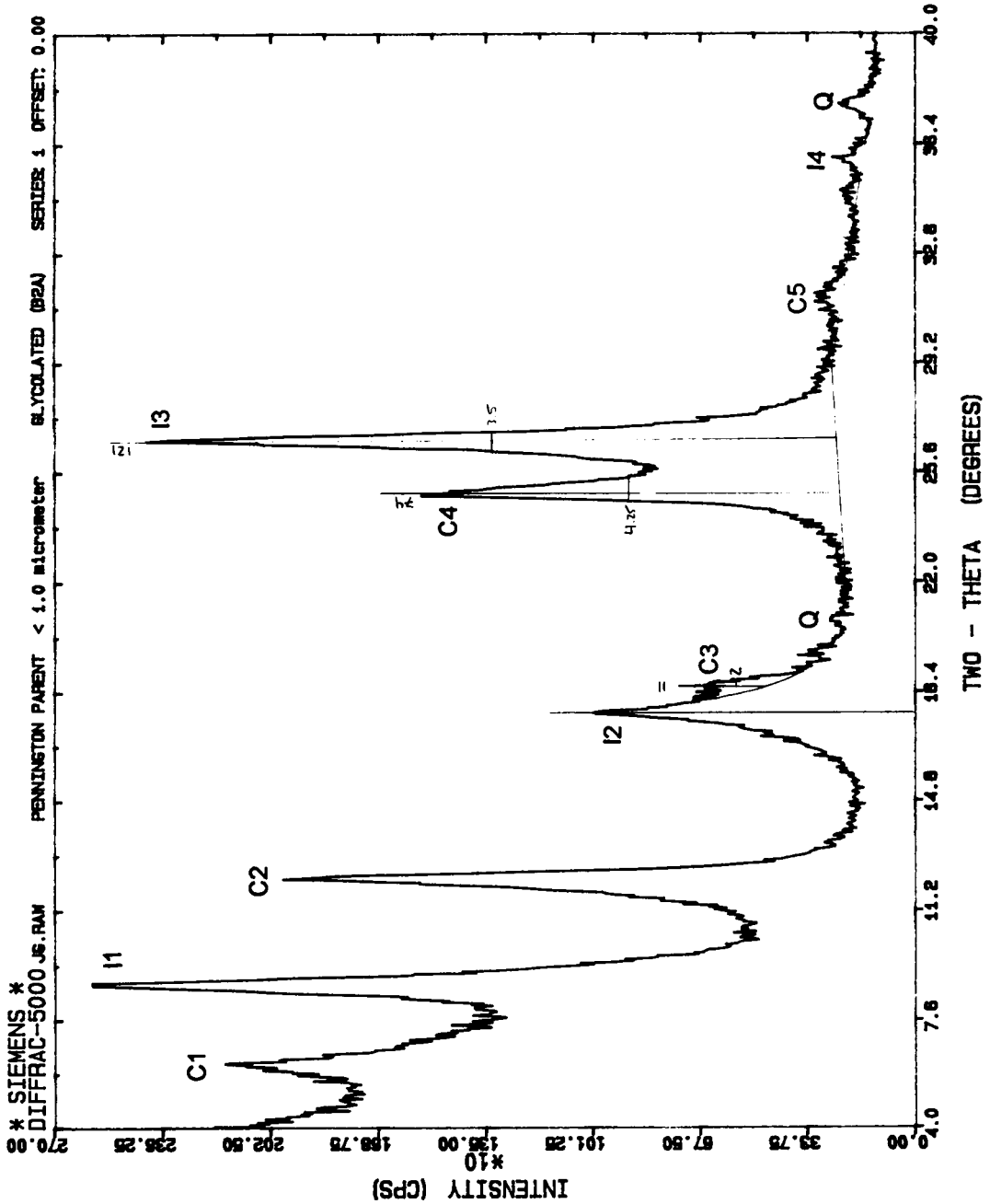
* SIEMENS *
DIFFRAC-5000 J6.RAM
PENNINGTON PARENT < 1.0 micrometer
GLYCOLATED (B2A)
SERIES: 1 OFFSET: 0.00
INTENSITY (CPS)
*10
TWO - THETA (DEGREES)
I1
I2
I3
I4
C1
C2
C3
C4
C5
Q
Q

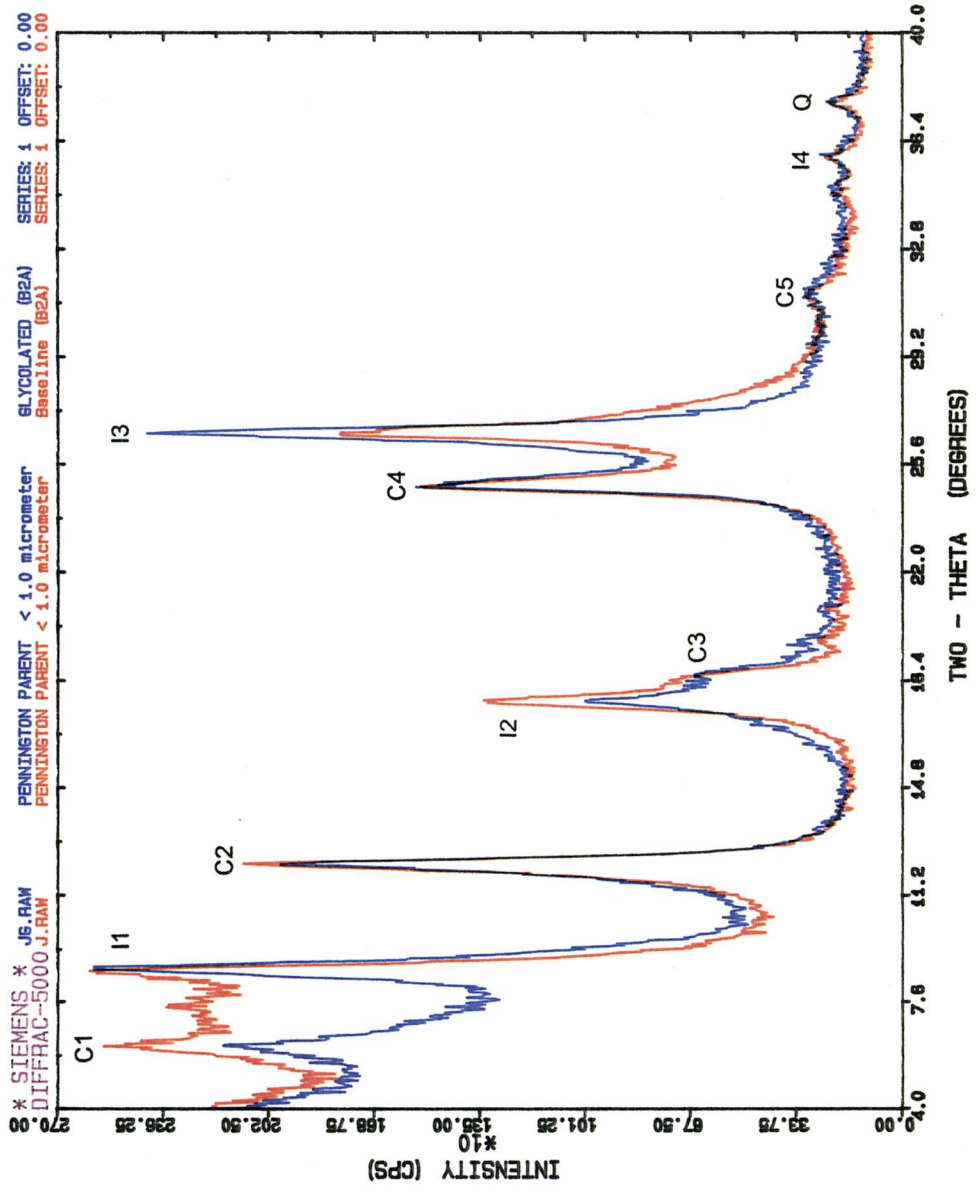
* SIEMENS * J6.RAW
DIFFRAC-5000 J.RAW
PENNINGTON PARENT < 1.0 micrometer GLYCOLATED (B2A) SERIES: 1 OFFSET: 0.00
PENNINGTON PARENT < 1.0 micrometer Baseline (B2A) SERIES: 1 OFFSET: 0.00
C1
I1
C2
I3
C4
I2
C3
C5
I4
Q
INTENSITY (CPS)
*10
0.00
33.75
67.50
101.25
135.00
168.75
202.50
236.25
270.00
4.0
7.6
11.2
14.8
18.4
22.0
25.6
29.2
32.8
36.4
40.0
TWO - THETA (DEGREES)

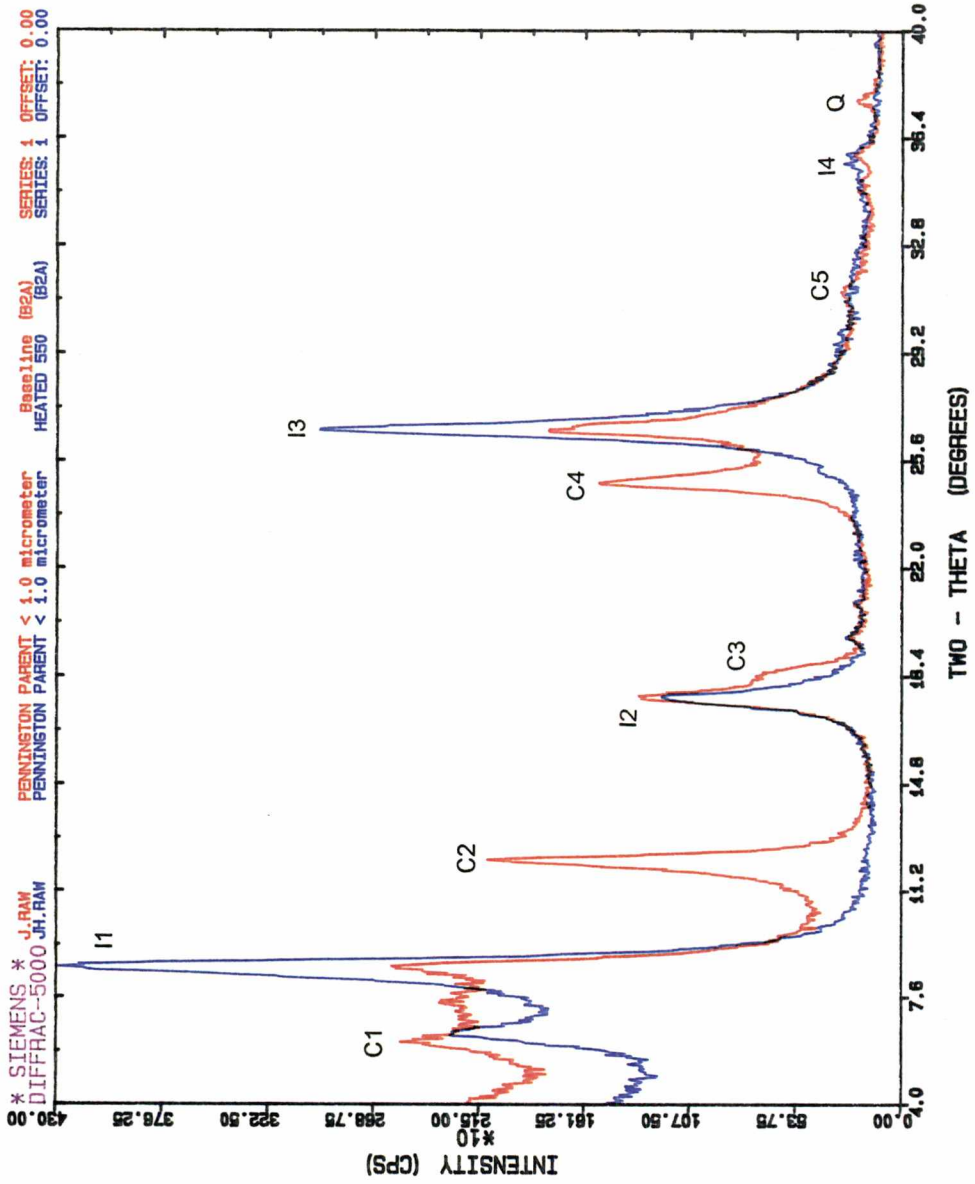
* SIEMENS *
DIFFRAC-5000
J.RAW
JH.RAW
PENNINGTON PARENT < 1.0 micrometer
PENNINGTON PARENT < 1.0 micrometer
Baseline (B2A)
HEATED 550 (B2A)
SERIES: 1 OFFSET: 0.00
SERIES: 1 OFFSET: 0.00
I1
C1
C2
I2
C3
I3
C4
C5
I4
Q
INTENSITY (CPS)
*10
430.00
376.25
322.50
268.75
215.00
161.25
107.50
53.75
0.00
4.0
7.6
11.2
14.8
18.4
22.0
25.6
29.2
32.8
36.4
40.0
TWO - THETA (DEGREES)

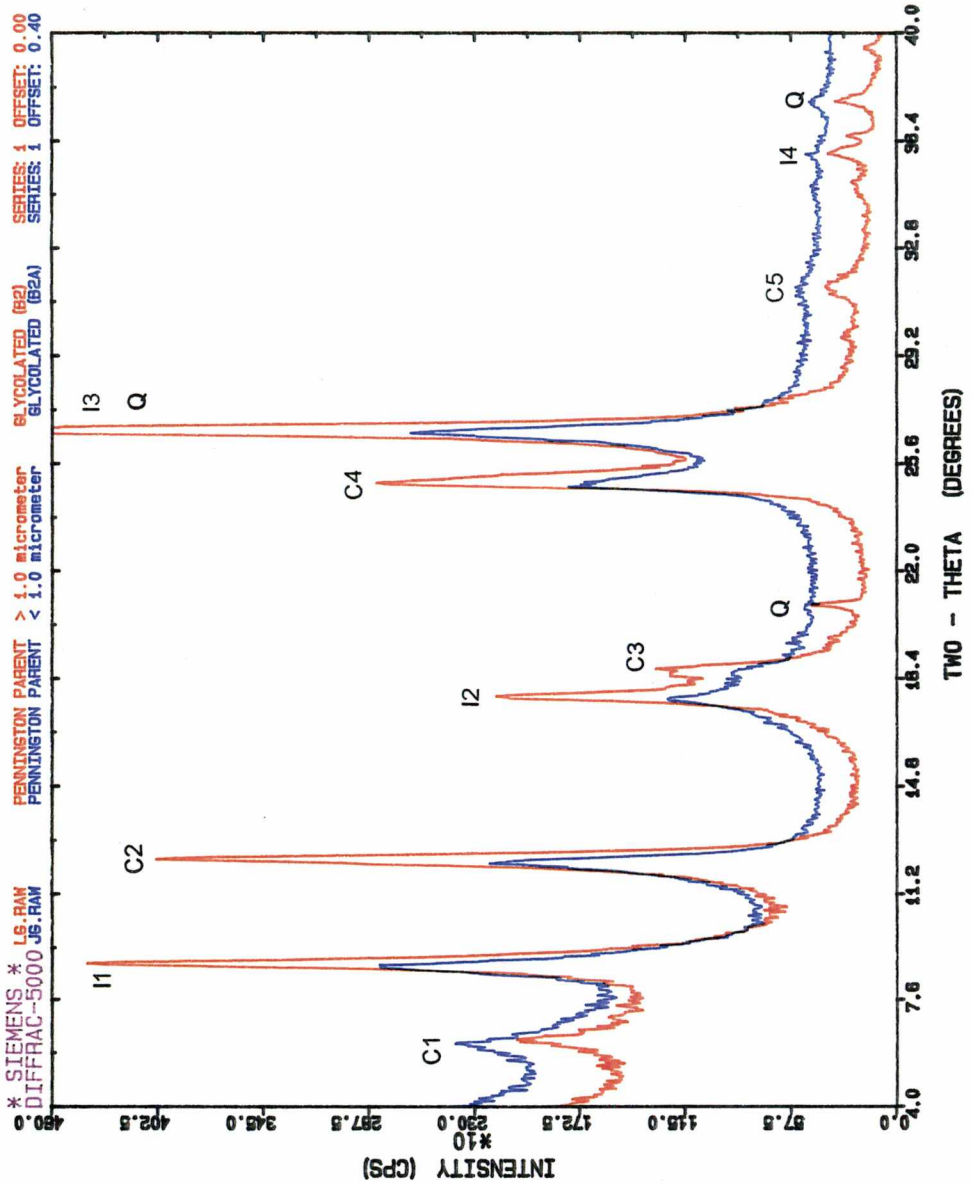
* SIEMENS *
DIFFRAC-5000
LG.RAW
JG.RAM
PENNINGTON PARENT > 4.0 micrometer
PENNINGTON PARENT < 4.0 micrometer
GLYCOLATED (G2)
GLYCOLATED (G2A)
SERIES: 1 OFFSET: 0.00
SERIES: 1 OFFSET: 0.40
I1
C1
C2
I2
C3
C4
I3
Q
C5
I4
Q
INTENSITY (CPS)
*10
TWO - THETA (DEGREES)

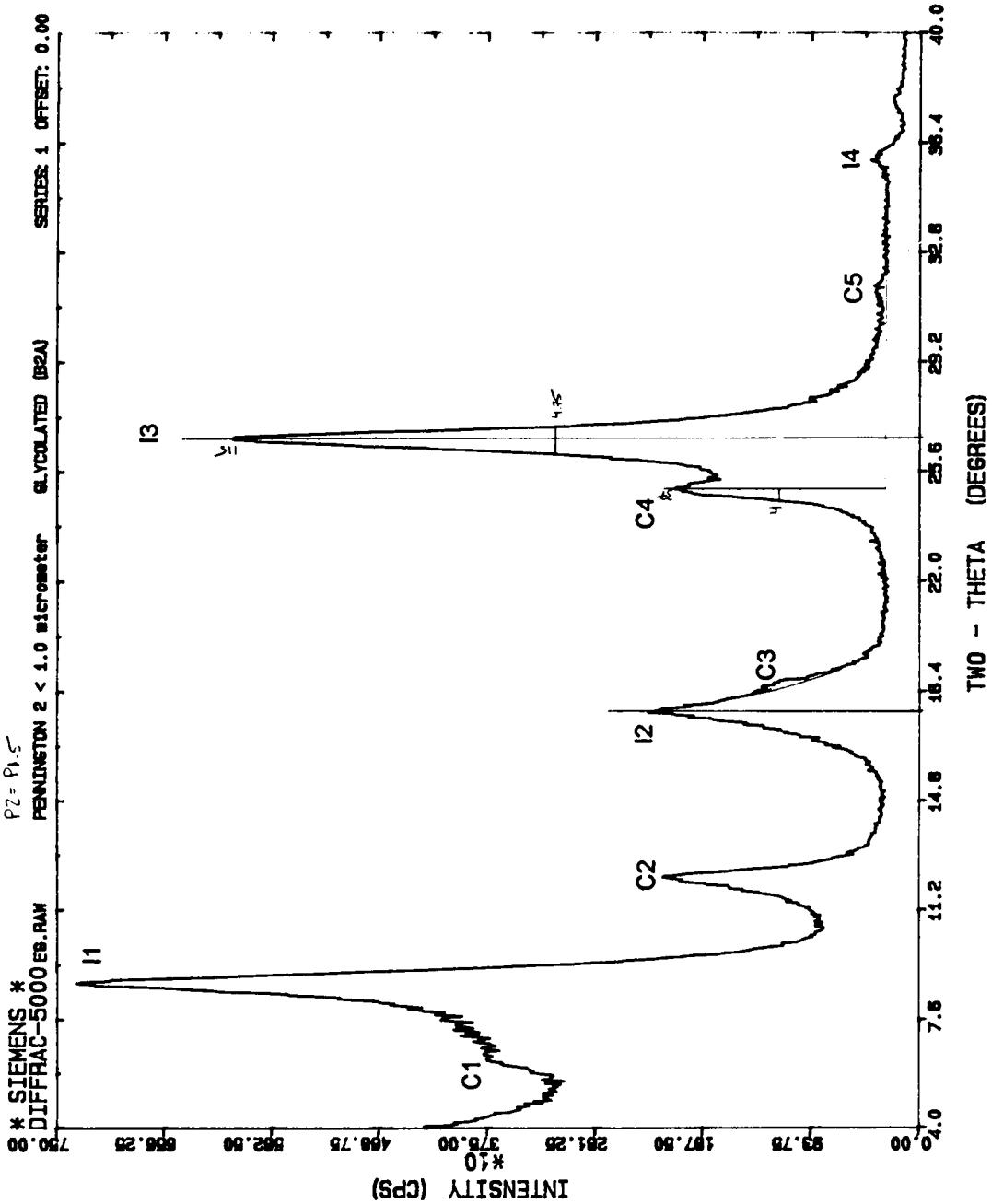
* SIEMENS *
DIFFRAC-5000
ES.RAW
PENNINGTON 2 < 1.0 micrometer
GLYCOLATED (B2A)
SERIES: 1 OFFSET: 0.00
P2= P1.5
I1
I2
I3
I4
C1
C2
C3
C4
C5
INTENSITY (CPS)
*10
TWO - THETA (DEGREES)

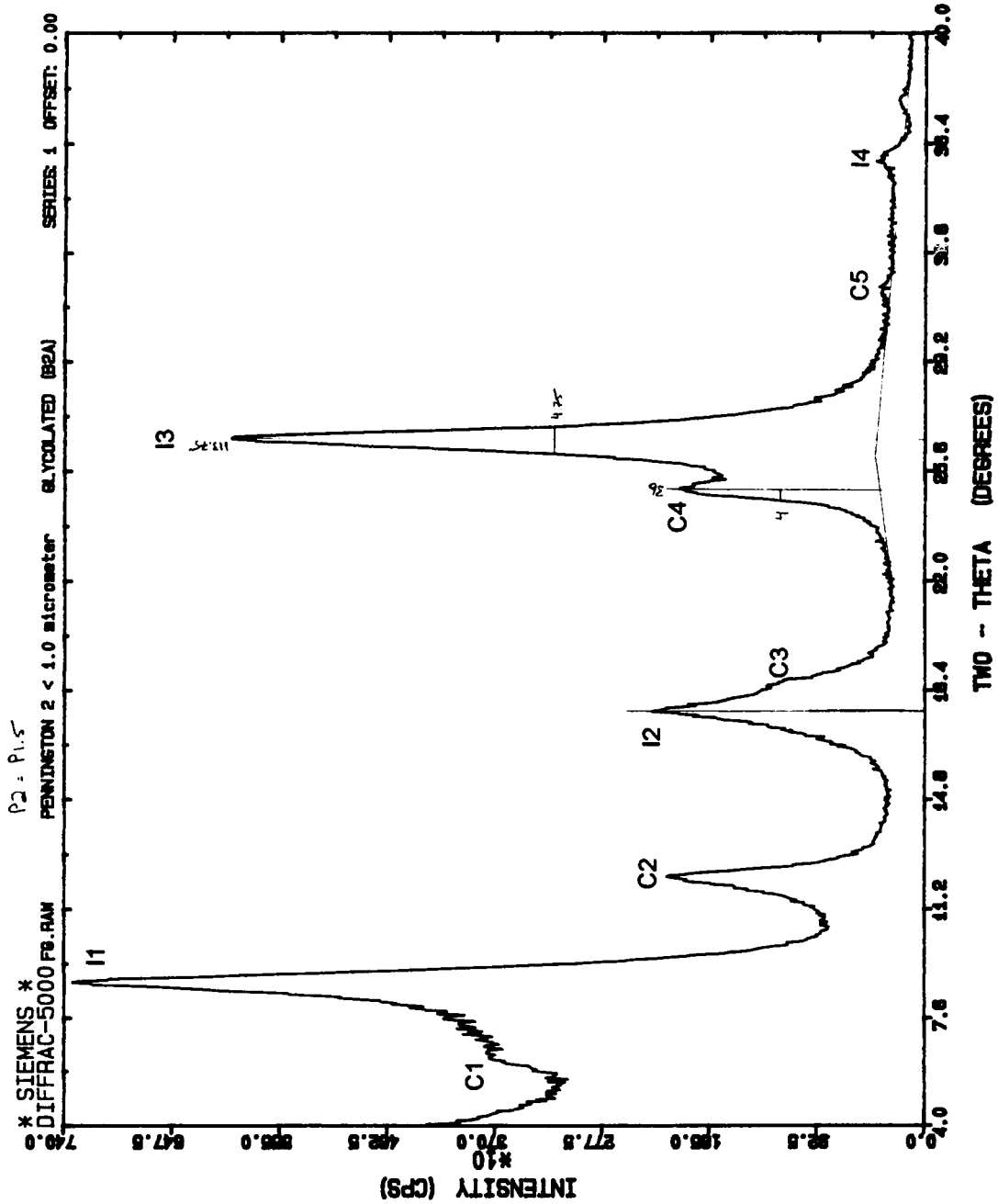
* SIEMENS *
DIFFRAC-5000
FB.RAW
PENNINGTON 2 < 1.0 micrometer
GLYCOLATED (B2A)
SERIES: 1 OFFSET: 0.00
I1
I2
I3
I4
C1
C2
C3
C4
C5
INTENSITY (CPS)
*10
TWO - THETA (DEGREES)

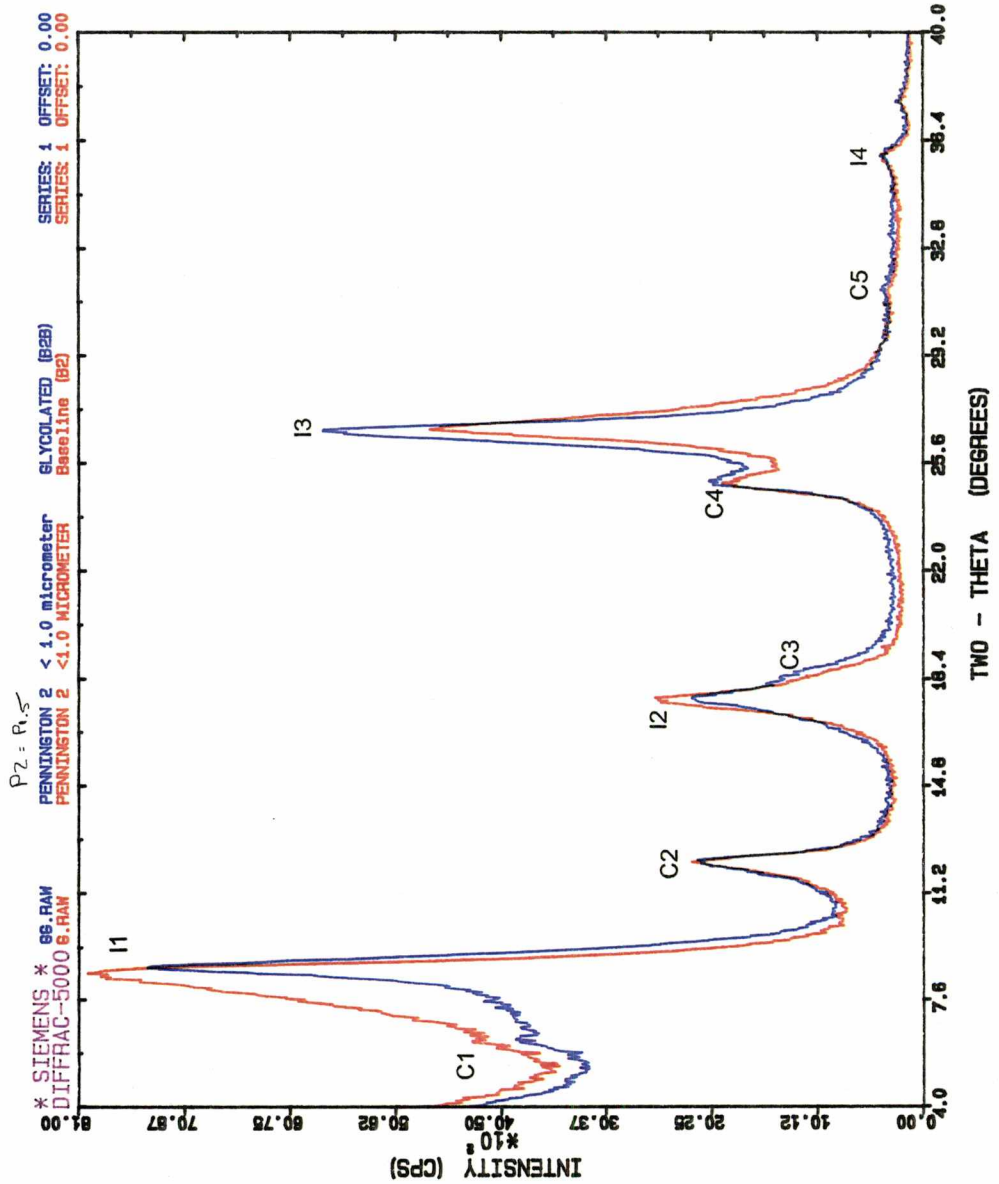
* SIEMENS *
DIFFRAC-5000
66.RAW
6.RAW
PENNINGTON 2 < 1.0 micrometer
PENNINGTON 2 <4.0 MICROMETER
GLYCOLATED (B2B)
Baseline (B2)
SERIES: 1 OFFSET: 0.00
SERIES: 1 OFFSET: 0.00
P2 = P1.5
I1
I2
I3
I4
C1
C2
C3
C4
C5
INTENSITY (CPS)
*10³
81.00
70.87
60.75
50.62
40.50
30.37
20.25
10.12
0.00
4.0
7.6
11.2
14.8
18.4
22.0
25.6
29.2
32.8
36.4
40.0
TWO - THETA (DEGREES)

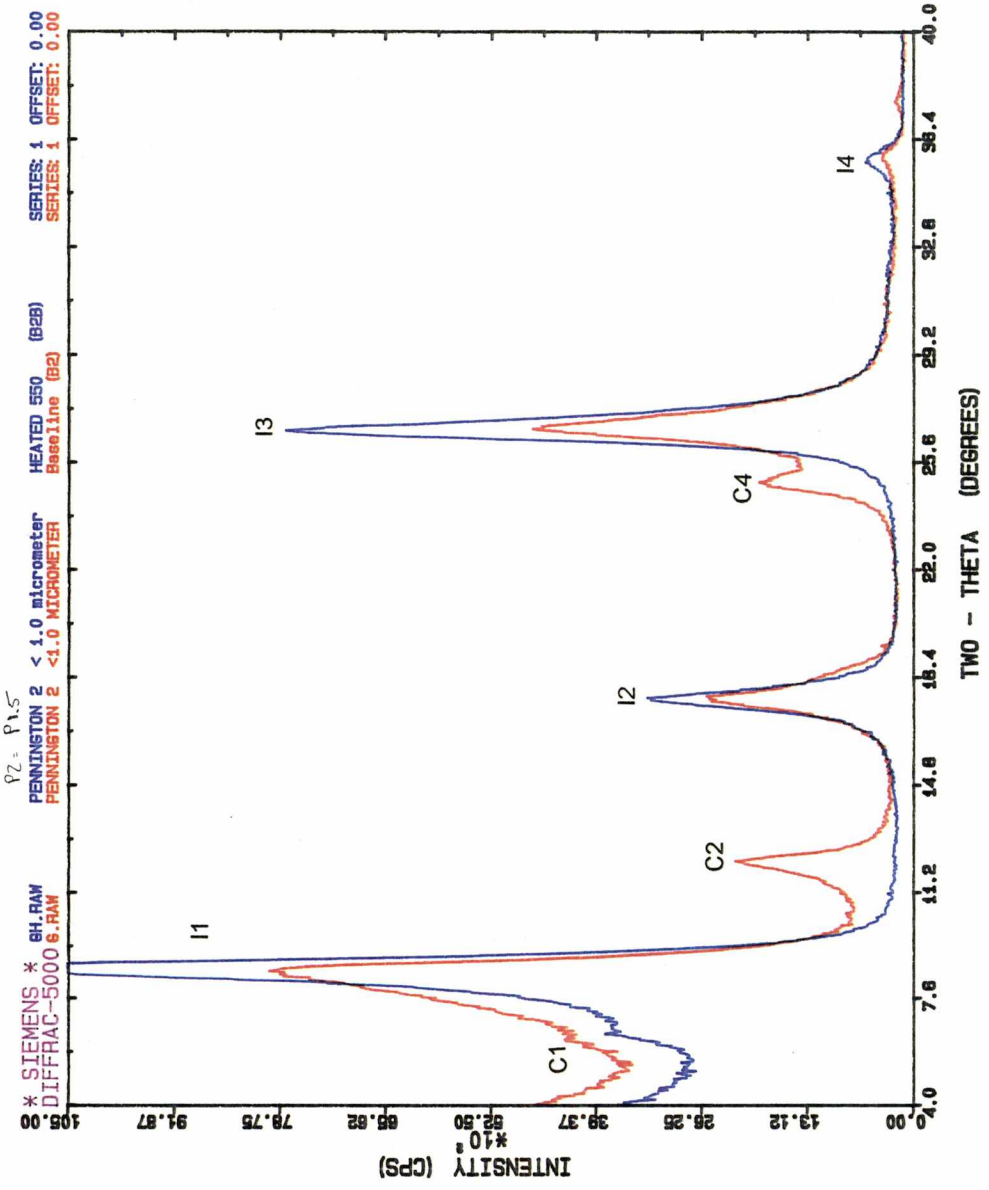
* SIEMENS *
DIFFRAC-5000
8H.RAW
6.RAW
PENNINGTON 2 < 1.0 micrometer
PENNINGTON 2 <1.0 MICROMETER
HEATED 550 (B2B)
Baseline (B2)
SERIES: 1 OFFSET: 0.00
SERIES: 1 OFFSET: 0.00
P2- P1.5
I1
I2
I3
I4
C1
C2
C4
INTENSITY (CPS)
*10^3
105.00
94.87
79.75
66.62
52.50
39.37
26.25
13.12
0.00
4.0
7.6
11.2
14.8
18.4
22.0
25.6
29.2
32.8
36.4
40.0
TWO - THETA (DEGREES)

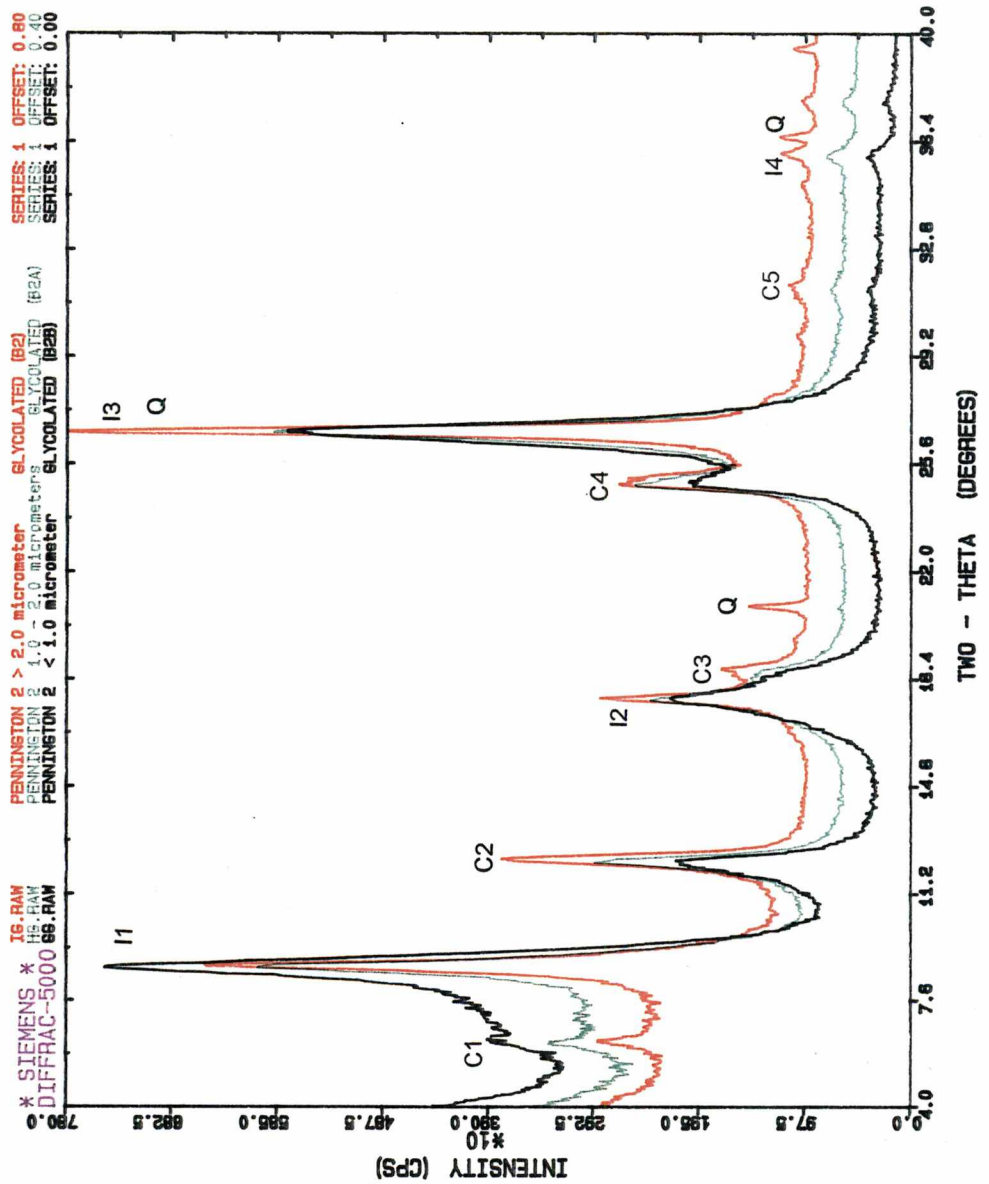
* SIEMENS *
DIFFRAC-5000
IG.RAW
HG.RAW
GG.RAW
PENNINGTON 2 > 2.0 micrometer
PENNINGTON 2 1.0 - 2.0 micrometers
PENNINGTON 2 < 1.0 micrometer
GLYCOLATED (B2)
GLYCOLATED (B2A)
GLYCOLATED (B2B)
SERIES: 1 OFFSET: 0.80
SERIES: 1 OFFSET: 0.40
SERIES: 1 OFFSET: 0.00
I1
C1
C2
I2
C3
Q
C4
I3
Q
C5
I4
Q
INTENSITY (CPS)
*10
780.0
682.5
585.0
487.5
390.0
292.5
195.0
97.5
0.0
4.0
7.6
11.2
14.8
18.4
22.0
25.6
29.2
32.8
36.4
40.0
TWO - THETA (DEGREES)

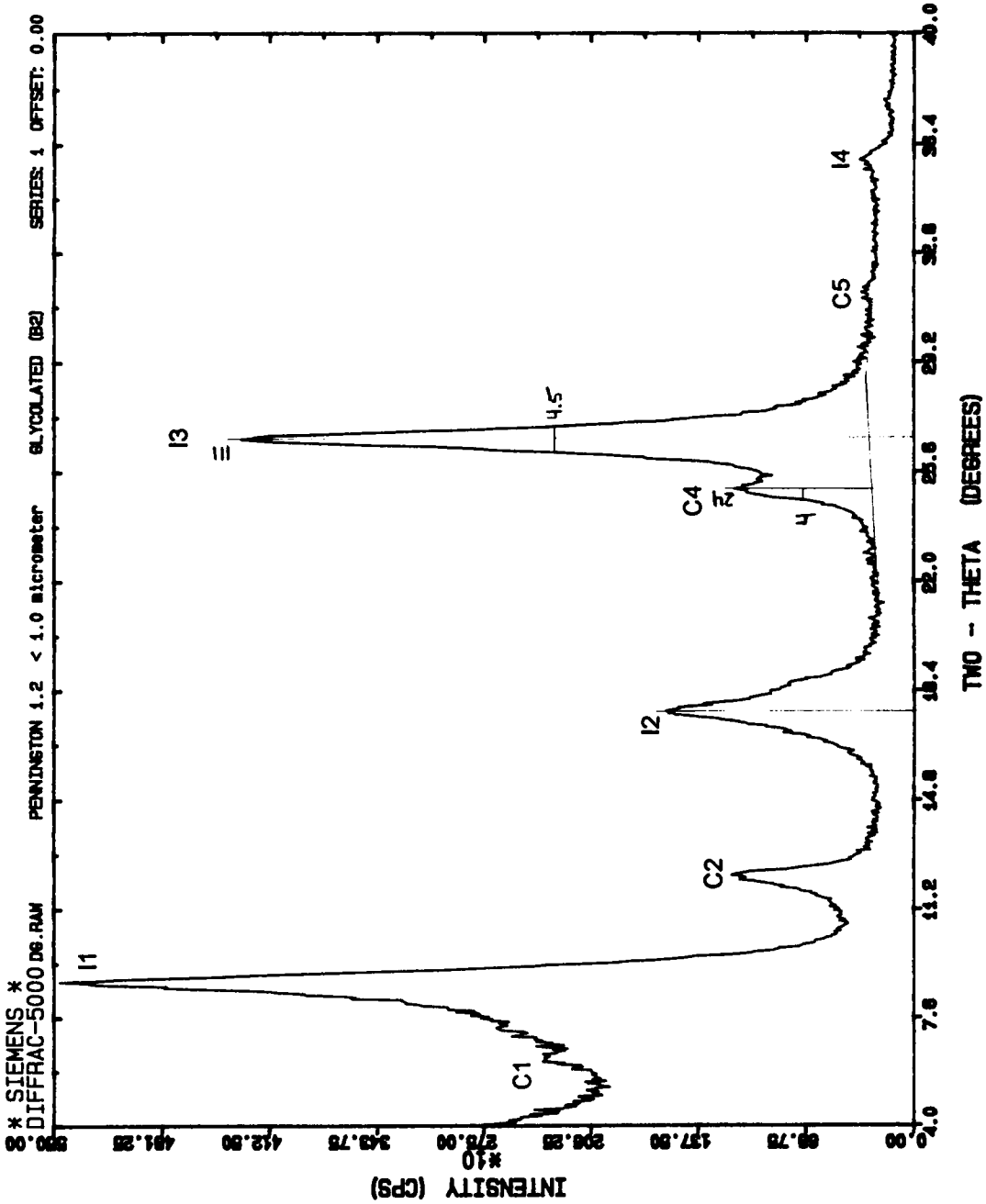
* SIEMENS *
DIFFRAC-5000 D8.RAW
PENNINGTON 1.2 < 1.0 micrometer GLYCOLATED (B2)
SERIES: 1 OFFSET: 0.00
I1
I2
I3
I4
C1
C2
C4
C5
4.5
4
INTENSITY (CPS)
*10
TWO - THETA (DEGREES)

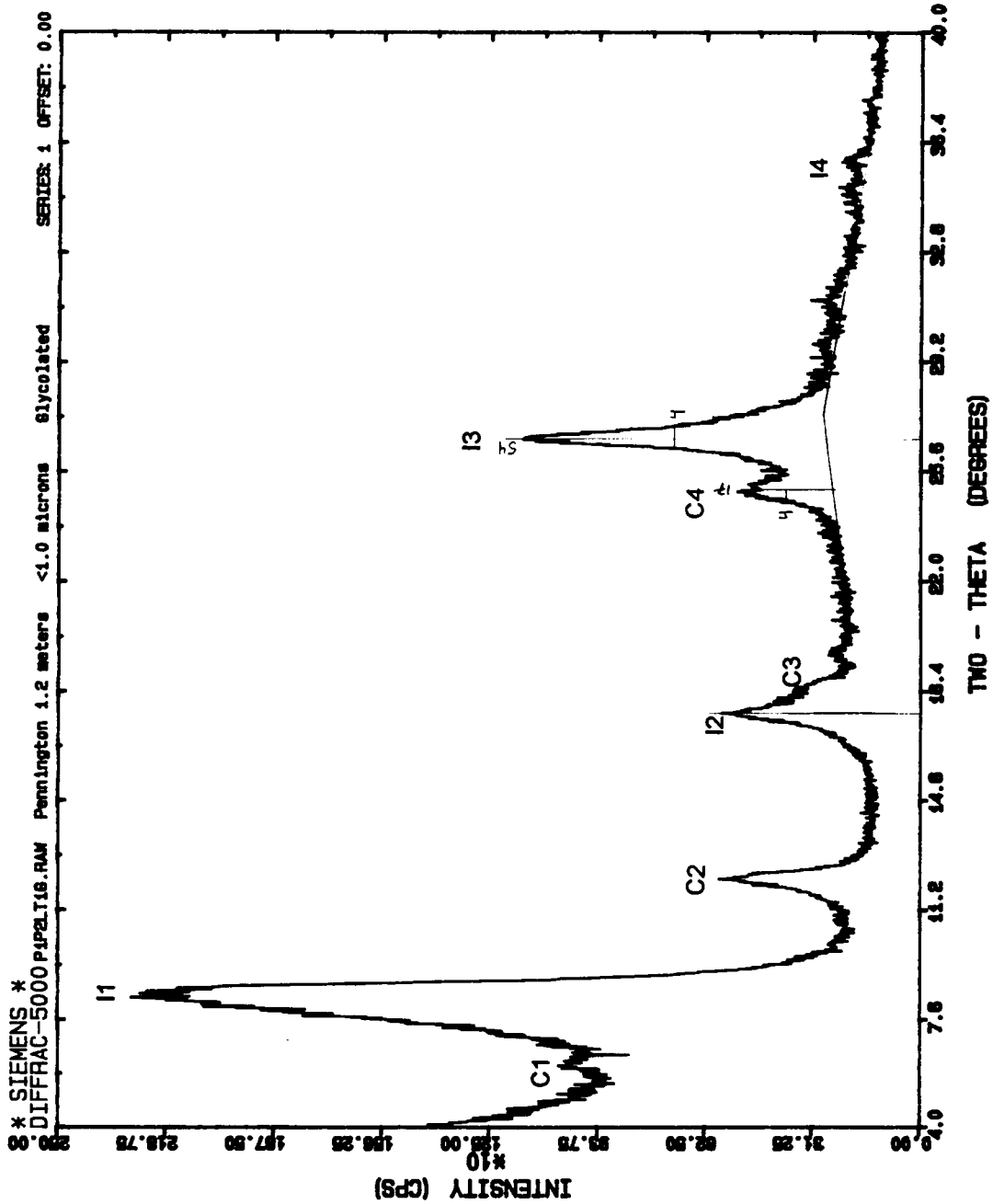
* SIEMENS *
DIFFRAC-5000 PJP2LT16.RAW Pennington 1.2 meters <1.0 microns Glycolated SERIES: 1 OFFSET: 0.00
INTENSITY (CPS)
*10
TWO - THETA (DEGREES)
I1
I2
I3
I4
C1
C2
C3
C4

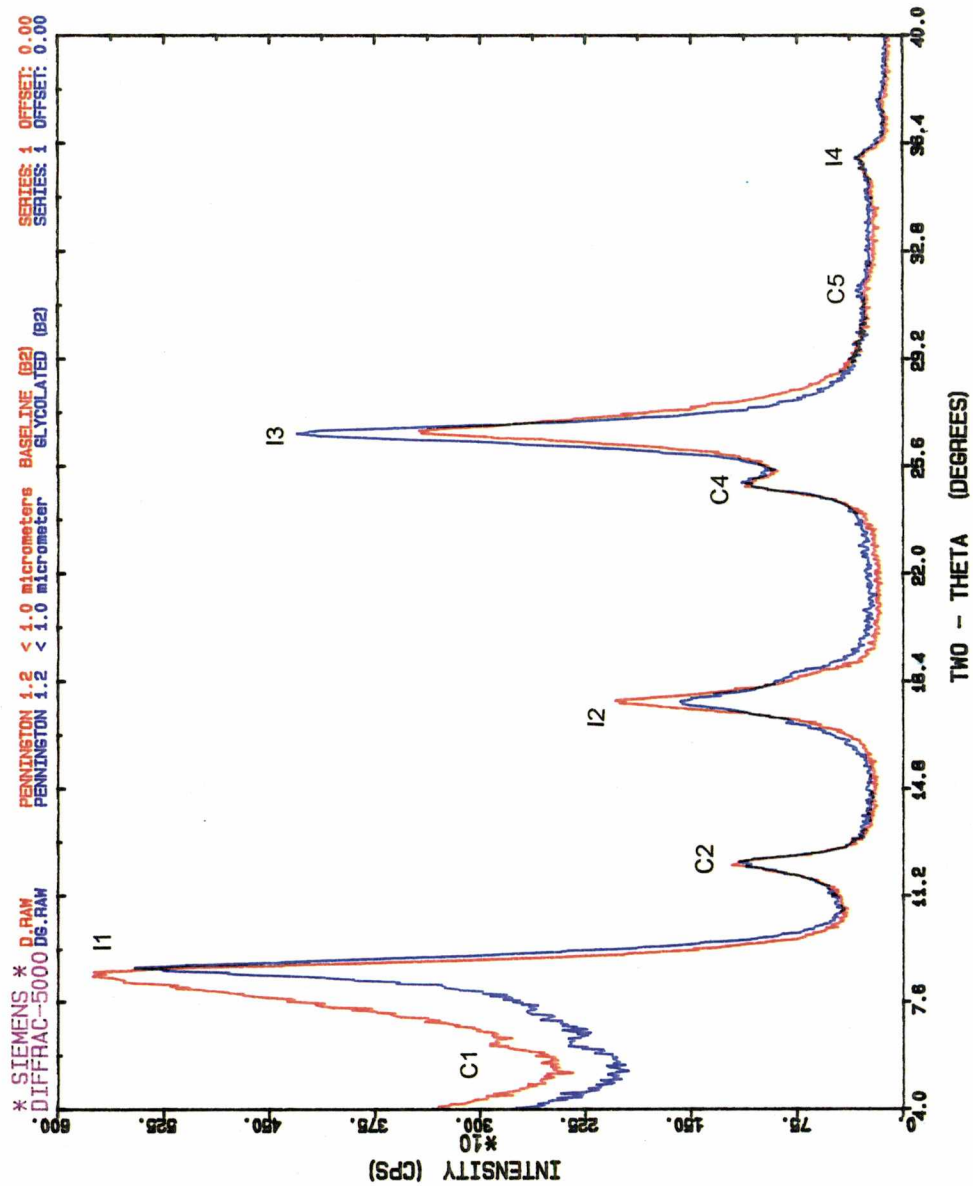
* SIEMENS *
DIFFRAC-5000
D.RAM
D6.RAW
PENNINGTON 1.2 < 1.0 micrometers
PENNINGTON 1.2 < 1.0 micrometer
BASELINE (B2)
GLYCOLATED (B2)
SERIES: 1 OFFSET: 0.00
SERIES: 1 OFFSET: 0.00
I1
I2
I3
I4
I5
C1
C2
C4
C5
INTENSITY (CPS)
*10
TWO - THETA (DEGREES)

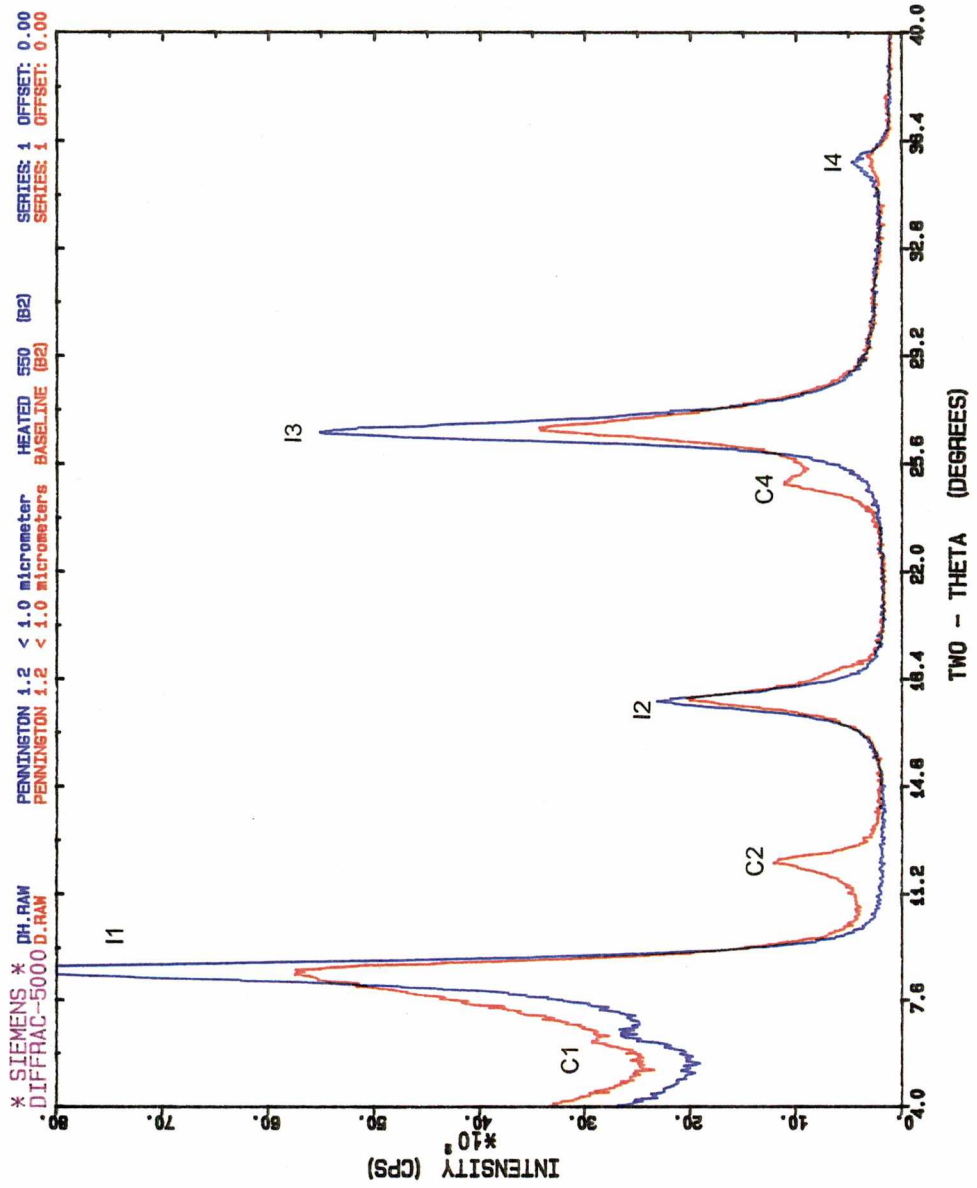
* SIEMENS *
DIFFRAC-5000
DH.RAW
D.RAW
PENNINGTON 1.2 < 1.0 micrometer HEATED 550 (B2)
PENNINGTON 1.2 < 1.0 micrometers BASELINE (B2)
SERIES: 1 OFFSET: 0.00
SERIES: 1 OFFSET: 0.00
I1
I2
I3
I4
C1
C2
C4
INTENSITY (CPS)
*10
TWO - THETA (DEGREES)

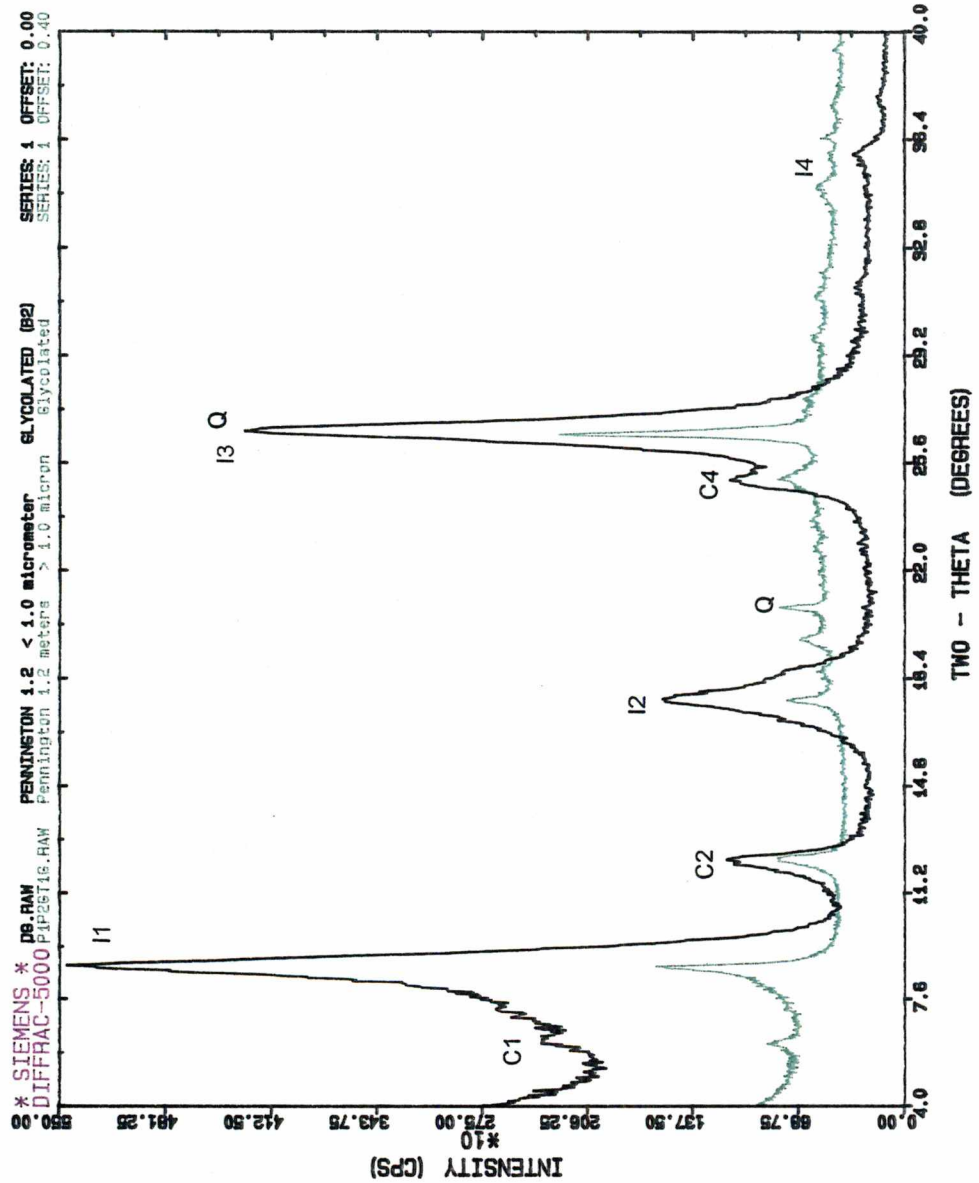
* SIEMENS * DB.RAW PENNINGTON 1.2 < 1.0 micrometer GLYCOLATED (B2) SERIES: 1 OFFSET: 0.00
DIFFRAC-5000 P1P26T16.RAW Pennington 1.2 meters > 1.0 micron Glycolated SERIES: 1 OFFSET: 0.40
I1
I3 Q
C1
C2
I2
Q
C4
I4
INTENSITY (CPS)
*10
550.00
481.25
412.50
343.75
275.00
206.25
137.50
68.75
0.00
4.0
7.6
11.2
14.8
18.4
22.0
25.6
29.2
32.8
36.4
40.0
TWO - THETA (DEGREES)

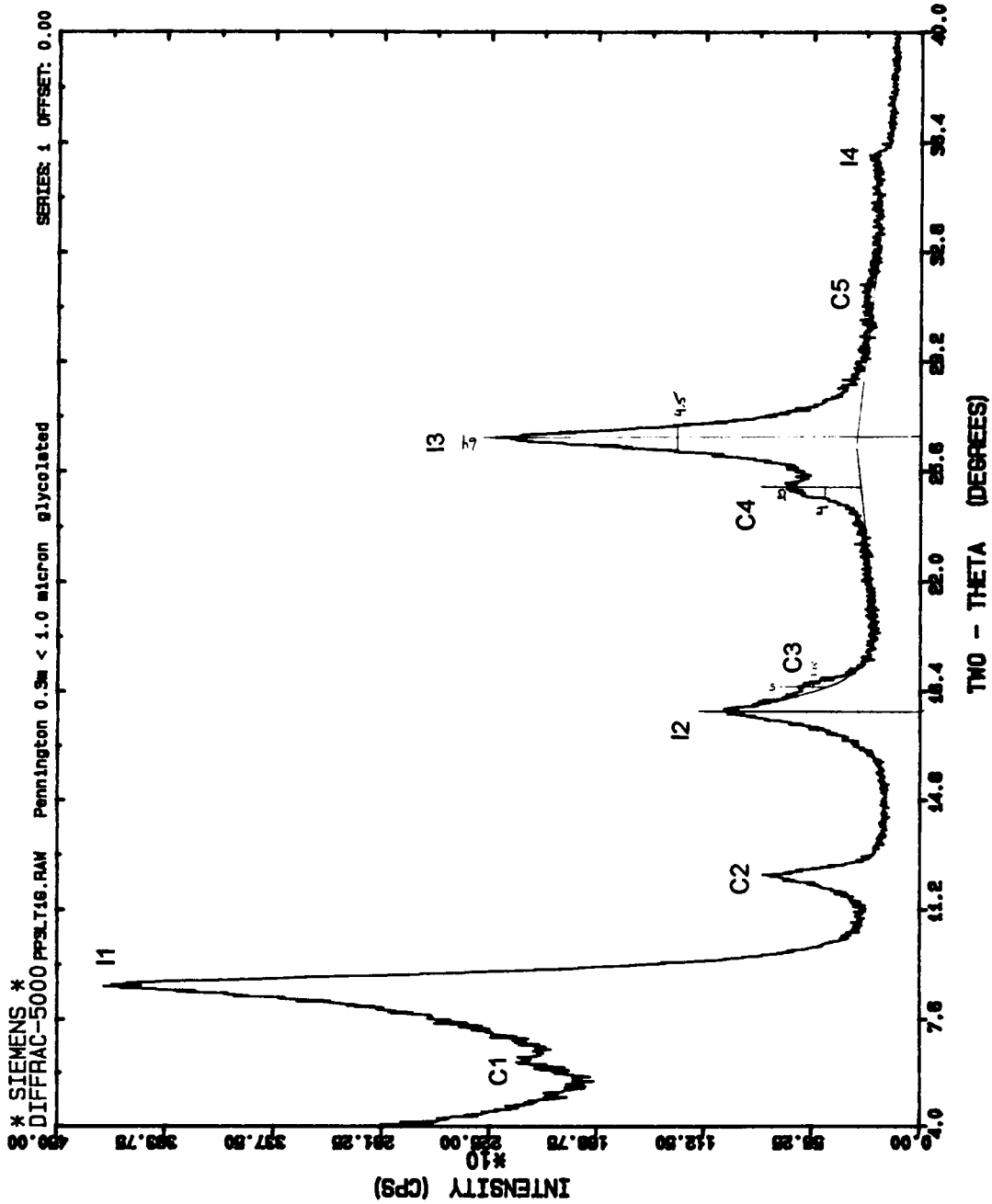
* SIEMENS *
DIFFRAC-5000 PPSL716.RAW Pennington 0.5m < 1.0 micron glycolated
SERIES: 1 OFFSET: 0.00
I1
I2
I3
I4
C1
C2
C3
C4
C5
INTENSITY (CPS)
*10
TWO - THETA (DEGREES)

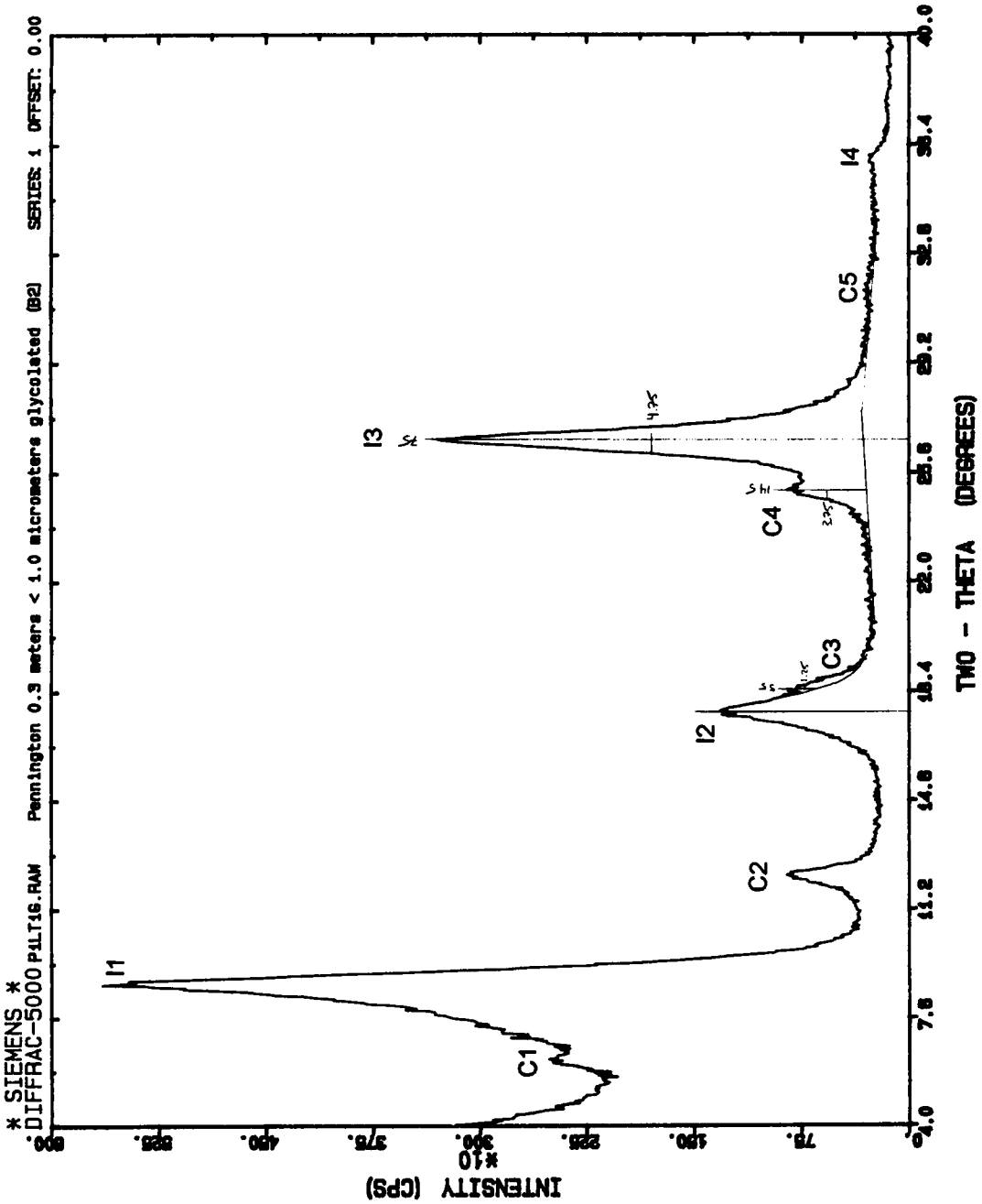
* SIEMENS *
DIFFRAC-5000 P&LT16.RAW Pennington 0.3 meters < 1.0 micrometers glycolated (B2) SERIES: 1 OFFSET: 0.00
INTENSITY (CPS)
*10
TWO - THETA (DEGREES)
I1
I2
I3
I4
C1
C2
C3
C4
C5

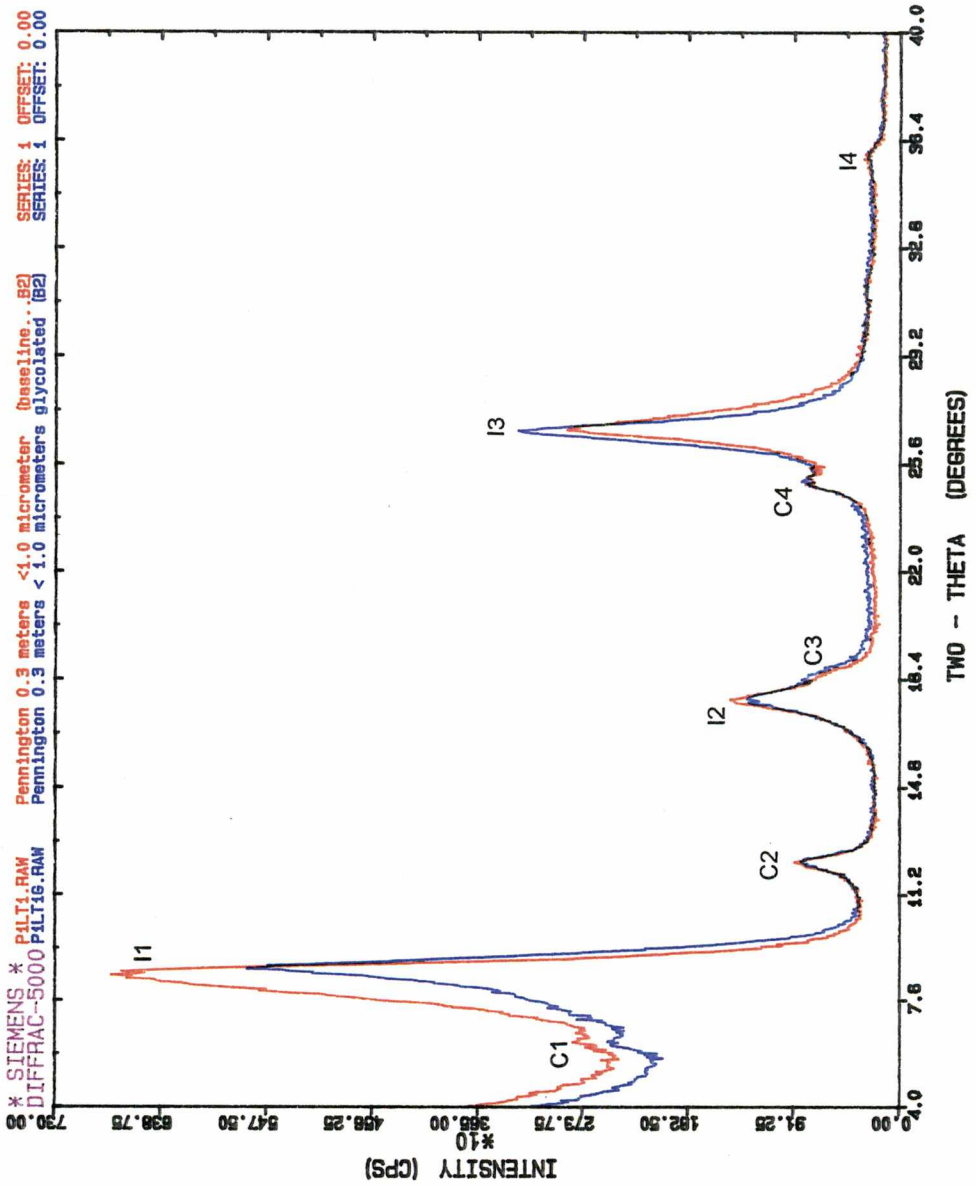
* SIEMENS * P4LT1.RAW Pennington 0.3 meters <1.0 micrometer (baseline...B2) SERIES: 1 OFFSET: 0.00
DIFFRAC-5000 P4LT16.RAW Pennington 0.3 meters < 1.0 micrometers glycolated (B2) SERIES: 1 OFFSET: 0.00
730.00
638.75
547.50
456.25
365.00
273.75
182.50
91.25
0.00
INTENSITY (CPS)
*10
4.0
7.6
11.2
14.8
18.4
22.0
25.6
29.2
32.8
36.4
40.0
TWO - THETA (DEGREES)
I1
I2
I3
I4
C1
C2
C3
C4

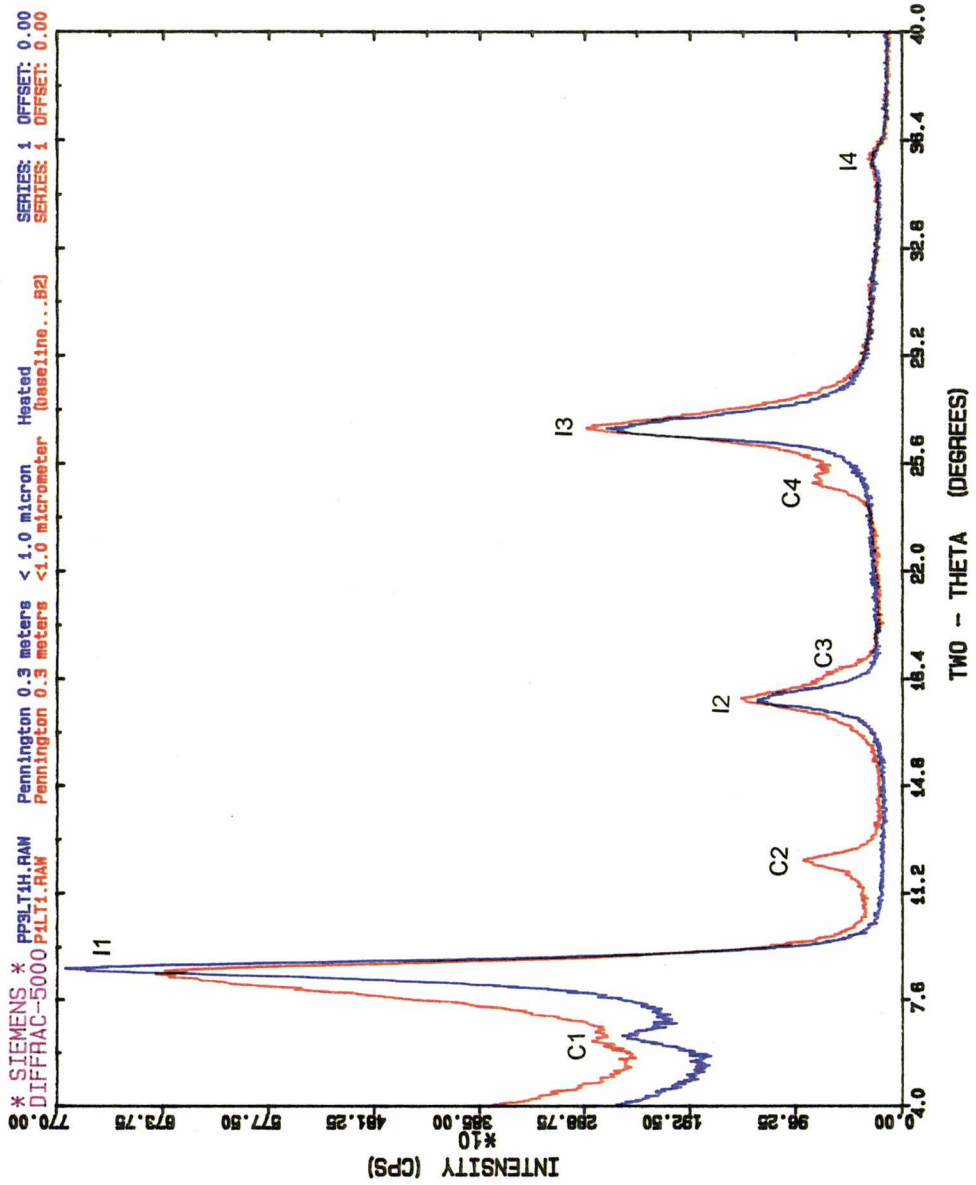
* SIEMENS * PP3LT1H.RAW Pennington 0.3 meters <1.0 micron Heated SERIES: 1 OFFSET: 0.00
DIFFRAC-5000 P1LT1.RAW Pennington 0.3 meters <1.0 micrometer (baseline...B2) SERIES: 1 OFFSET: 0.00
I1
I2
I3
I4
C1
C2
C3
C4
INTENSITY (CPS)
*10
770.00
673.75
577.50
481.25
385.00
288.75
192.50
96.25
.00
4.0
7.6
11.2
14.8
18.4
22.0
25.6
29.2
32.8
36.4
40.0
TWO - THETA (DEGREES)

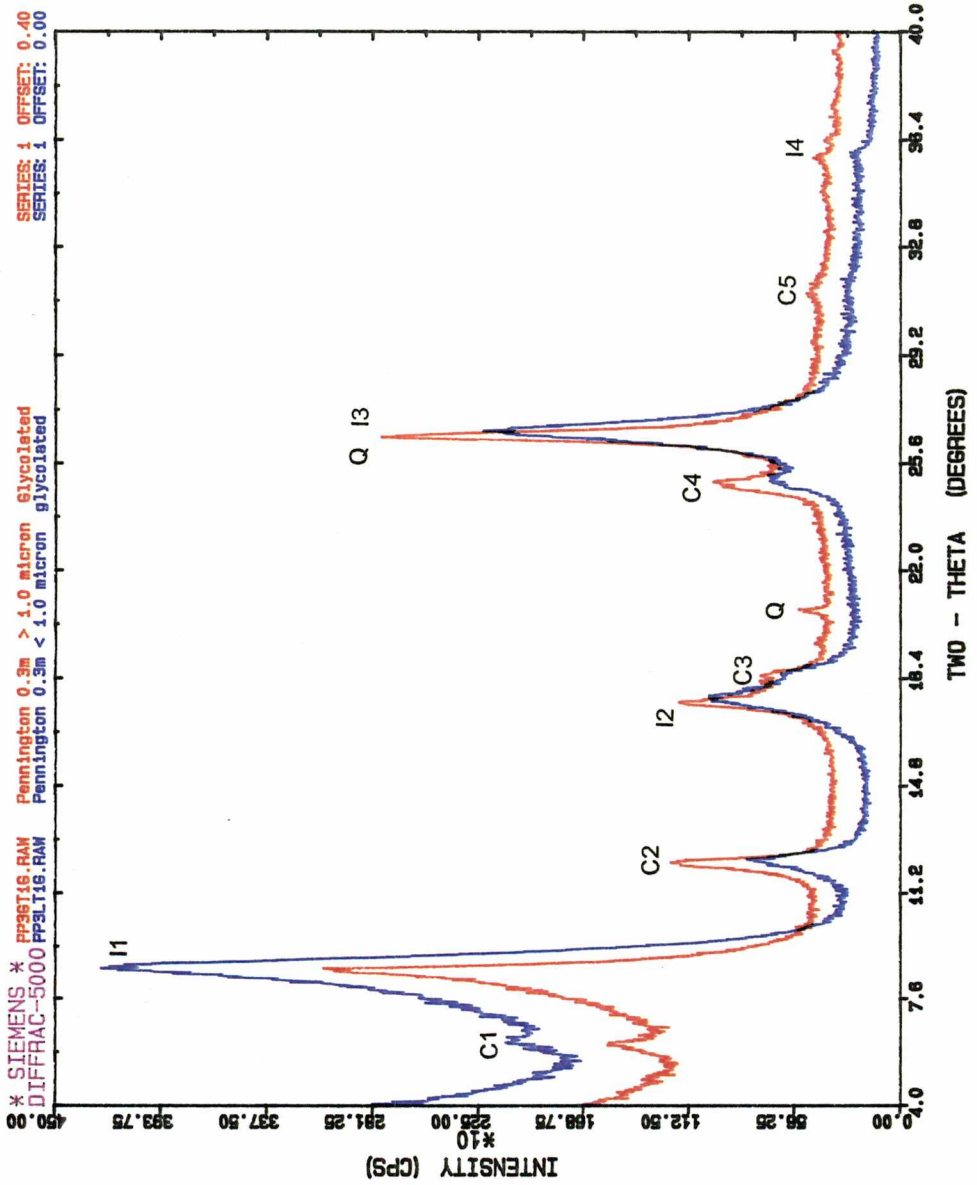
* SIEMENS *
DIFFRAC-5000
PP3GT16.RAM
PP3LT16.RAM
Pennington 0.3m > 1.0 micron Glycolated
Pennington 0.3m < 1.0 micron glycolated
SERIES: 1 OFFSET: 0.40
SERIES: 1 OFFSET: 0.00
I1
C1
C2
I2
C3
Q
C4
Q I3
C5
I4
INTENSITY (CPS)
*10
450.00
393.75
337.50
281.25
225.00
168.75
112.50
56.25
.00
4.0
7.6
11.2
14.8
18.4
22.0
25.8
29.2
32.8
36.4
40.0
TWO - THETA (DEGREES)

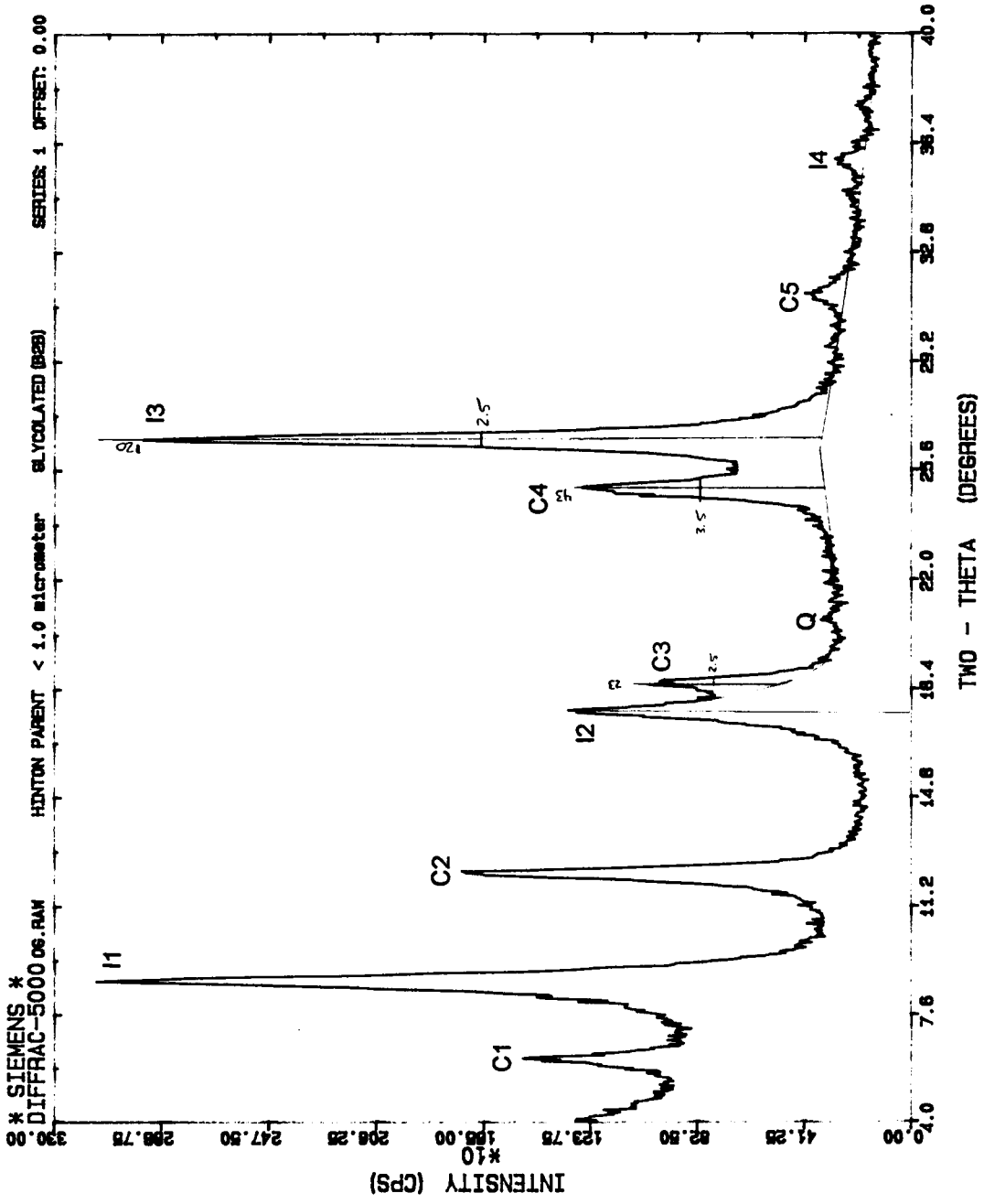
* SIEMENS *
DIFFRAC-5000 06.RAW
HINTON PARENT < 1.0 micrometer GLYCOLATED (B2B)
SERIES: 1 OFFSET: 0.00
I1
C1
C2
I2
C3
Q
C4
I3
C5
I4
INTENSITY (CPS)
*10
330.00
288.78
247.50
206.25
165.00
123.78
82.50
41.25
0.00
4.0
7.6
11.2
14.8
18.4
22.0
25.6
29.2
32.8
36.4
40.0
TWO - THETA (DEGREES)

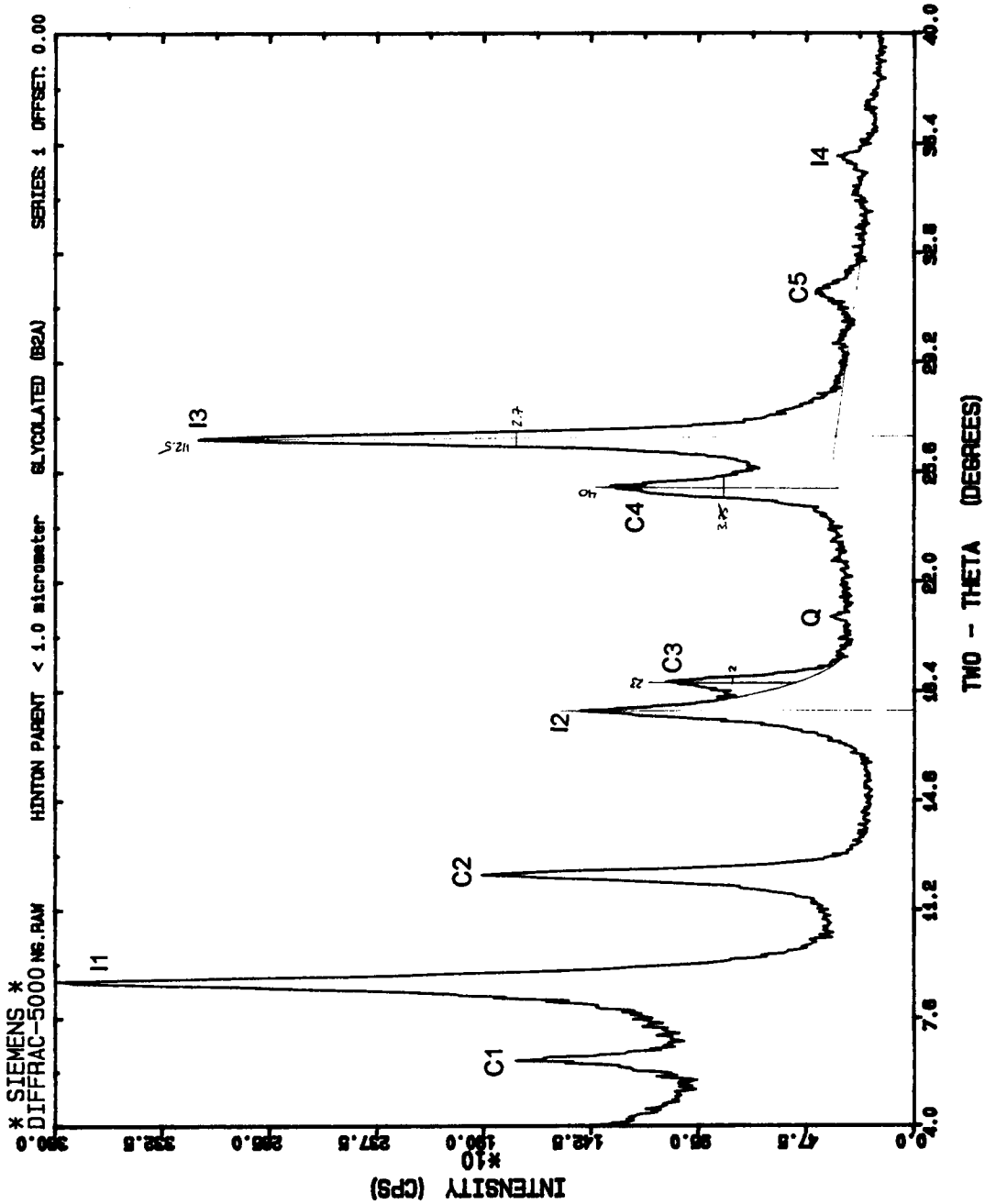
* SIEMENS *
DIFFRAC-5000 NG.RAW
HINTON PARENT < 1.0 micrometer GLYCOLATED (B2A)
SERIES: 1 OFFSET: 0.00
INTENSITY (CPS)
*10
TWO - THETA (DEGREES)
I1
I2
I3
I4
C1
C2
C3
C4
C5
Q

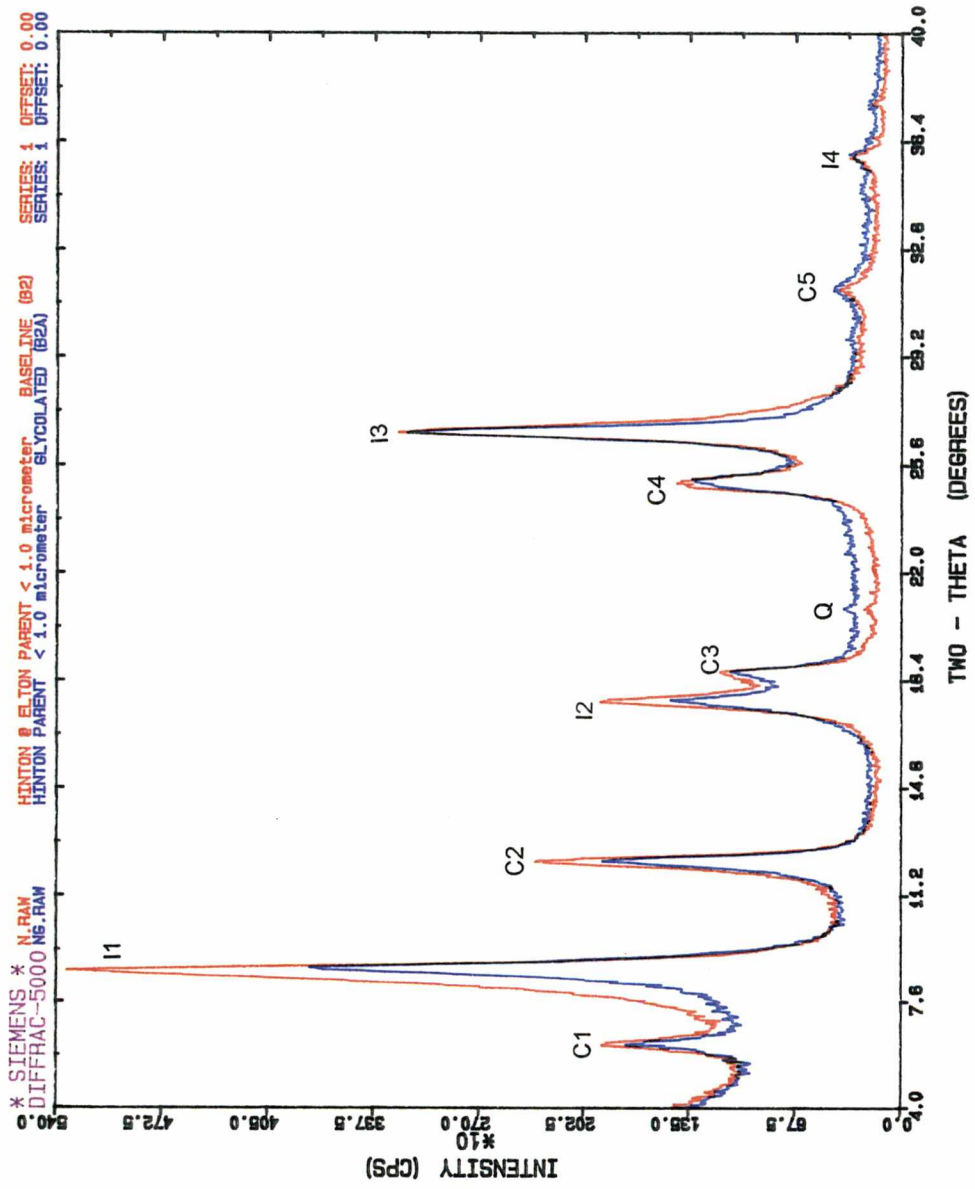
* SIEMENS * N.RAW
DIFFRAC-5000 N6.RAW
HINTON @ ELTON PARENT < 1.0 micrometer BASELINE (B2)
HINTON PARENT < 1.0 micrometer GLYCOLATED (B2A)
SERIES: 1 OFFSET: 0.00
SERIES: 1 OFFSET: 0.00
INTENSITY (CPS)
*10
540.0
472.5
405.0
337.5
270.0
202.5
135.0
67.5
0.0
4.0
7.6
11.2
14.8
18.4
22.0
25.6
29.2
32.8
36.4
40.0
TWO - THETA (DEGREES)
I1
I2
I3
I4
C1
C2
C3
C4
C5
Q

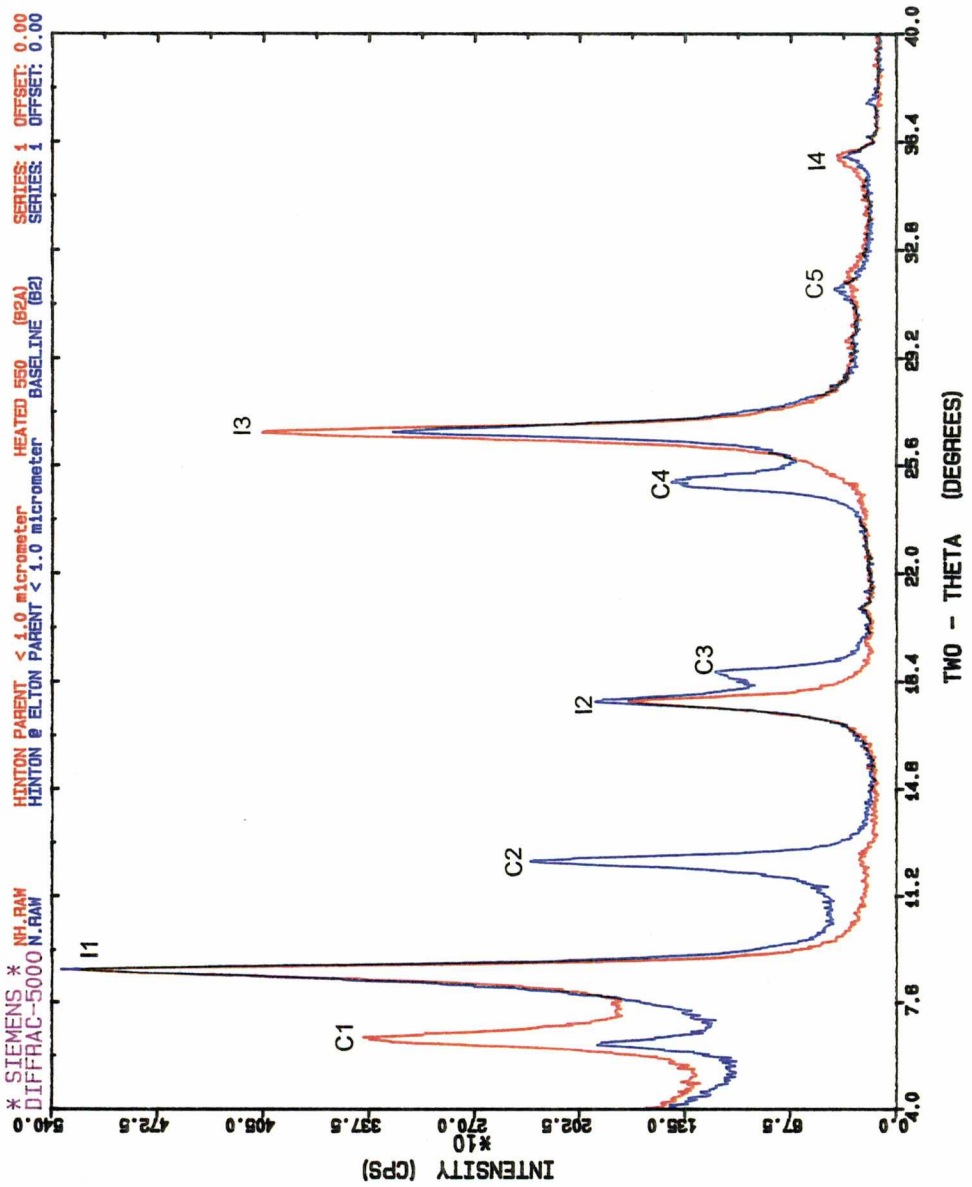
* SIEMENS *
DIFFRAC-5000
NH.RAW
N.RAW
HINTON PARENT < 1.0 micrometer HEATED 550 (B2A)
HINTON @ ELTON PARENT < 1.0 micrometer BASELINE (B2)
SERIES: 1 OFFSET: 0.00
SERIES: 1 OFFSET: 0.00
I1
I2
I3
I4
C1
C2
C3
C4
C5
INTENSITY (CPS)
*10
540.0
472.5
405.0
337.5
270.0
202.5
135.0
67.5
0.0
4.0
7.8
11.2
14.8
18.4
22.0
25.6
29.2
32.8
36.4
40.0
TWO - THETA (DEGREES)

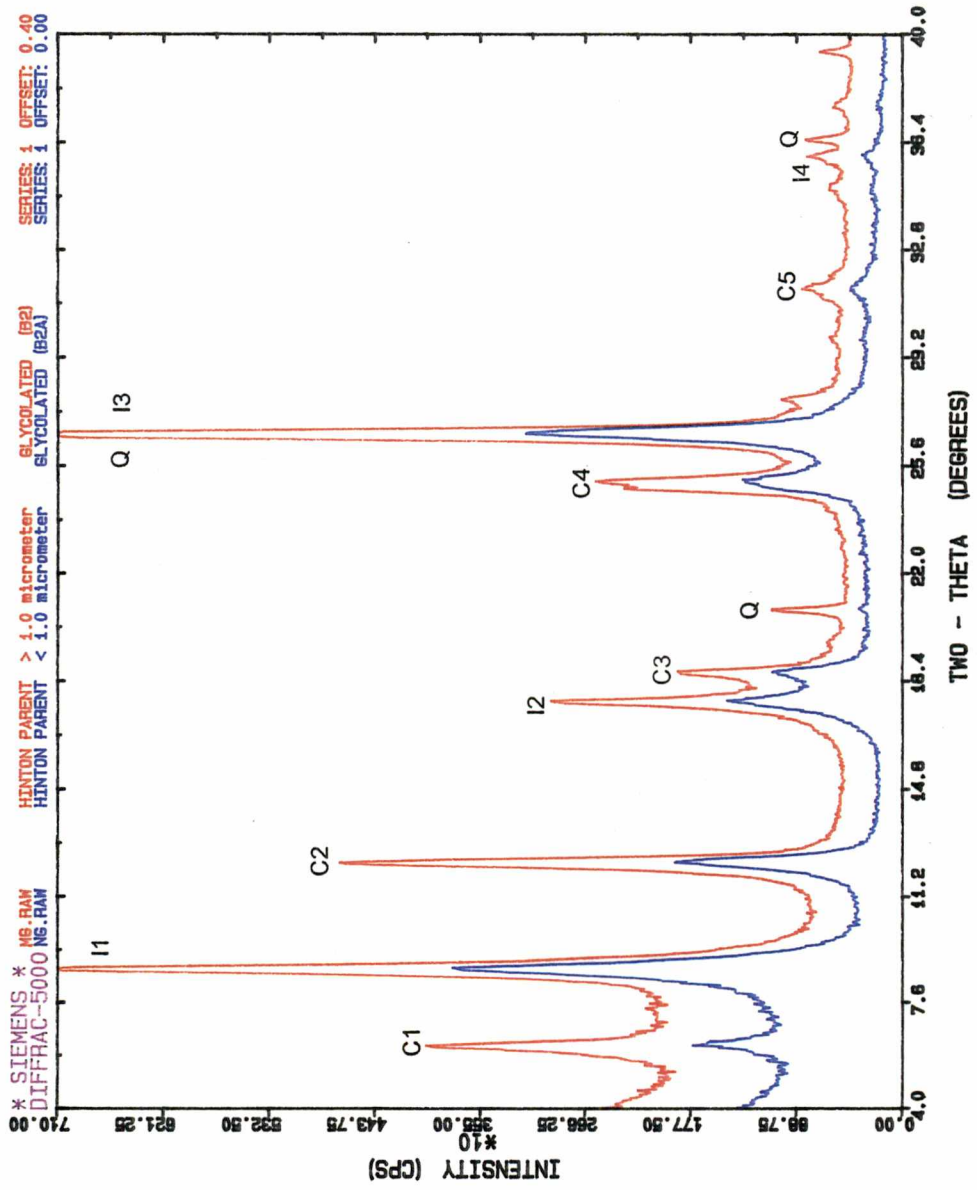
* SIEMENS *
DIFFRAC-5000
MG.RAW
MG.RAW
HINTON PARENT > 1.0 micrometer
HINTON PARENT < 1.0 micrometer
GLYCOLATED (B2)
GLYCOLATED (B2A)
SERIES: 1 OFFSET: 0.40
SERIES: 1 OFFSET: 0.00
I1
C1
C2
I2
C3
Q
C4
Q
I3
C5
I4
Q
740.00
621.25
532.50
443.75
355.00
266.25
177.50
88.75
0.00
*10
INTENSITY (CPS)
4.0
7.6
11.2
14.8
18.4
22.0
25.6
29.2
32.8
36.4
40.0
TWO - THETA (DEGREES)

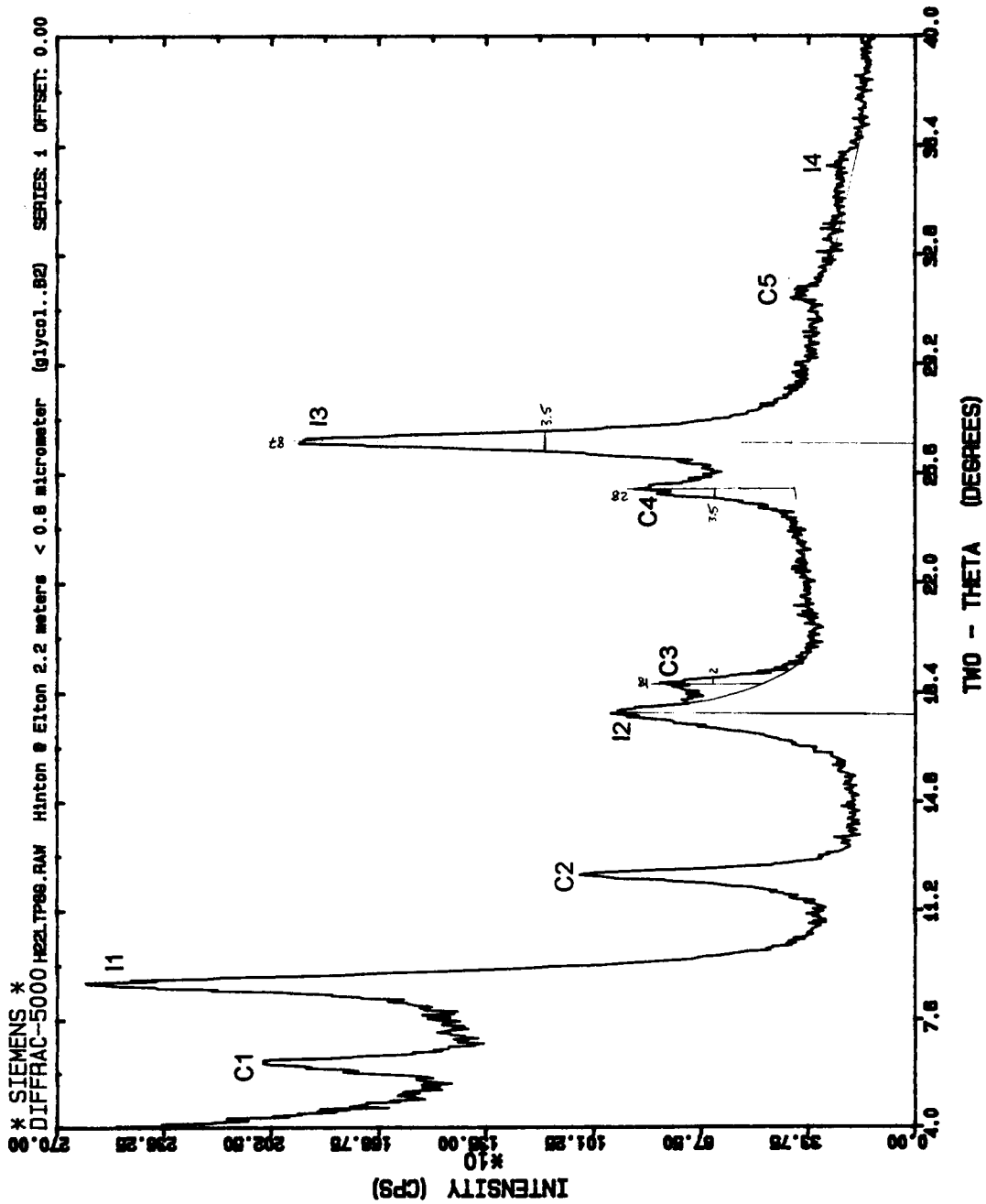
* SIEMENS *
DIFFRAC-5000 H22\TP68.RAW Hinton @ Elton 2.2 meters < 0.8 micrometer (glycol..82) SERIES: 1 OFFSET: 0.00
I1
C1
C2
I2
C3
C4
I3
C5
I4
INTENSITY (CPS)
*10
TWO - THETA (DEGREES)

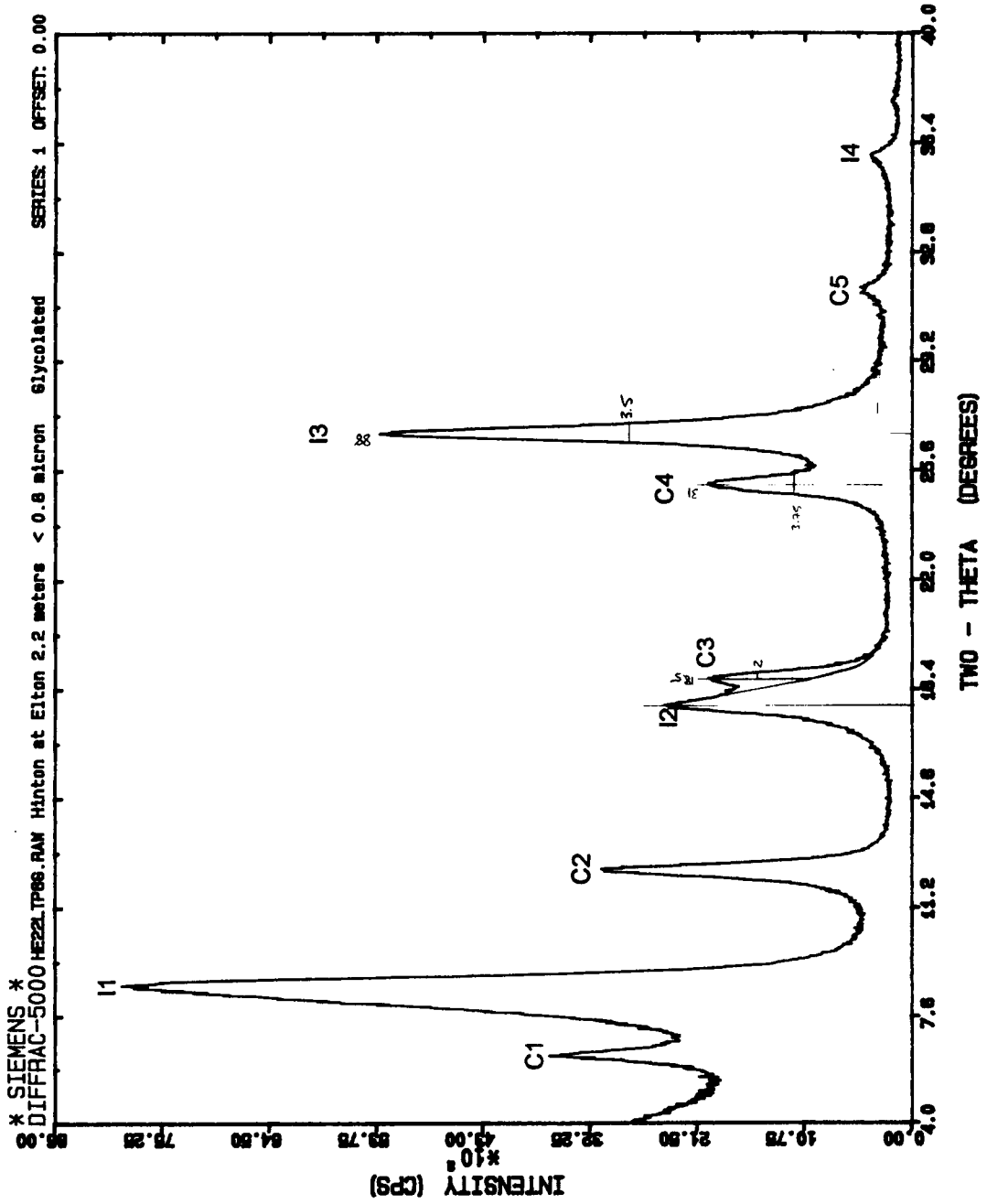
* SIEMENS *
DIFFRAC-5000 HE22LTP88.RAW Hinton at Elton 2.2 meters < 0.8 micron Glycolated SERIES: 1 OFFSET: 0.00
I1
C1
C2
I2
C3
I3
C4
C5
I4
INTENSITY (CPS)
*10³
TWO - THETA (DEGREES)

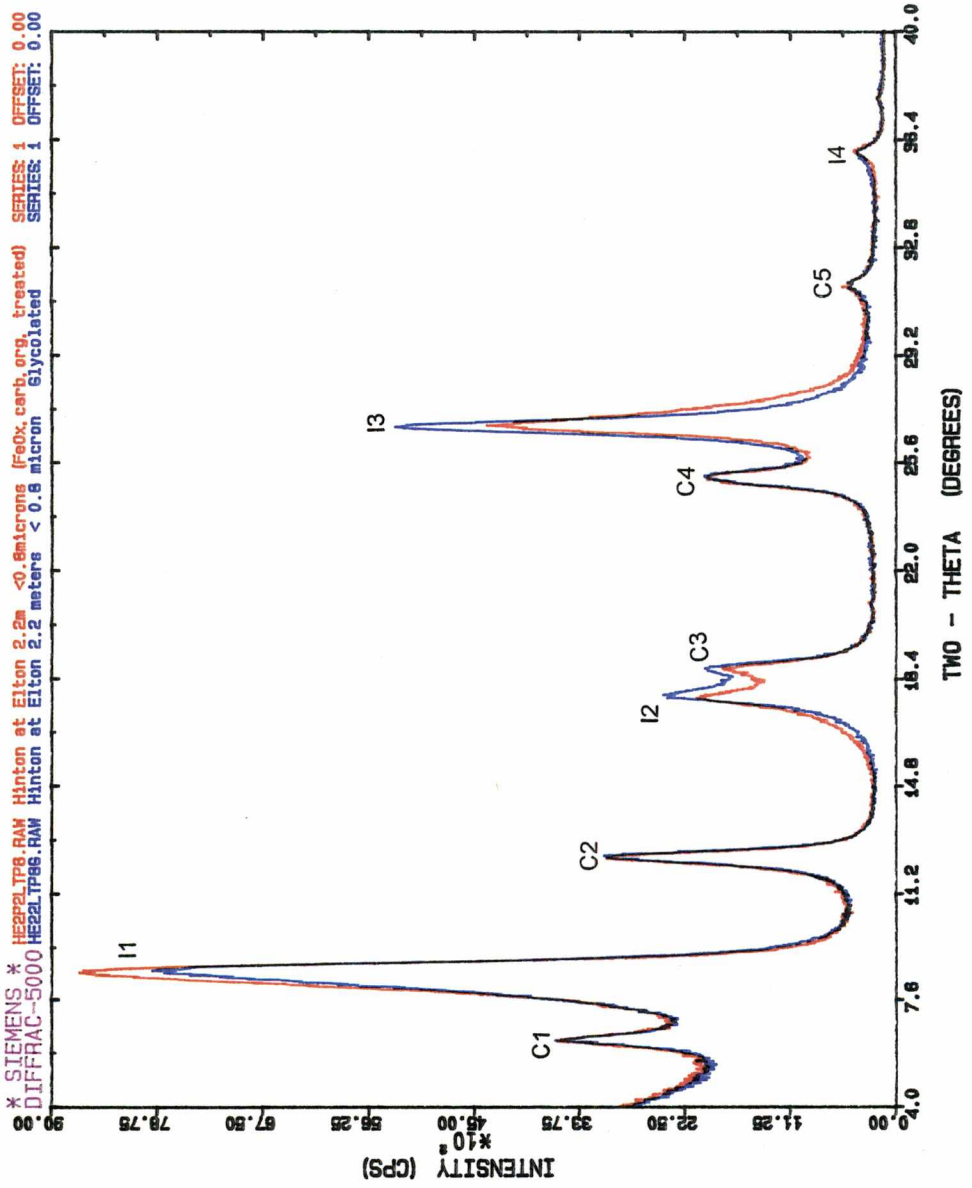
* SIEMENS *
DIFFRAC-5000
HE22LTP8.RAW Hinton at Elton 2.2m <0.8microns (FeOx,carb,org, treated) SERIES: 1 OFFSET: 0.00
HE22LTP86.RAW Hinton at Elton 2.2 meters < 0.8 micron Glycolated SERIES: 1 OFFSET: 0.00
I1
C1
C2
I2
C3
C4
I3
C5
I4
INTENSITY (CPS)
*10
90.00
78.75
67.50
56.25
45.00
33.75
22.50
11.25
0.00
4.0
7.6
11.2
14.8
18.4
22.0
25.6
29.2
32.8
36.4
40.0
TWO - THETA (DEGREES)

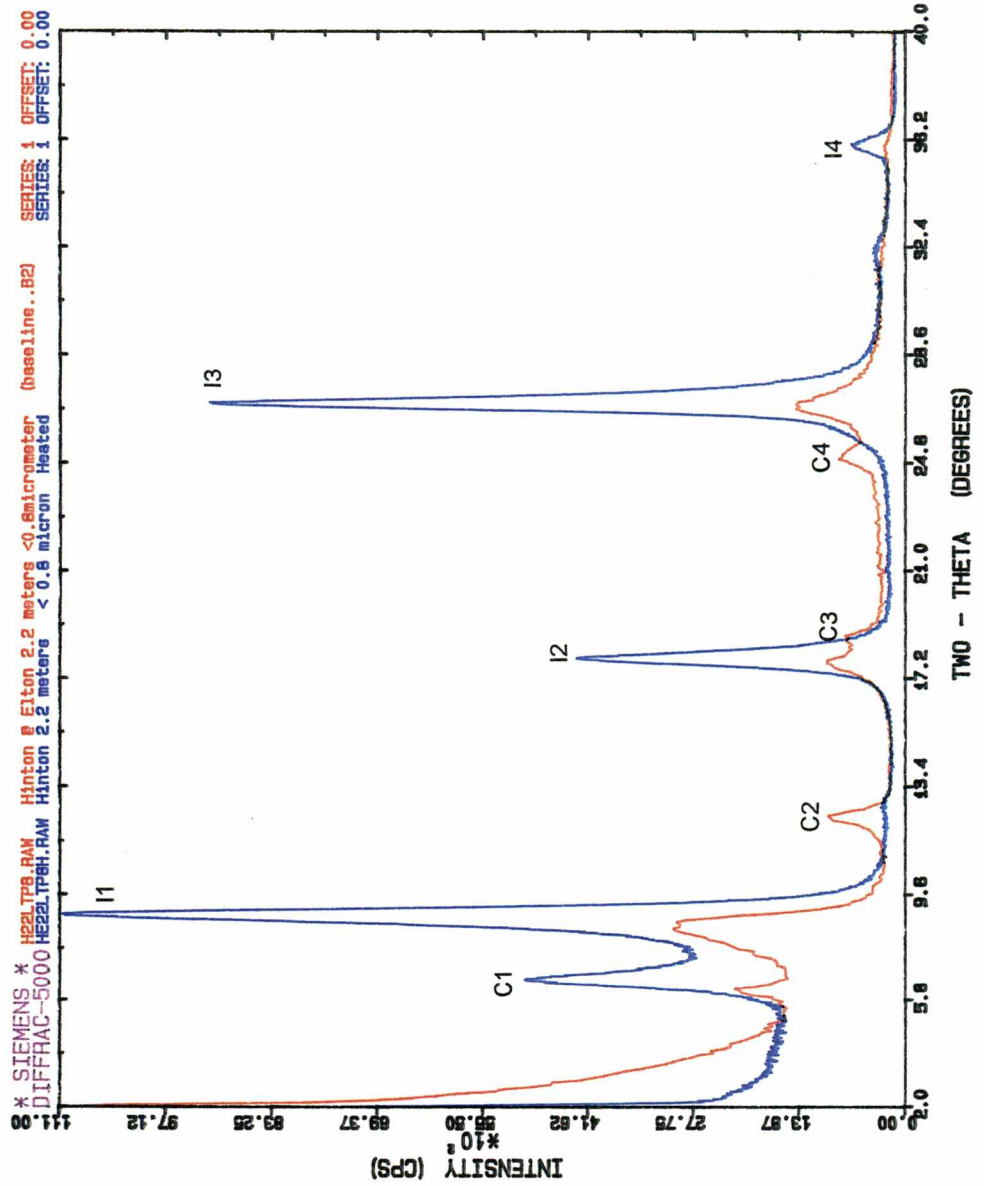
* SIEMENS *
DIFFRAC-5000
H22LTP8.RAW Hinton @ Elton 2.2 meters <0.8micrometer (baseline..B2) SERIES: 1 OFFSET: 0.00
H22LTP8H.RAW Hinton 2.2 meters < 0.8 micron Heated SERIES: 1 OFFSET: 0.00
I1
I2
I3
I4
C1
C2
C3
C4
INTENSITY (CPS)
*10
TWO - THETA (DEGREES)

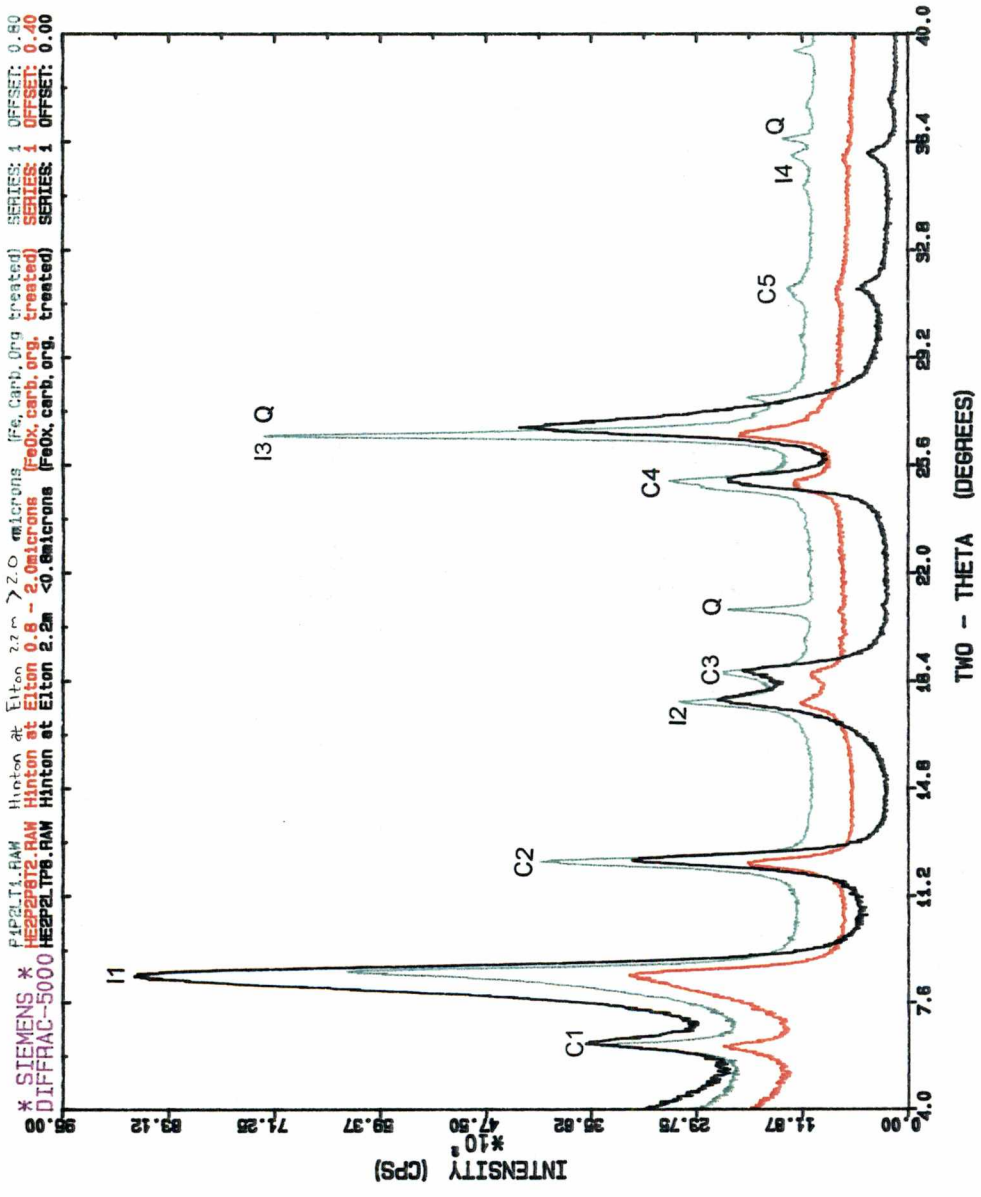
* SIEMENS * DIFFRAC-5000
F4P2LT1.RAW Hinton at Elton 2.2m >2.0 microns (Fe, Carb, Org treated) SERIES: 1 OFFSET: 0.80
HE2PP8T2.RAW Hinton at Elton 0.8 - 2.0microns (FeOx, carb, org, treated) SERIES: 1 OFFSET: 0.40
HE2P2LTP6.RAW Hinton at Elton 2.2m <0.8microns (FeOx, carb, org, treated) SERIES: 1 OFFSET: 0.00
I1
C1
C2
I2
C3
Q
C4
I3
Q
C5
I4
Q
INTENSITY (CPS)
*10³
95.00
83.12
71.25
59.37
47.50
35.62
23.75
11.87
0.00
4.0
7.8
11.2
14.8
18.4
22.0
25.6
29.2
32.8
36.4
40.0
TWO - THETA (DEGREES)

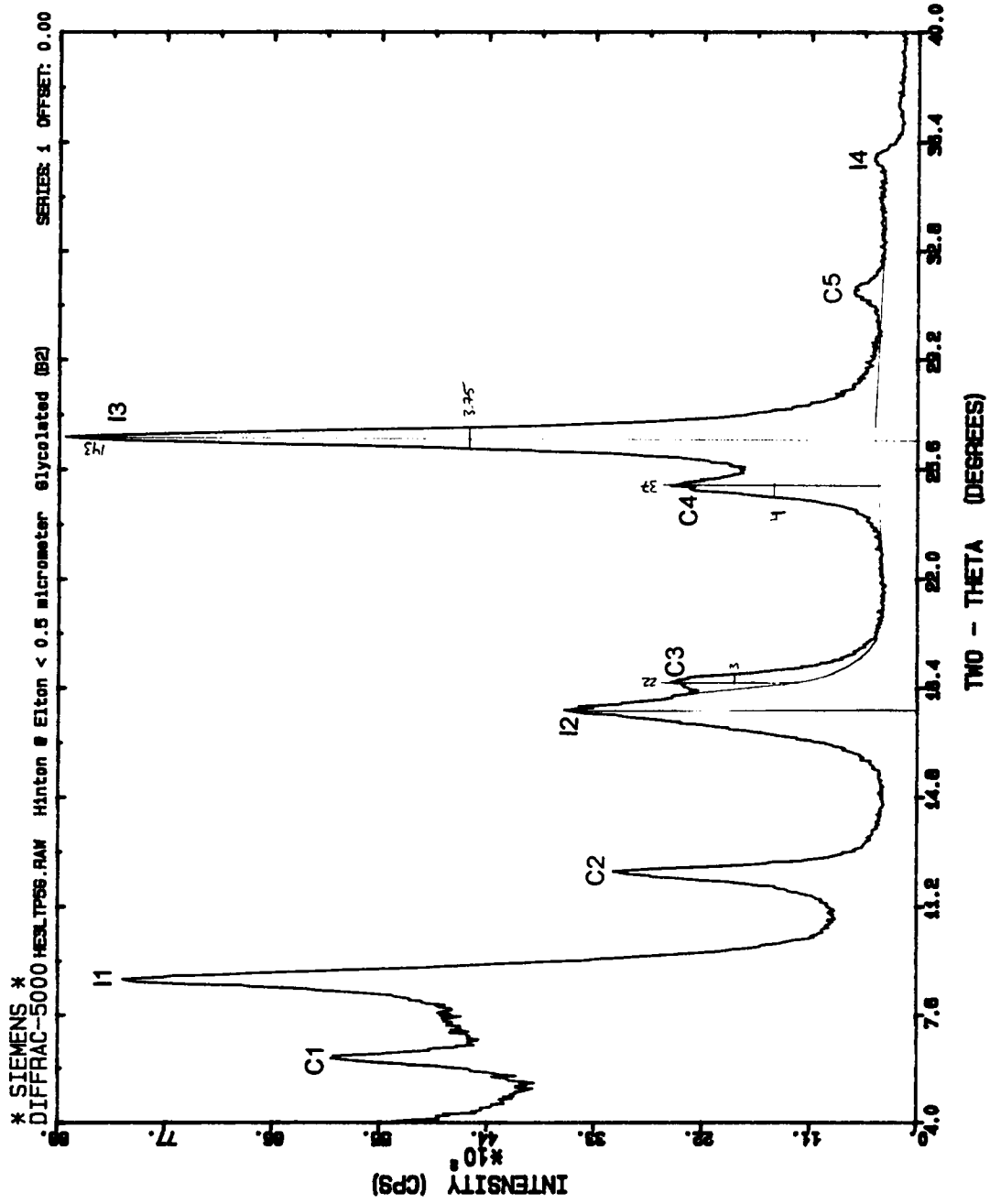
* SIEMENS *
DIFFRAC-5000 HEXLTP56.RAW Hinton @ Elton < 0.5 micrometer Glycolated (B2) SERIES: 1 OFFSET: 0.00
I1
C1
C2
I2
C3
C4
I3
C5
I4
3.345
INTENSITY (CPS)
*10
TWO - THETA (DEGREES)

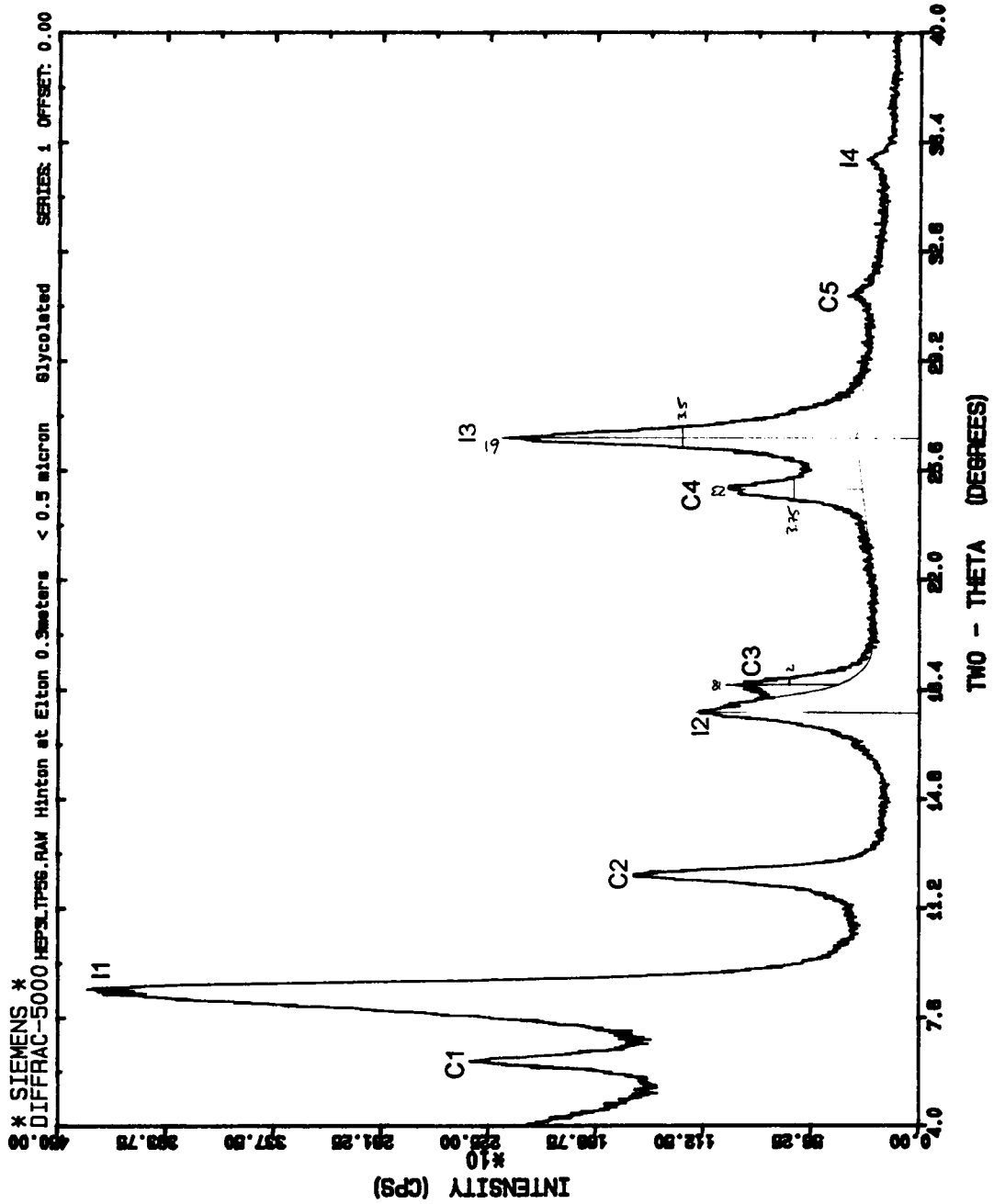
* SIEMENS *
DIFFRAC-5000 HEPSLTPSG.RAW Hinton at Elton 0.5meters < 0.5 micron Glycolated SERIES: 1 OFFSET: 0.00
I1
C1
C2
I2
C3
C4
I3
C5
I4
INTENSITY (CPS)
*10
TWO - THETA (DEGREES)

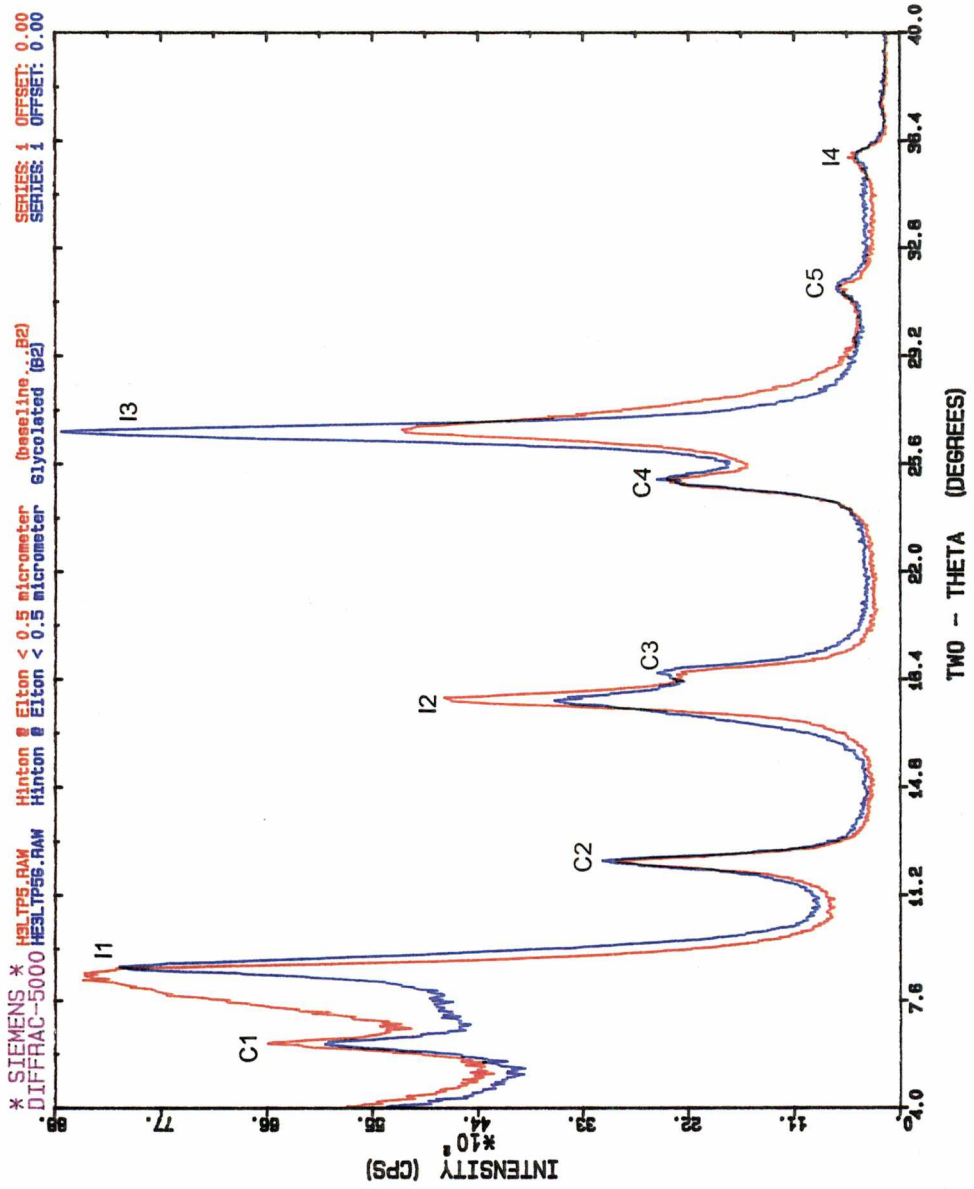
* SIEMENS *
DIFFRAC-5000
H3LTP5.RAW
H3LTP5G.RAW
Hinton @ Elton < 0.5 micrometer
Hinton @ Elton < 0.5 micrometer
(baseline...B2)
Glycolated (B2)
SERIES: 1 OFFSET: 0.00
SERIES: 1 OFFSET: 0.00
I1
I2
I3
I4
I5
C1
C2
C3
C4
C5
INTENSITY (CPS)
*10
TWO - THETA (DEGREES)

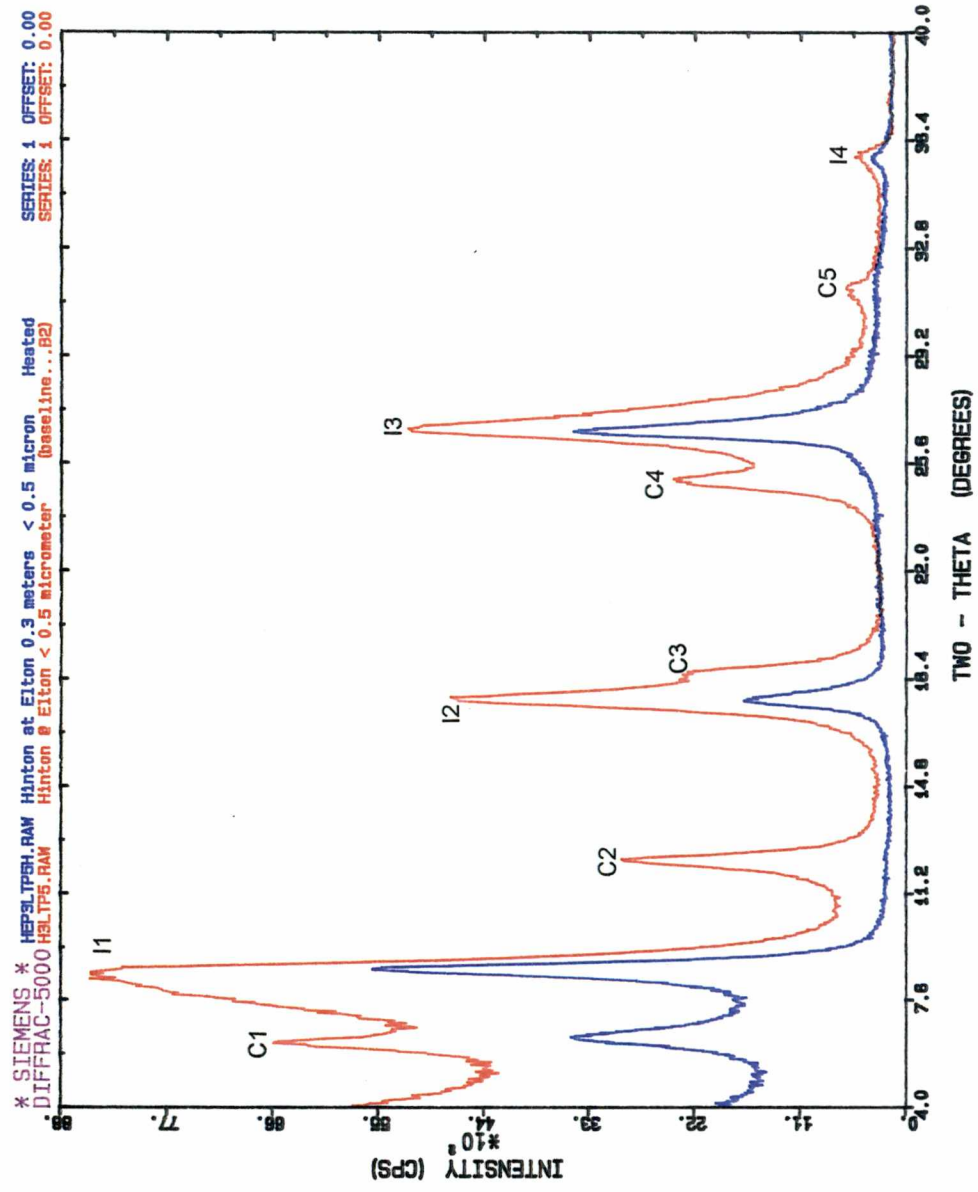
* SIEMENS * HEP3LTP5H.RAW Hinton at Elton 0.3 meters < 0.5 micron Heated SERIES: 1 OFFSET: 0.00
DIFFRAC-5000 H3LTP5.RAW Hinton @ Elton < 0.5 micrometer (baseline...B2) SERIES: 1 OFFSET: 0.00
I1
I2
I3
I4
C1
C2
C3
C4
C5
INTENSITY (CPS)
*10³
88.
77.
66.
55.
44.
33.
22.
11.
4.0
7.6
11.2
14.8
18.4
22.0
25.6
29.2
32.8
36.4
40.0
TWO - THETA (DEGREES)

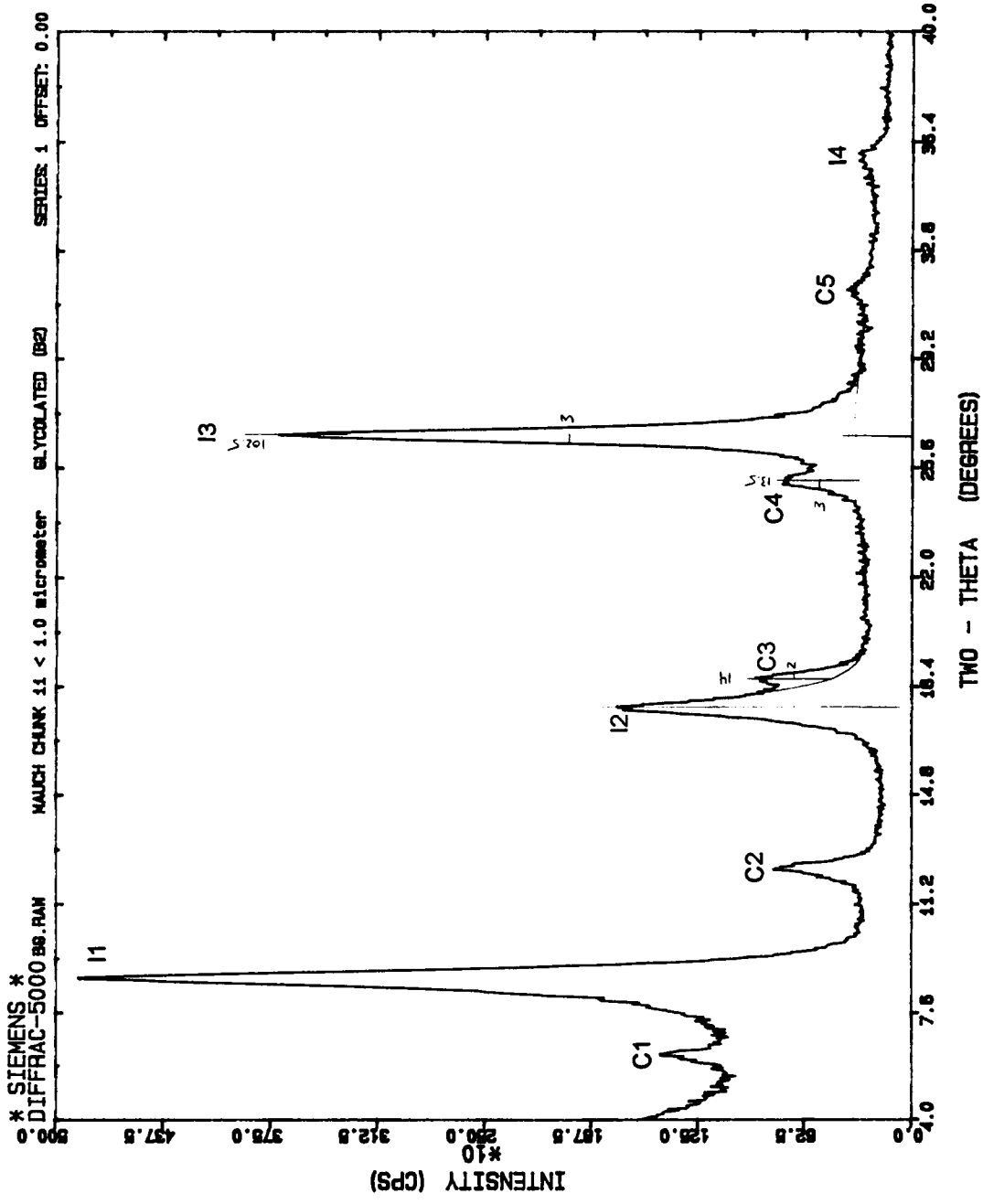
* SIEMENS *
DIFFRAC-5000 BG.RAW
KAUCH CHUNK 11 < 1.0 micrometer GLYCOLATED (B2)
SERIES: 1 OFFSET: 0.00
I1
I2
I3
I4
C1
C2
C3
C4
C5
INTENSITY (CPS)
*10
TWO - THETA (DEGREES)

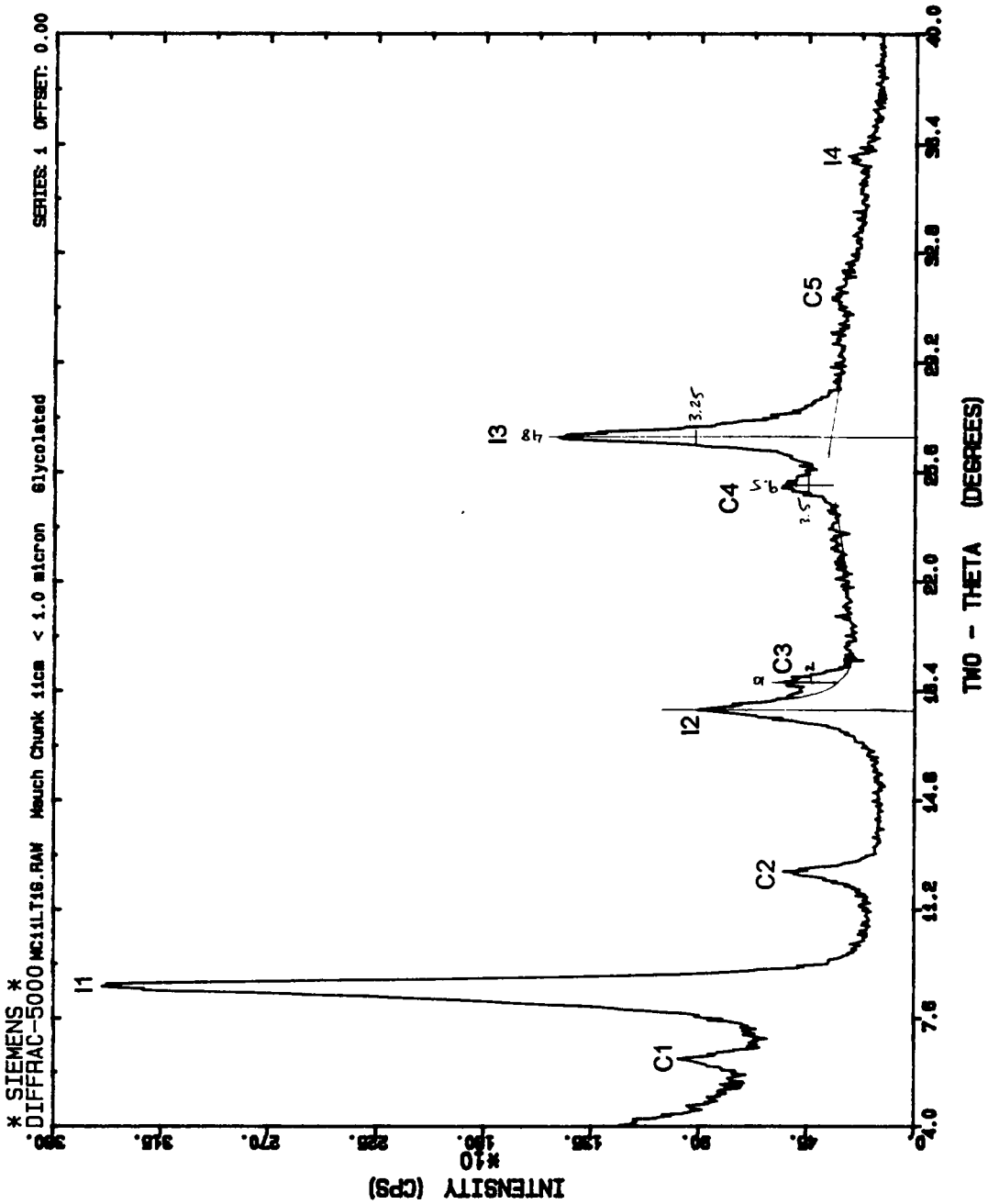
* SIEMENS *
DIFFRAC-5000 MC11LT16.RAW Mauch Chunk 11cm < 1.0 micron Glycolated SERIES: 1 OFFSET: 0.00
I1
C1
C2
I2
C3
C4
I3
I4
C5
3.25
4.8
INTENSITY (CPS)
*10
TWO - THETA (DEGREES)

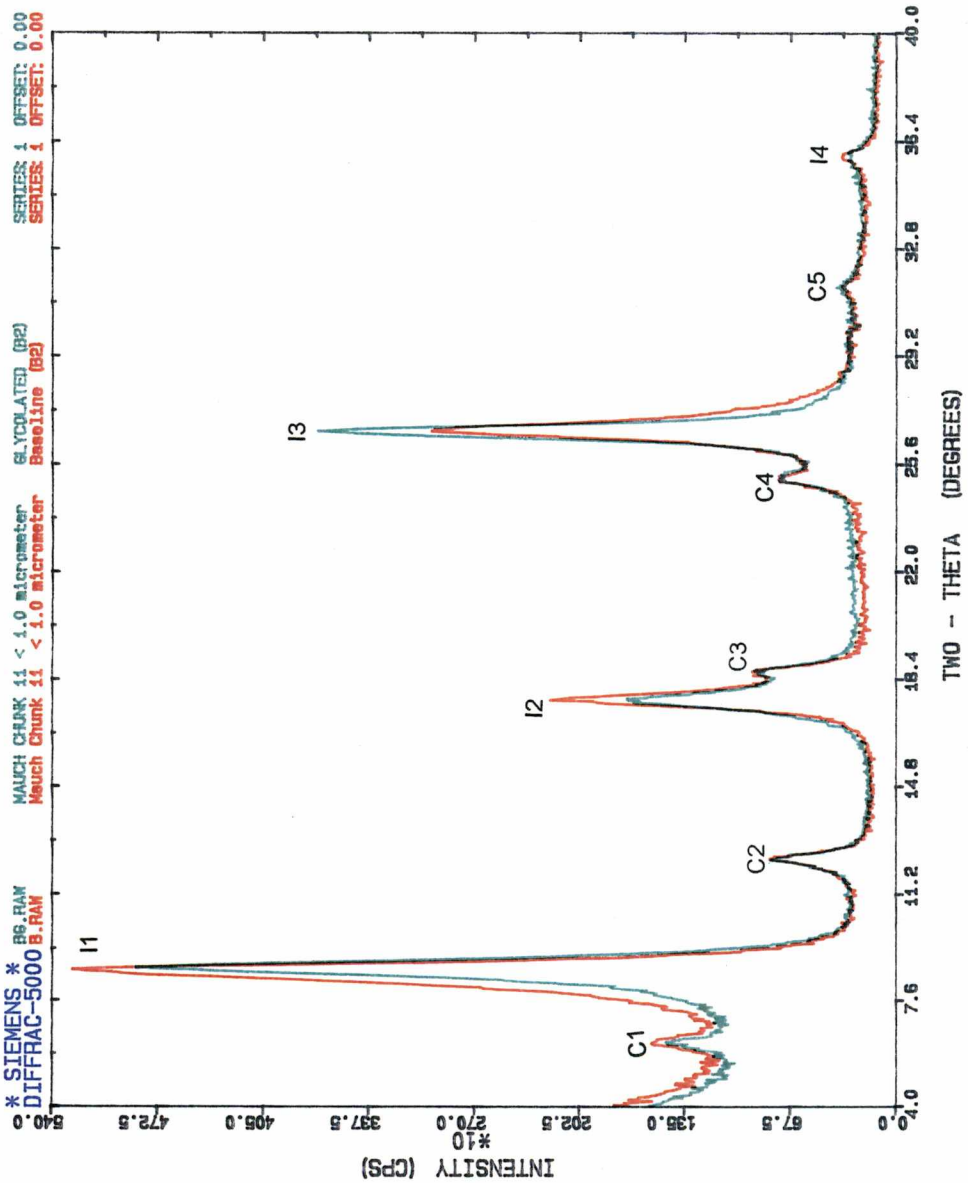
* SIEMENS *
DIFFRAC-5000
BG.RAW
B.RAW
MAUCH CHUNK 11 < 1.0 micrometer
Mauch Chunk 11 < 1.0 micrometer
GLYCOLATED (B2)
Baseline (B2)
SERIES: 1 OFFSET: 0.00
SERIES: 1 OFFSET: 0.00
I1
I2
I3
I4
C1
C2
C3
C4
C5
INTENSITY (CPS)
*10
540.0
472.5
405.0
337.5
270.0
202.5
135.0
67.5
0.0
4.0
7.6
11.2
14.8
18.4
22.0
25.6
29.2
32.8
36.4
40.0
TWO - THETA (DEGREES)

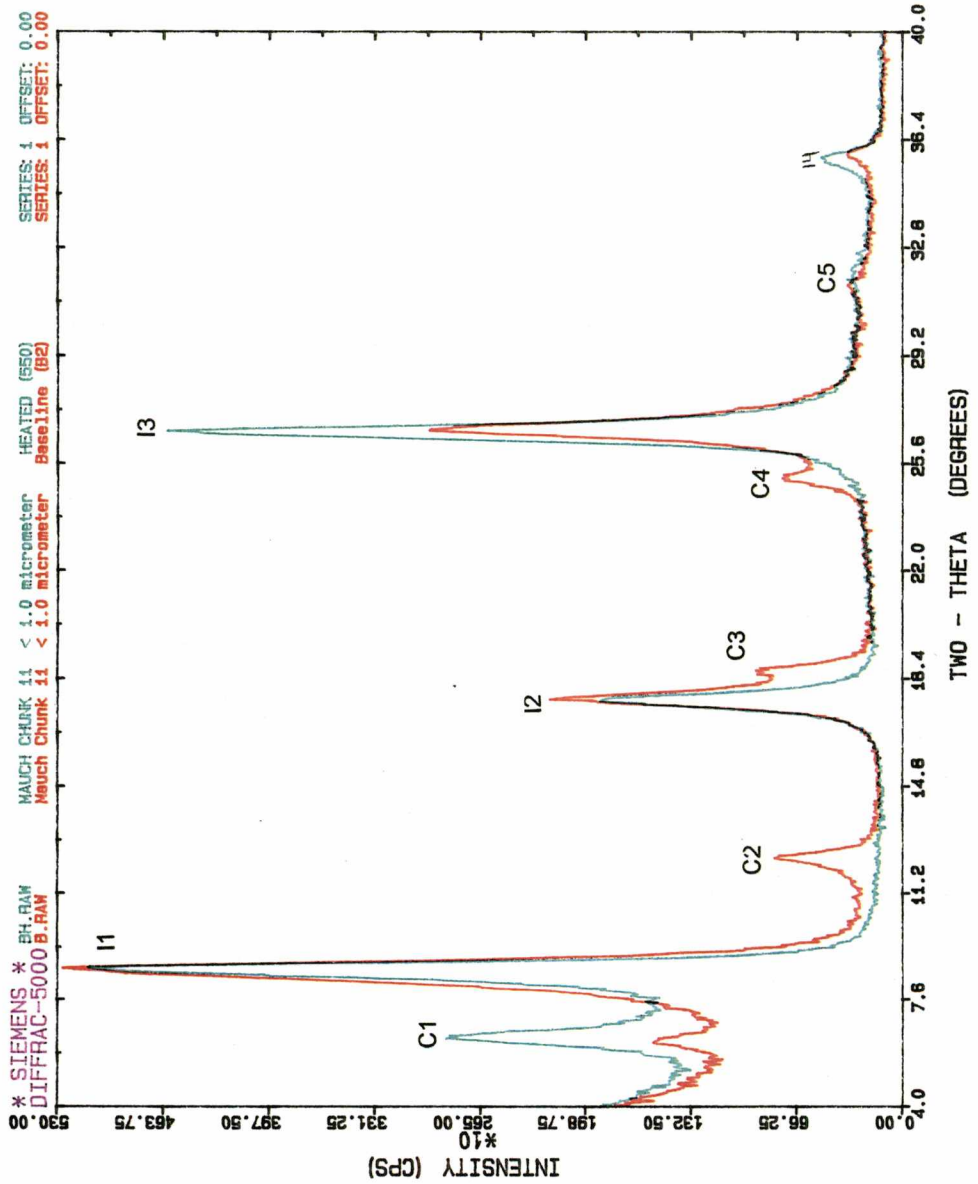
* SIEMENS *
DIFFRAC-5000
BH.RAW
B.RAW
MAUCH CHUNK 11 < 1.0 micrometer HEATED (550)
Mauch Chunk 11 < 1.0 micrometer Baseline (B2)
SERIES: 1 OFFSET: 0.00
SERIES: 1 OFFSET: 0.00
I1
I2
I3
I4
C1
C2
C3
C4
C5
530.00
463.75
397.50
331.25
265.00
198.75
132.50
66.25
0.00
*10
INTENSITY (CPS)
4.0
7.6
11.2
14.8
18.4
22.0
25.6
29.2
32.8
36.4
40.0
TWO - THETA (DEGREES)

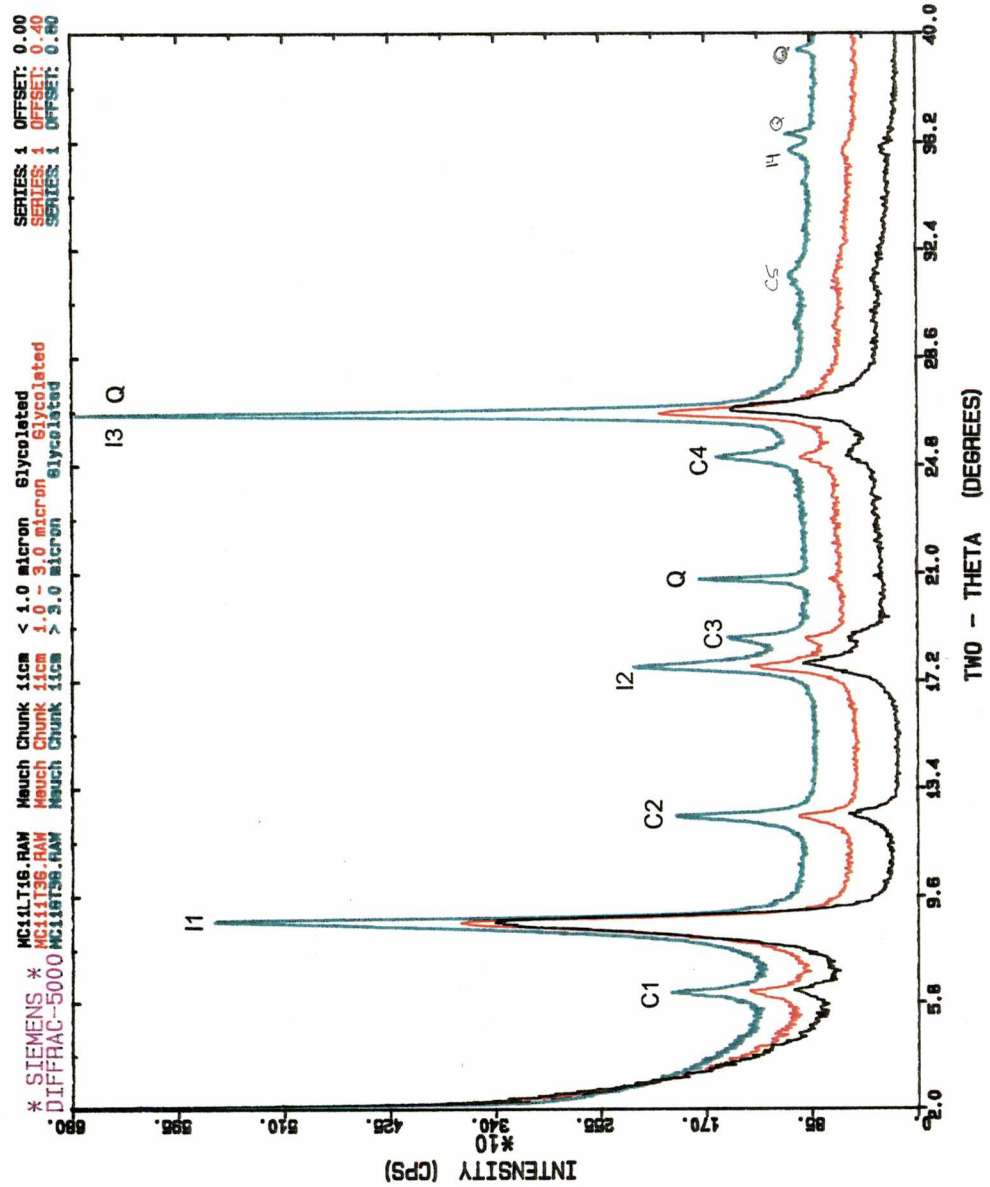
* SIEMENS *
DIFFRAC-5000
MC11LT16.RAM Hauch Chunk 11cm < 1.0 micron Glycolated
MC111T36.RAM Hauch Chunk 11cm 1.0 - 3.0 micron Glycolated
MC116T36.RAM Hauch Chunk 11cm > 3.0 micron Glycolated
SERIES: 1 OFFSET: 0.00
SERIES: 1 OFFSET: 0.40
SERIES: 1 OFFSET: 0.80
I1
I2
I3
Q
C1
C2
C3
C4
INTENSITY (CPS)
*10
680.
595.
510.
425.
340.
255.
170.
85.
2.0
5.8
9.6
13.4
17.2
21.0
24.8
28.6
32.4
36.2
40.0
TWO - THETA (DEGREES)

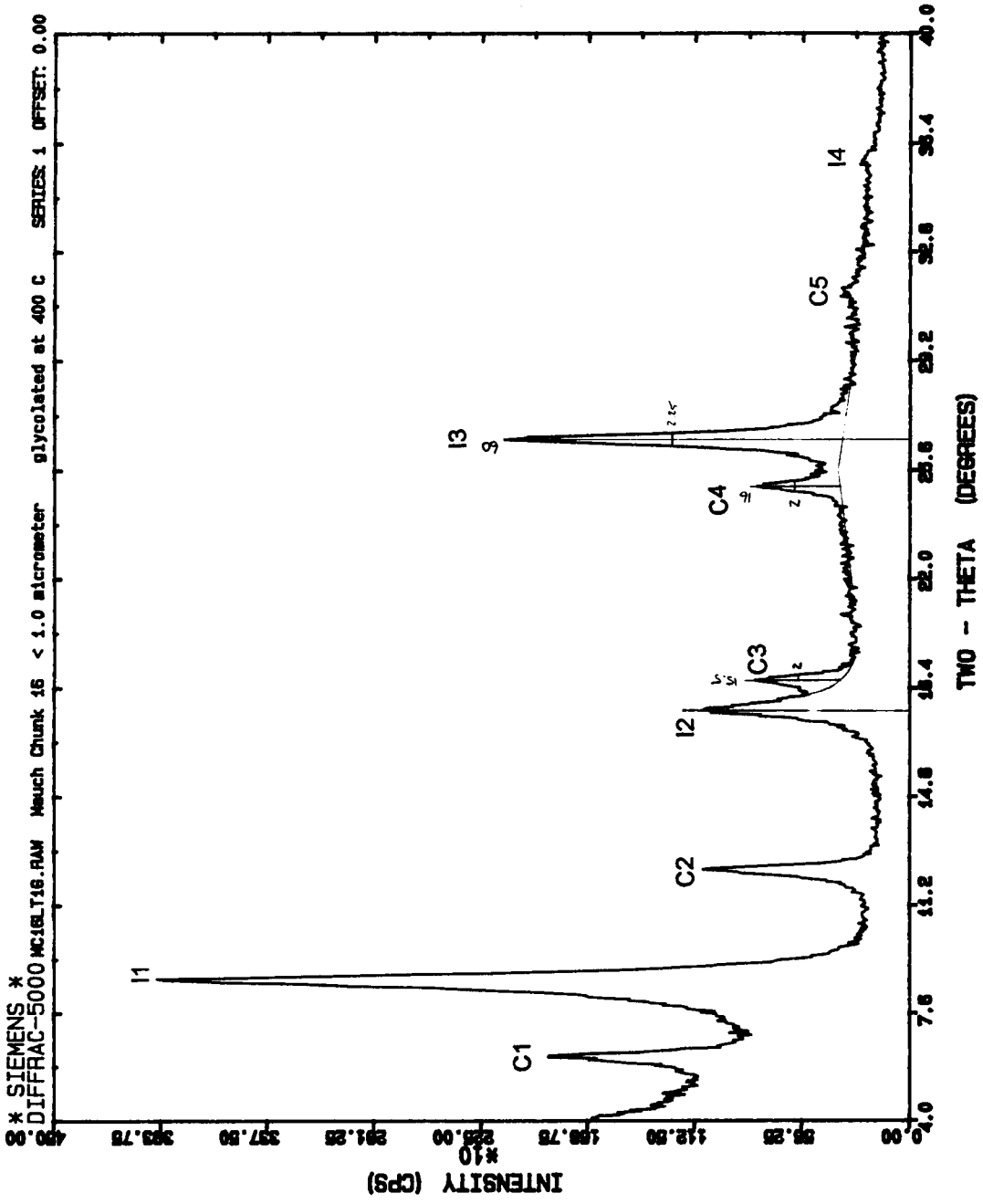
* SIEMENS *
DIFFRAC-5000 MC16LT16.RAW Mauch Chunk 16 < 1.0 micrometer glycolated at 400 C SERIES: 1 OFFSET: 0.00
INTENSITY (CPS)
*10
TWO - THETA (DEGREES)
I1
I2
I3
I4
C1
C2
C3
C4
C5

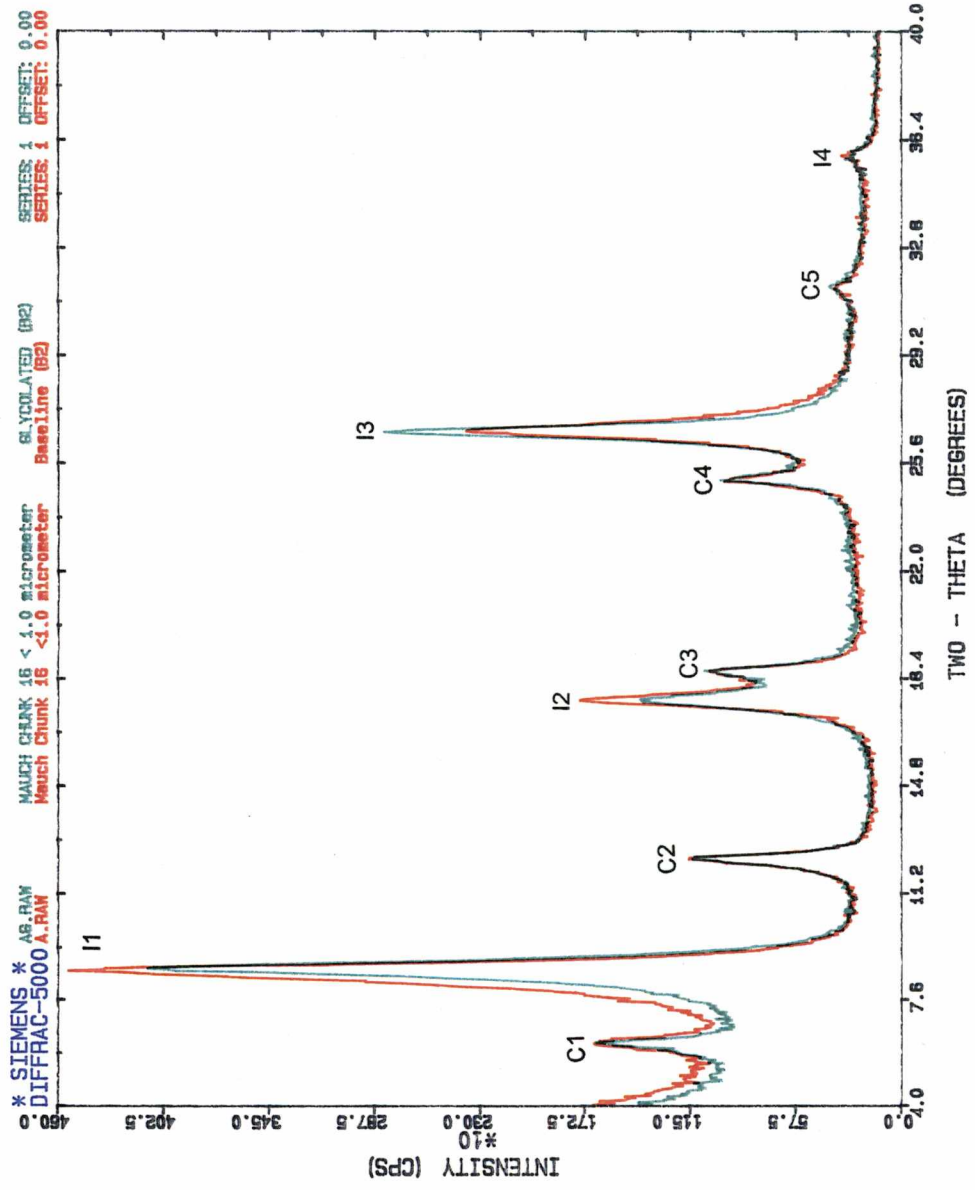
* SIEMENS *
DIFFRAC-5000
AR.RAW
A.RAM
MAUCH CHUNK 16 < 1.0 micrometer
Mauch Chunk 16 <1.0 micrometer
GLYCOLATED (B2)
Baseline (B2)
SERIES: 1 OFFSET: 0.00
SERIES: 1 OFFSET: 0.00
I1
I2
I3
I4
C1
C2
C3
C4
C5
460.0
402.5
345.0
287.5
230.0
172.5
115.0
57.5
0.0
*10
INTENSITY (CPS)
4.0
7.6
11.2
14.8
18.4
22.0
25.6
29.2
32.8
36.4
40.0
TWO - THETA (DEGREES)

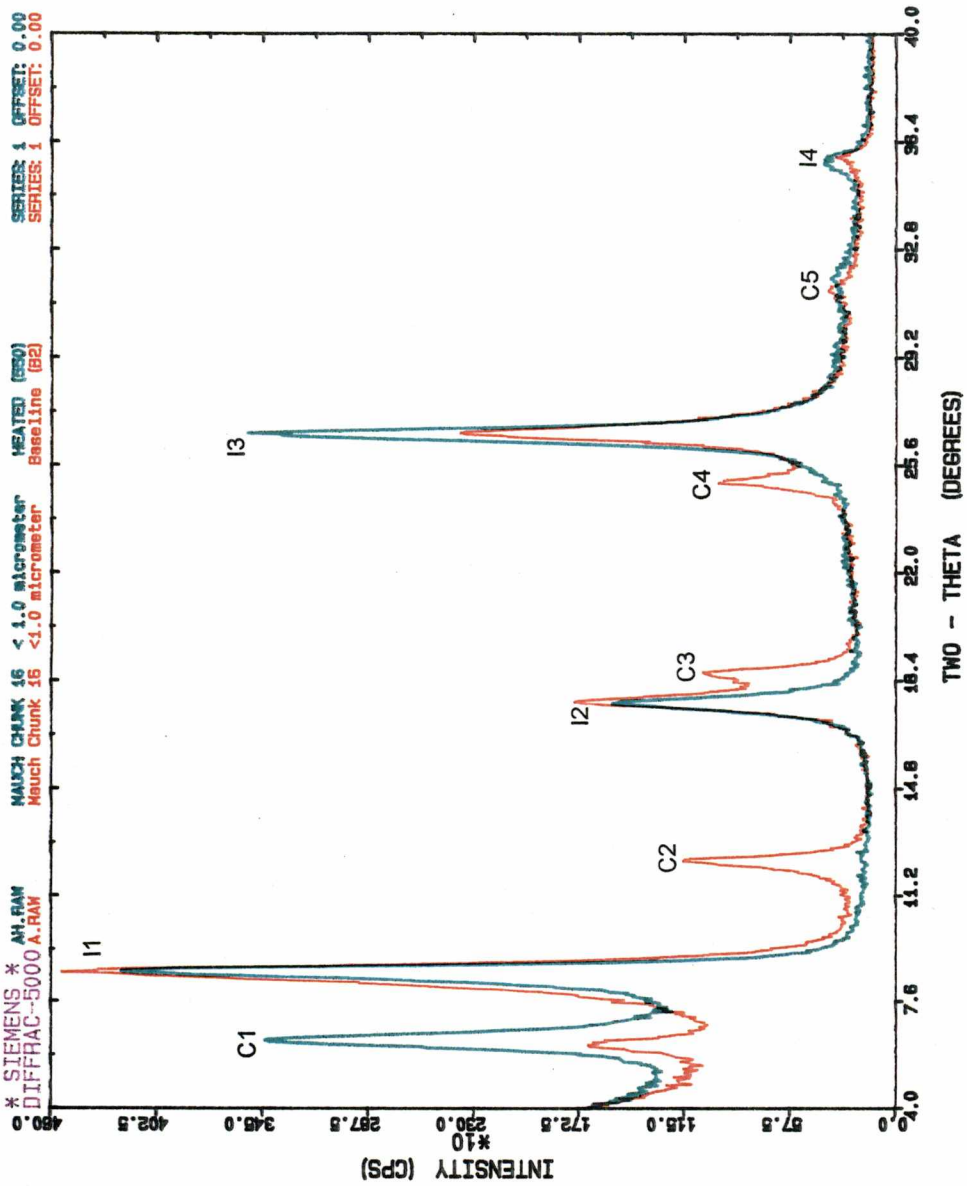
* SIEMENS *
DIFFRAC-5000
AH.RAW
A.RAW
MAUCH CHUNK 16
Mauch Chunk 16
< 1.0 micrometer
<1.0 micrometer
HEATED (850)
Baseline (B2)
SERIES: 1 OFFSET: 0.00
SERIES: 1 OFFSET: 0.00
I1
I2
I3
I4
C1
C2
C3
C4
C5
INTENSITY (CPS)
*10
TWO - THETA (DEGREES)

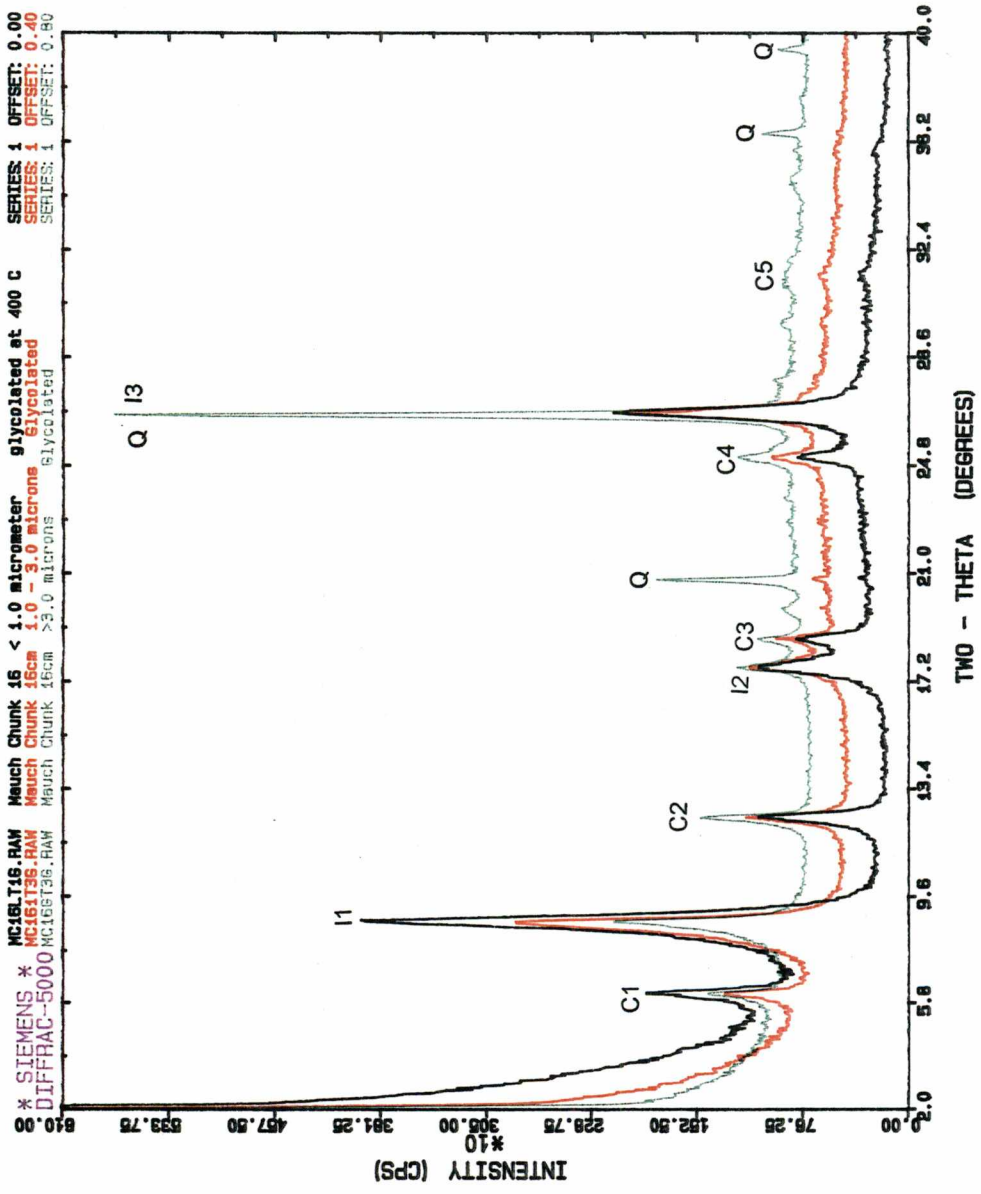
* SIEMENS *
DIFFRAC-5000
MC16LT16.RAW Mauch Chunk 16 < 1.0 micrometer glycolated at 400 C
MC16IT36.RAW Mauch Chunk 16cm 1.0 - 3.0 microns Glycolated
MC16ST36.RAW Mauch Chunk 16cm >3.0 microns Glycolated
SERIES: 1 OFFSET: 0.00
SERIES: 1 OFFSET: 0.40
SERIES: 1 OFFSET: 0.80
I1
I2
I3
C1
C2
C3
C4
C5
Q
INTENSITY (CPS)
*10
TWO - THETA (DEGREES)

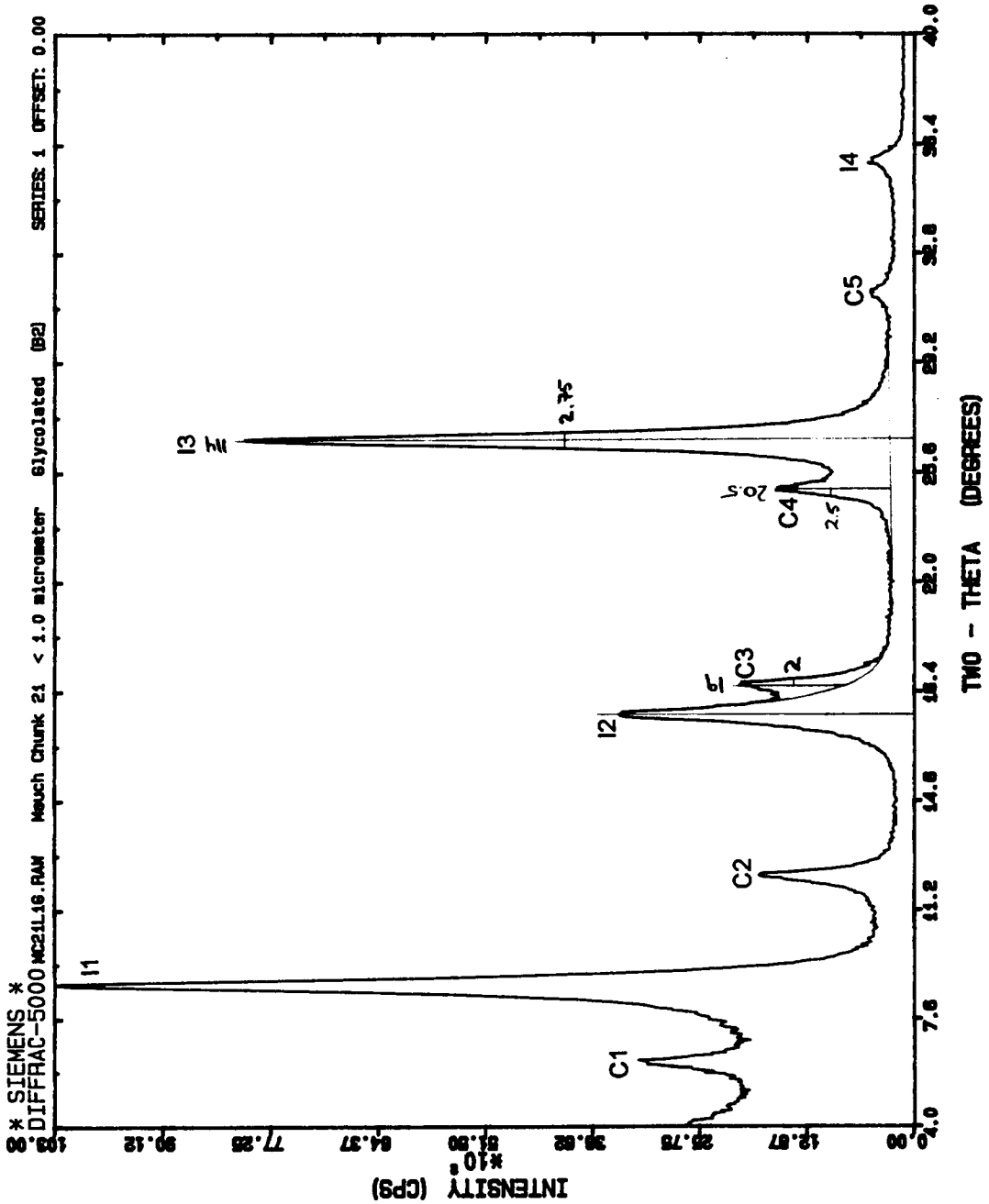
* SIEMENS *
DIFFRAC-5000 MC21L16.RAM Mauch Chunk 21 < 1.0 micrometer Glycolated (B2) SERIES: 1 OFFSET: 0.00
I1
C1
C2
I2
C3
I3
C4
C5
I4
2.75
2θ.5
2.5
INTENSITY (CPS)
*10³
TWO - THETA (DEGREES)

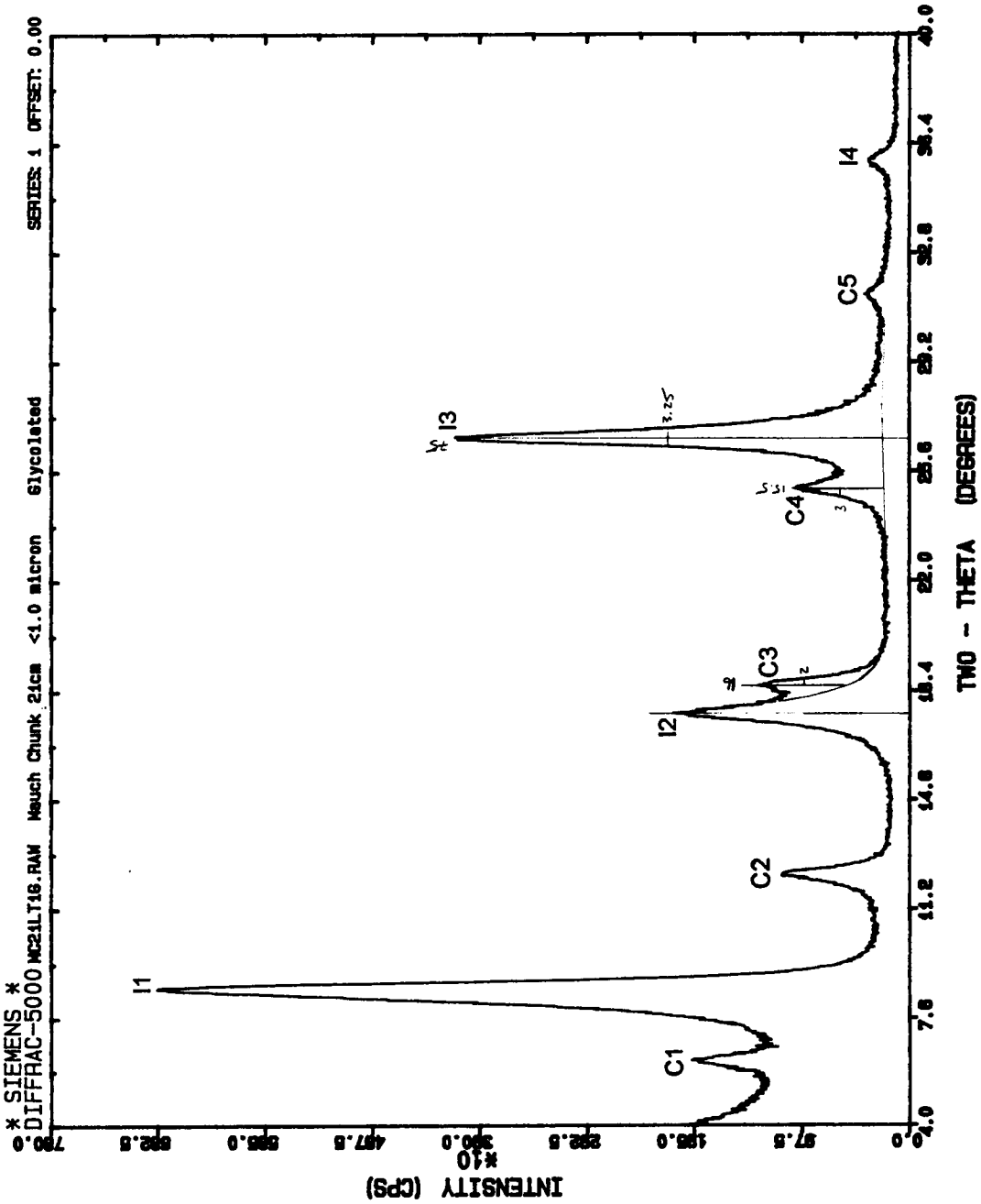
* SIEMENS *
DIFFRAC-5000 MG21LT16.RAM Mauch Chunk 21cm <1.0 micron Glycolated SERIES: 1 OFFSET: 0.00
I1
I2
I3
I4
C1
C2
C3
C4
C5
INTENSITY (CPS)
*10
TWO - THETA (DEGREES)

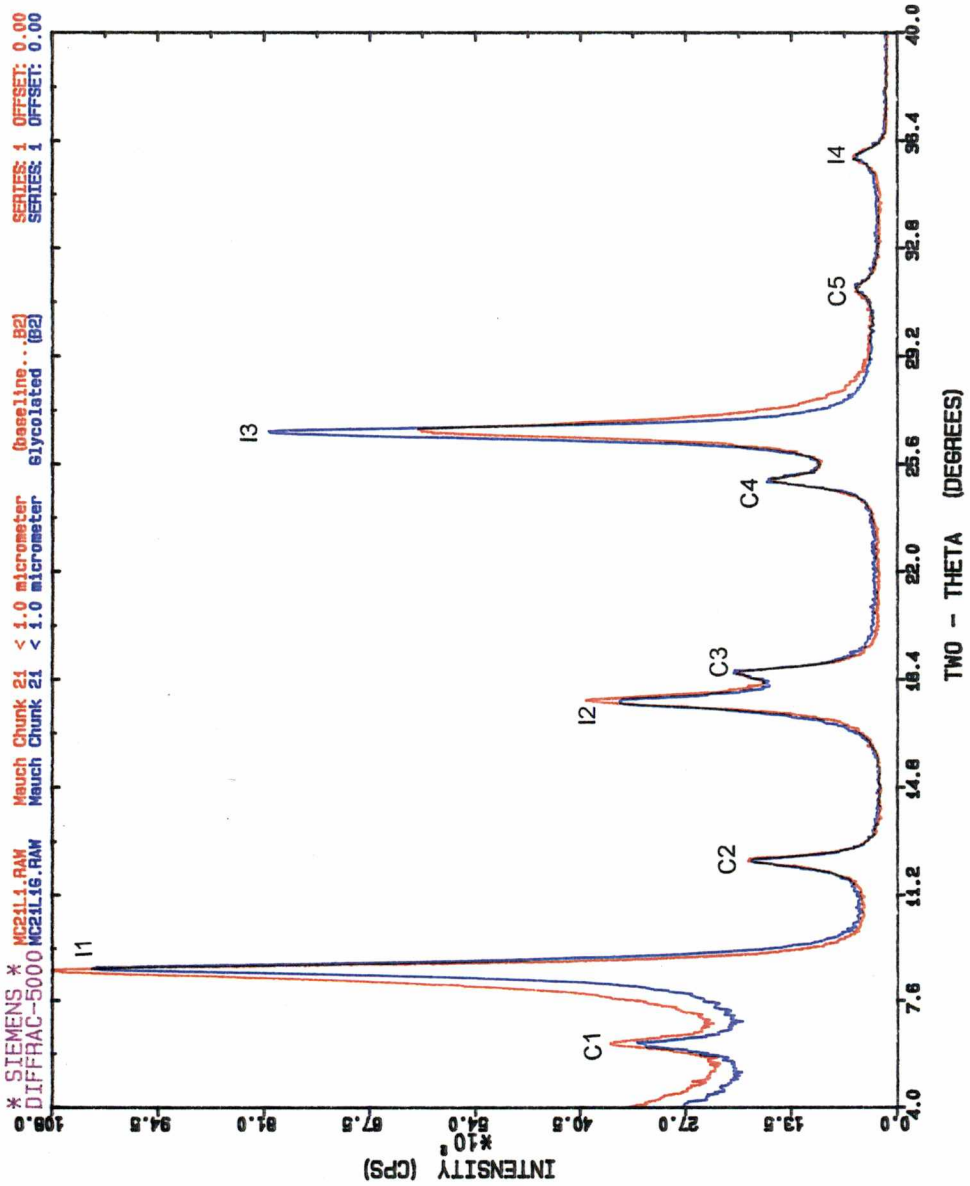
* SIEMENS *
DIFFRAC-5000
MC2114.RAW Mauch Chunk 21 < 1.0 micrometer (baseline...B2)
MC2116.RAW Mauch Chunk 21 < 1.0 micrometer Glycolated (B2)
SERIES: 1 OFFSET: 0.00
SERIES: 1 OFFSET: 0.00
I1
I2
I3
I4
C1
C2
C3
C4
C5
INTENSITY (CPS)
*10³
TWO - THETA (DEGREES)

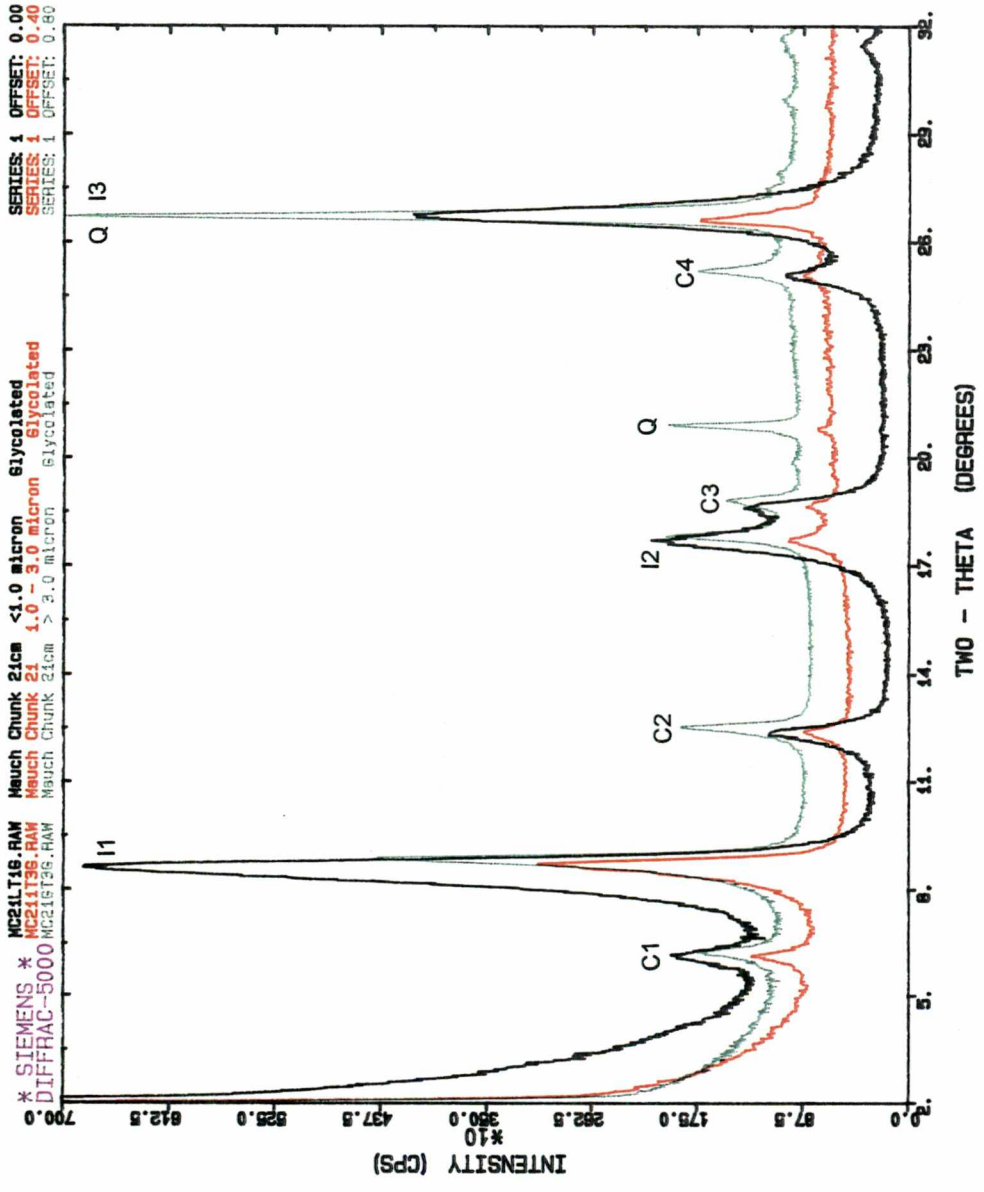
* SIEMENS *
DIFFRAC-5000
MC21LT16.RAM Mauch Chunk 21cm <1.0 micron Glycolated
MC211T36.RAM Mauch Chunk 21 1.0 - 3.0 micron Glycolated
MC21GT36.RAM Mauch Chunk 21cm > 3.0 micron Glycolated
SERIES: 1 OFFSET: 0.00
SERIES: 1 OFFSET: 0.40
SERIES: 1 OFFSET: 0.80
I1
I2
I3
Q
C1
C2
C3
C4
INTENSITY (CPS)
*10
700.0
612.5
525.0
437.5
350.0
262.5
175.0
87.5
0.0
2.
5.
8.
11.
14.
17.
20.
23.
26.
29.
32.
TWO - THETA (DEGREES)

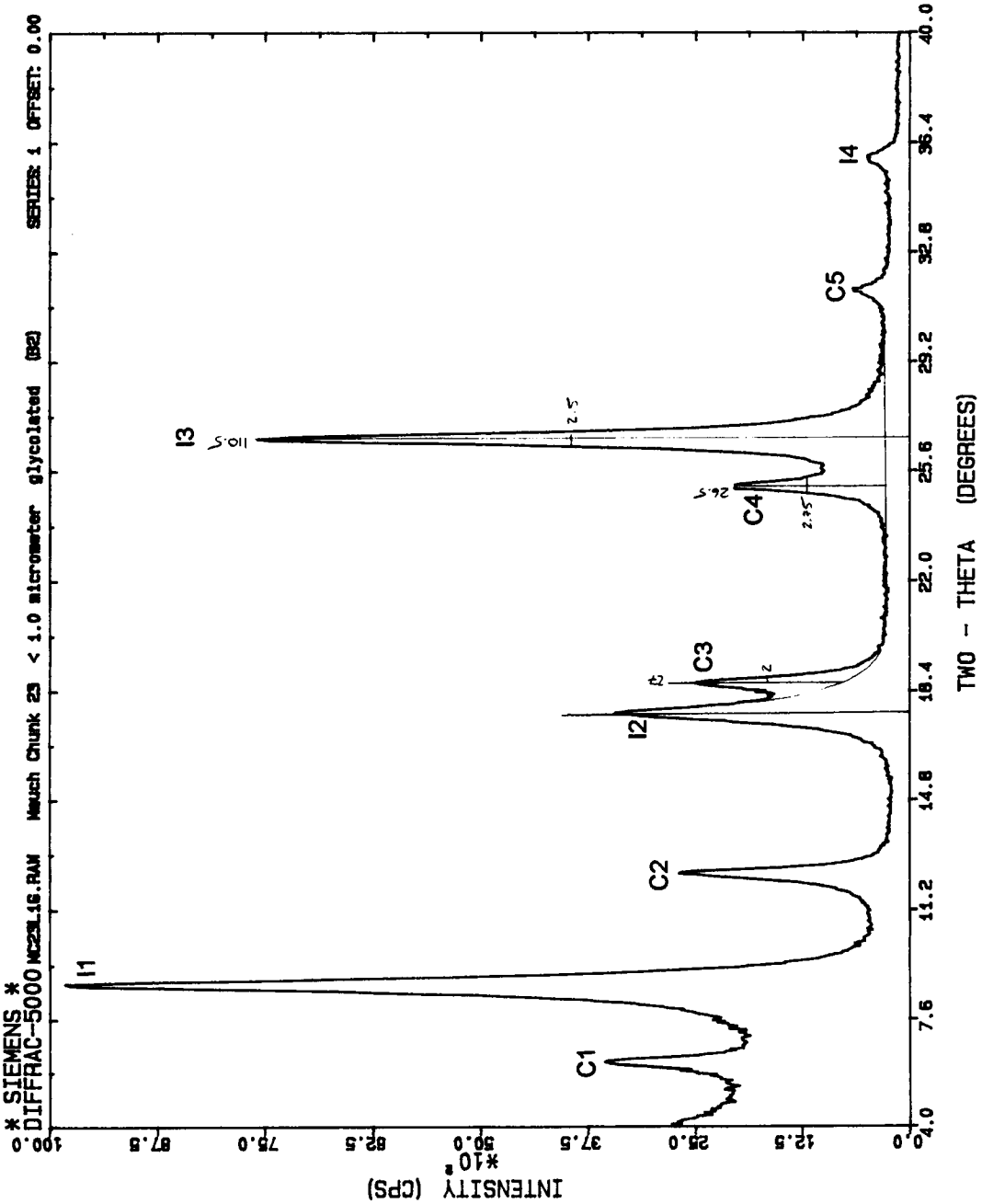
* SIEMENS *
DIFFRAC-5000
Mauch Chunk 23 < 1.0 micrometer glycolated (B2)
SERIES: 1 OFFSET: 0.00
I1
C1
C2
I2
C3
I3
C4
C5
I4
INTENSITY (CPS)
*10²
TWO - THETA (DEGREES)

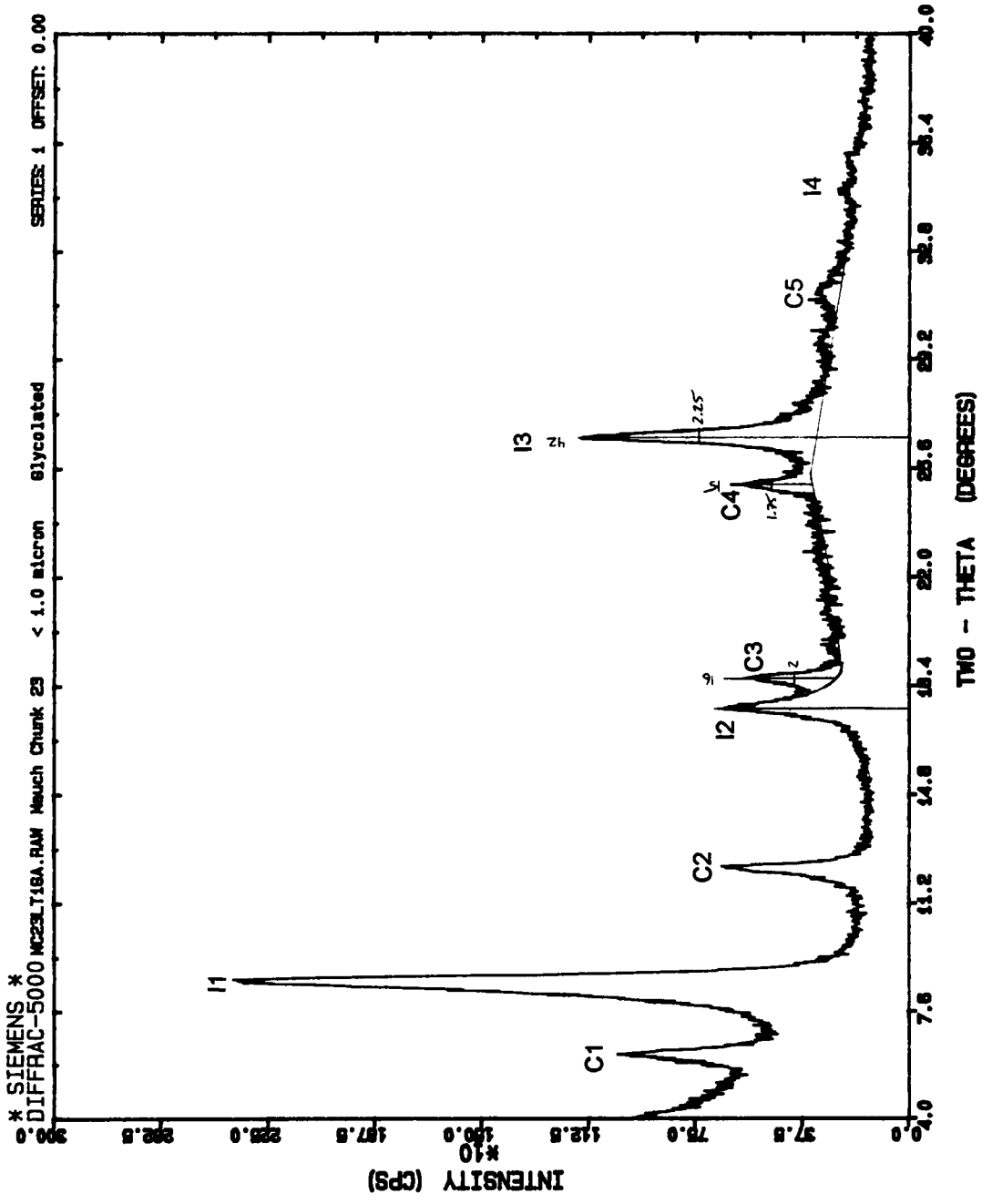
* SIEMENS *
DIFFRAC-5000 MC23LT18A.RAW Mauch Chunk 23 < 1.0 micron Glycolated SERIES: 1 OFFSET: 0.00
INTENSITY (CPS)
*10
TWO - THETA (DEGREES)
I1
I2
I3
I4
C1
C2
C3
C4
C5

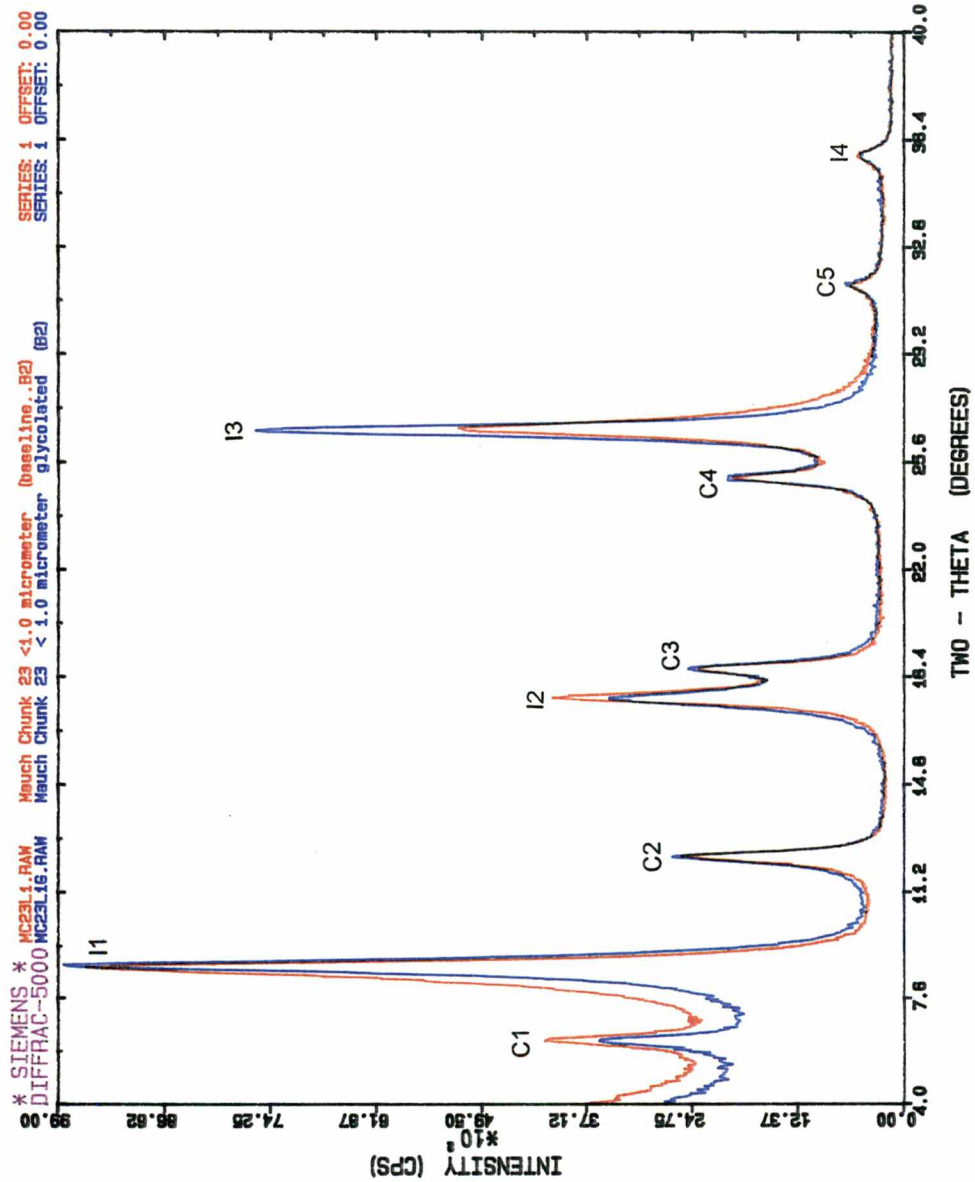
* SIEMENS *
DIFFRAC-5000
MC23L1.RAW Mauch Chunk 23 <1.0 micrometer (baseline,.B2) SERIES: 1 OFFSET: 0.00
MC23L16.RAW Mauch Chunk 23 < 1.0 micrometer glycolated (B2) SERIES: 1 OFFSET: 0.00
I1
I2
I3
I4
C1
C2
C3
C4
C5
99.00
86.62
74.25
61.87
49.50
37.12
24.75
12.37
0.00
INTENSITY (CPS)
*10³
4.0
7.6
11.2
14.8
18.4
22.0
25.6
29.2
32.8
36.4
40.0
TWO - THETA (DEGREES)

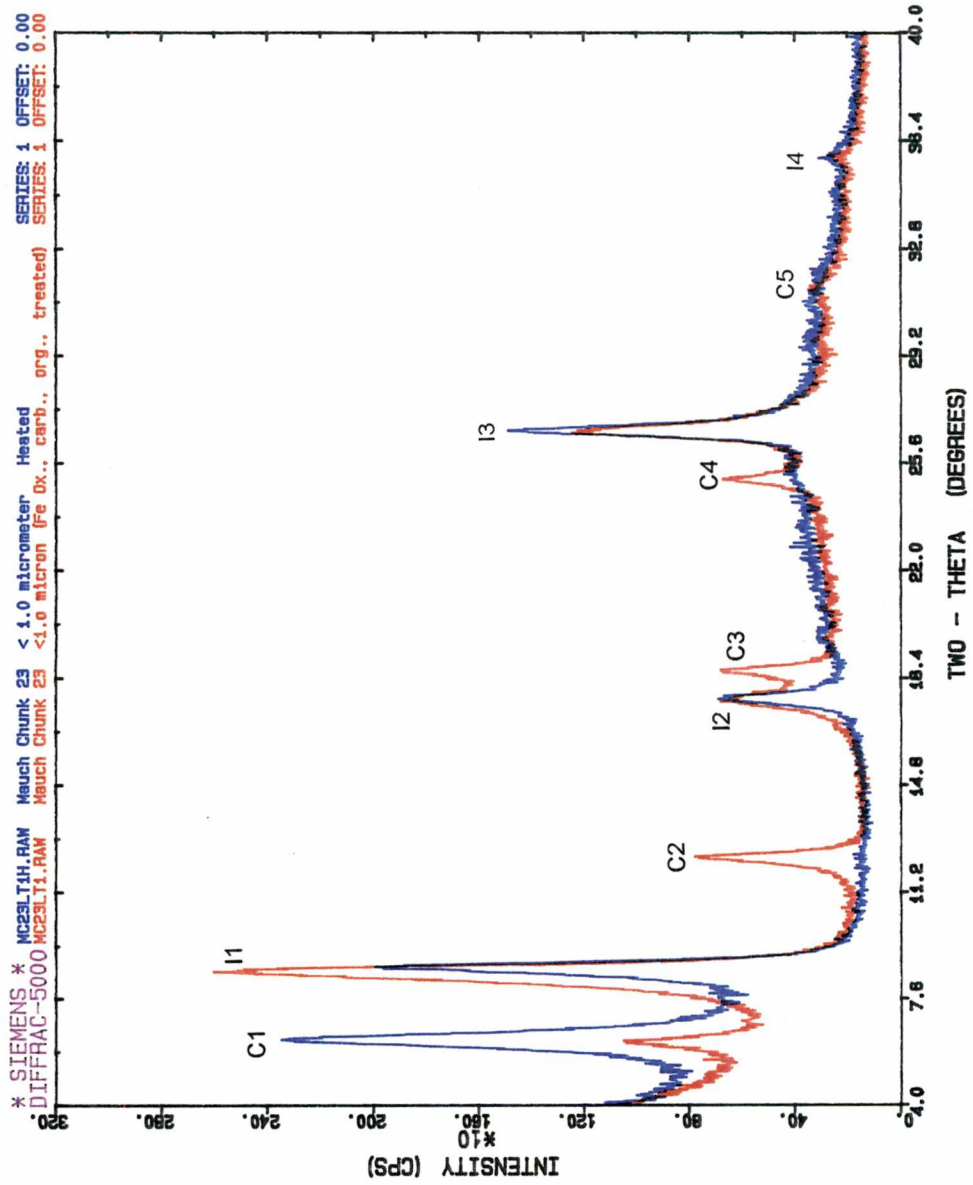
* SIEMENS *
DIFFRAC-5000
MC23LT1H.RAW Mauch Chunk 23 < 1.0 micrometer Heated SERIES: 1 OFFSET: 0.00
MC23LT1.RAW Mauch Chunk 23 <1.0 micron (Fe Ox., carb., org., treated) SERIES: 1 OFFSET: 0.00
INTENSITY (CPS)
*10
320.
280.
240.
200.
160.
120.
80.
40.
0.0
7.8
11.2
14.8
18.4
22.0
25.6
29.2
32.8
36.4
40.0
TWO - THETA (DEGREES)
I1
C1
C2
I2
C3
C4
I3
C5
I4

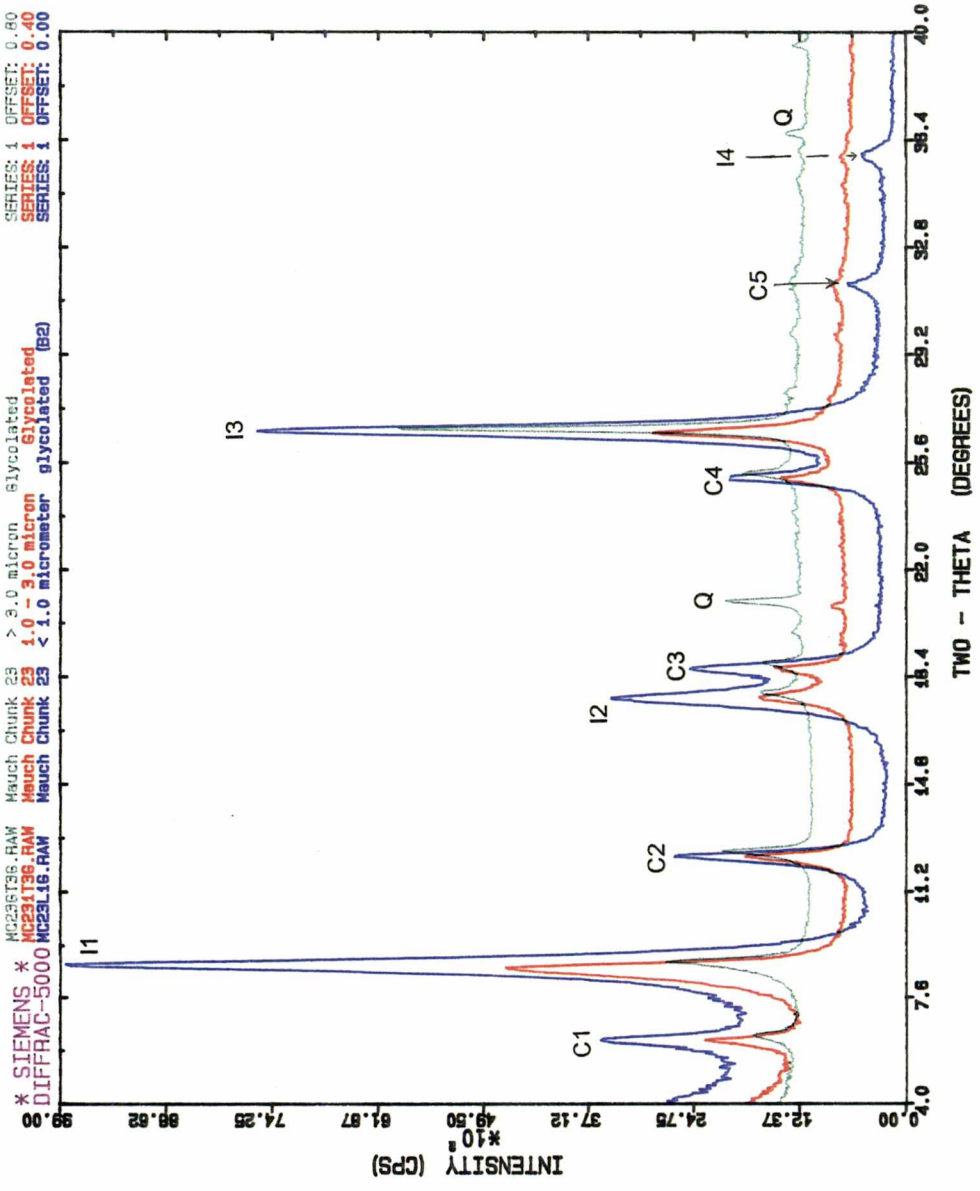
* SIEMENS *
DIFFRAC-5000
MC231736.RAW Mauch Chunk 23 > 3.0 micron Glycolated
MC231736.RAW Mauch Chunk 23 1.0 - 3.0 micron Glycolated
MC23L16.RAW Mauch Chunk 23 < 1.0 micrometer glycolated (B2)
SERIES: 1 OFFSET: 0.80
SERIES: 1 OFFSET: 0.40
SERIES: 1 OFFSET: 0.00
I1
I2
I3
I4
C1
C2
C3
C4
C5
Q
Q
INTENSITY (CPS)
*10^3
99.00
88.62
74.25
61.87
49.50
37.12
24.75
12.37
0.00
4.0
7.6
11.2
14.8
18.4
22.0
25.6
29.2
32.8
36.4
40.0
TWO - THETA (DEGREES)

APPENDIX C:
SILICATE OXYGEN ANALYSIS

SAMPLE	SILICATE #*	% YIELD**	δ^{18}O SMOW	AVE.
M23< 1.0μm	Sill-52-6	88-93	+13.18	
M23< 1.0μm	Sill-54-6	89-95	+11.19	
M23< 1.0μm	Sill-54-7	90-96	+12.74	12.36 +/- .6‰
M23< 1.0μm	Sill-66-5	92-98	+11.95	
M23< 1.0μm	Sill-77-3	96-102	+12.74	
M21< 1.0μm	Sill-53-2	89-93	+11.86	11.97 +/- .08‰
M21< 1.0μm	Sill-53-3	91-96	+12.08	
M16< 1.0μm	Sill-65-3	93-97	+12.35	12.16 +/- .15‰
M16< 1.0μm	Sill-72-2	90-96	+11.98	
M11< 1.0μm	Sill-49-2	89-92	+12.18	12.16 +/- .02‰
M11<1.0μm	Sill-49-3	89-94	+12.13	
H.3< 0.5μm	Sill-51-2	90-95	+15.16	15.15 +/- .004‰
H.3< 0.5μm	Sill-51-3	88-93	+15.14	
H2.2< 0.8μm	Sill-53-5	91-96	+15.06	14.97 +/- .07‰
H2.2< 0.8μm	Sill-55-4	89-94	+14.88	
HP < 1.0μm	Sill-68-7	94-100	+14.25	14.66 +/- .2‰
HP < 1.0μm	Sill-75-5	90-96	+14.82	
HP < 1.0μm	Sill-74-3	91-97	+14.92	
P.3< 1.0μm	Sill-51-5	87-91	+16.76	17.37 +/- .4‰
P.3< 1.0μm	Sill-55-2	85-88	+17.37	
P.3< 1.0μm	Sill-63-2	89-93	+17.38	
P.3< 1.0μm	Sill-64-6	92-96	+17.98	
P1.2 < 1.0 μm	Sill-47-2	85-88	+16.82	16.62 +/- .3‰
P1.2 < 1.0 μm	Sill-47-3	87-90	+16.08	
P1.2 < 1.0 μm	Sill-48-8	87-90	+16.67	
P1.2 < 1.0 μm	Sill-50-8	87-90	+16.90	
P1.5 <1.0μm	Sill-55-3	90-95	+17.04	17.57 +/- .4‰
P1.5 <1.0μm	Sill-63-5	93-97	+18.12	
P1.5 <1.0μm	Sill-63-3	93-97	+17.56	
PP < 1.0μm	Sill-67-3	89-99	+16.27	16.74 +/- .3‰
PP < 1.0μm	Sill-73-7	89-99	+17.24	
PP < 1.0μm	Sill-74-2	90-100	+16.70	

APPENDIX C (continued)

SAMPLE	SILICATE #*	% YIELD**	AVE. δ^{18}O SMOW
NBS-28	Ave. Rv 2-8***	> 95%	9.56 +/- .25 %
MAPS	Ave. Rv 2-8	> 95%	9.61 +/- .30%

* Refers to sample name in silicate book 2. Last digit in number refers to reaction vessel used for that sample

** % Yield is represented by a range to account for the possibility of both Fe and Mg-chlorites.

*** Average standard values for reaction vessels (RV) 2-8.

APPENDIX D:

CARBONATE ISOTOPE ANALYSIS

SAMPLE	δ^{13}C PDB	δ^{18}0 PDB	δ^{18}O SMOW	AVE.
HE2N2L1	-12.80	-11.90	+18.64	
HE2N3L1	-10.89	-13.52	+16.97	
HE2N4L1	-9.39	-11.10	+19.47	18.54
HE2N4L2	-9.31	-10.67	+19.91	
HE2N4L4	-9.84	-12.80	+17.71	
HE2.2N4L1	-10.97	-12.96	+17.55	
HE2.2N4L2	-10.72	-10.93	+19.64	18.70
HE2.2N4L4	-10.46	-11.65	+18.90	

AVERAGE CHIHUAHUAN CALCITE STANDARD: 21.25 +/- .20 SMOW
-9.372 +/- .20 PDB

APPENDIX E:

CHEMICAL TREATMENTS TO REMOVE CHLORITE

Several preliminary were performed to validate the interpretations made in this investigation. The most important of these was to attempt to quantify the effects chlorite had on the oxygen isotope composition of the finest clay size fraction. Limited sample supply prevented attempts at the physical separation of chlorite from illite using a Franz magnetic separator. However, chlorite percentages in selected samples were successfully reduced by washing samples in 10% HCl for 30 minutes at 90^{0}C . It was hoped that oxygen values of these treated samples would be displaced relative to untreated samples; and that these trends would allow a semi-quantitative estimate of the effects of chlorite, based on the amount of chlorite removed. Unfortunately two problems were encountered. First, following the repeated washes (up to 10) necessary to reduce chlorite, a quartz peak appeared in the XRD plots. Whether this quartz is a small percentage of actual quartz that was being masked by chlorite, or if this quartz was produced by the HCl treatments is not known. Experiments will have to be performed to evaluate these possibilities. The second problem encountered was that oxygen isotope analysis of the treated samples showed that every sample, regardless of the paleosol it was from, had exactly the same $\delta^{18}O$ value. This uniformity strongly suggests that the HCl used in these treatments affected the oxygen isotope composition of the clays.

VITA

Brian Thomas Sheldon was born in the small town of New Hartford, New York to Herbert and Signe Sheldon on March 28, 1968. A childhood spent in the fields, woods, and ravines that were his backyard instilled a strong appreciation for the outdoors, including the damage it could do to a boy's frame. Brian's curiosity and interest in the outdoors were further enhanced by his parents, who took the family hiking and camping on a number of occasions to such places as the near-by lakes and mountains of the Adirondacks.

Brian attended New Hartford Jr. High and High School, during which time two biology teachers, Mr. Reno Johnson and Mr. Peter Goodfriend, and his ecology teacher Mr. Douglas Pens, were instrumental in firmly establishing his interests in the sciences. In the Fall of 1986 Brian entered the State University of New York College at Geneseo as a biochemistry major, but was quickly saved and introduced to geology be Dr. P.D. Boger. Dr. Boger (Bowg) still serves as one of Brian's mentors, with the exception that Dr. Boger loves computers and Brian would rather CRUSH them. Brian spent the summer of 1991 working at the U.S. Geological Survey-Water Resources Division in Durango, Colorado as a National Association of Geology Teachers Summer Internship awardee. Brian graduated from Geneseo in December of 1991, and entered the Masters program at the University of Tennessee, Knoxville in the following Fall.

Brian has aspirations to hike the Appalachian Trail and the 46 High Peaks of the Adirondacks. Getting a job is also on his list of things to do (kind of). Currently he is looking forward to his marriage with Amy Halleran, time off (just a little) to play, and to fretting his Martin guitar as much as he has fretted over the formatting of this thesis.